Channel pattern prediction in Dutch streams

Harkema, Tom
WAGENINGEN UNIVERSITY AND RESEARCH | 30-08-2019

Author:

T. T. L. Harkema

Registration number:

950817306010

Course:

MSc. Thesis

Soil Geography and Earth Surface Dynamics

SGL-80436

Supervisors:

Drs. J. H. J. Candel

Dr. B. Makaske

Cover pictures by:

Britt Albers

Date:

30-08-2019

Acknowledgements

First of all, I would like to express my gratitude towards Jasper for his help and supervision during this thesis. Especially the help with fieldwork and brainstorm sessions were very much appreciated. I would also like to thank my second supervisor Bart for his time, help and sharing of expertise for this thesis. The help of Britt, Fay, Niels and Noortje during the fieldwork was very much appreciated, they made the long and hard days more bearable while their expertise also helped lift some of the weight. Furthermore, I would like to thank Alice and Erna for their assistance in the OSL laboratory and data analysis and Wobbe for his supervision with the texture analysis. Lastly, I would like to thank my parents and grandparents for lending me their cars for the fieldwork and moral support, without them I could not have done this.

Abstract

For centuries rivers have been altered by human interference through canalisation and river management. Recently, many restoration projects have started to return rivers to their natural state to improve the quality of the rivers and their ecosystems. Knowledge of the morphodynamics of these rivers is essential to minimize further management. The stability diagram as presented by Kleinhans and Van den Berg (2011) has some predictive capabilities of the morphodynamics of rivers, but has not been tested and used yet for smaller streams. The stability diagram, which is based on stream power and the median grain size of a river, does not include the bank strength, while this is presumed to be an important factor for the morphodynamics of a river.

To test the predictive capability of the stability diagram, 19 Dutch streams were selected to be investigated and plotted. For each stream a bend was extensively studied in the field and soil descriptions were made of both the inner and the outer bank. Site descriptions were made and soil samples were gathered to test the effect of silt-plus-clay cohesion and vegetation cover on the lateral activity and bank strength. The fieldwork campaign was done to determine any lateral activity for these rivers in order to check them against their position in the stability diagram. Texture analysis of the material in the streambanks was carried out to determine the silt-plus-clay content. A decision table was produced to translate field observations and DEM data into the ability for a stream to laterally migrate. Optically stimulated luminescence (OSL) was used to determine the age of deposition of point bars for a selection of these streams. These data combined with historical maps were used to check the results of the decision table and to correctly indicate the lateral activity of these streams.

The decision table was correct in indicating the lateral activity in 8 out of 9 streams that were dated through OSL and should therefore be usable for other streams as well. Most streams plot within the field of the stability diagram that matches their lateral activity, four streams, however, do not. This cannot be explained by the addition of silt-plus-clay cohesion and vegetation cover. Most Dutch streams are surrounded by coversands which also make up most of their bed and bank material. This makes the silt-plus-clay fraction a less important bank resistance factor within the Netherlands. The presence of organic matter in the banks, either as peat or otherwise, does seem to influence the bank strength and lateral activity of these streams in particular. Three of the four "misplotted" streams were surrounded and probably limited in their lateral migration by peat and organic matter. It is therefore deemed necessary that organic matter in the streambanks is taken into account in the stability diagram.

In conclusion, a significant amount of streams were laterally active. For Dutch streams the stability diagram works rather well as "predictor" already. Organic matter as a source of bank resistance should be added to the stability diagram in order to further improve it for the Dutch streams in particular. The inclusion of the silt-plus-clay fraction or vegetation cover is of less importance for Dutch streams, but should be considered in regions with higher levels of silt and clay.

Table of Contents

1. Introduction

Rivers have been altered by human interference for several centuries (Notebaert and Verstraeten, 2010). Some rivers are able to restore their "natural" state using autogenic restoration. Many streams are, however, limited in their autogenic restoration capabilities through the lack of lateral activity and therefore require help with restoration to a "natural" state (Dépret et al., 2015). Many streams are currently being restored or have been restored in the recent past. In the period of 2010 – 2015 over 2400 km of Dutch streams have undergone some sort of restoration project (Makaske and Maas, 2015). Essential in these restoration projects is knowledge on the morphodynamics of these streams in order to minimize further management (Eekhout and Hoitink, 2014).

Much research has already been done on large lowland river morphological dynamics and evolution. In the Netherlands, rivers like the Rhine and the Meuse have been studied thoroughly due to their effect on the landscape and the Dutch population (Berendsen and Stouthamer, 2002; Gouw and Erkens, 2007; Kleinhans et al., 2011). Less is known about the morphodynamics of smaller lowland rivers and streams and their influence on the landscape. The recent efforts to restore canalised streams have also sparked a need for information on these streams. In-depth studies have already been conducted on particular rivers such as the Overijsselse Vecht (Candel et al., 2018; Quik and Wallinga, 2018), the Dommel (Kamstra, 2018; Kijm, 2018) and the Drentsche Aa (Candel et al., 2017). However, a broader study, investigating and comparing a multitude of smaller rivers and streams is still lacking.

It has been proven difficult to "predict" the morphodynamics of a river by relating just its stream power to the bedload grain size. Discriminators above which certain river patterns, such as meandering or braided, are formed can be established using these two parameters (Van den Berg, 1995). It is, however, still not possible to indicate the exact range where certain patterns can occur within the stability diagram without failure using just these two factors. The stability diagram as presented by Van den Berg has since been extended to include more discriminators for high energy river systems. The dataset was improved by excluding river systems that have been influenced by human alterations and therefore did not meet the requirements of the stability diagram (Kleinhans and Van den Berg, 2011). The diagram was further improved for laterally stable rivers through research on the upper Columbia River (Makaske et al., 2009). Streams and rivers in the lower part of the spectrum are still underrepresented and require extra attention. Makaske stated that the diagram should also work for streams and smaller rivers even though there is a large difference in scale between these and large rivers. Smaller rivers are more likely to be affected by random and mostly local external factors, such as a tree falling in the river, than larger rivers such as the Rhine (Makaske et al., 2016).

A possible improvement on the existing stability diagram (Fig. 1) is the addition of a third parameter or axis that acts as a proxy for the bank erodibility or strength. The stability diagram as presented by Kleinhans and Van den Berg (2011) was not meant to serve as a predictor of channel patterns, but does have some general predictive capabilities. With the addition of this third parameter the stability diagram might function more as a predictor of the channel pattern instead of an indicator of discriminators between channel patterns. Currently only the median grain size (D_{50}) is taken into account, both on the x-axis as well as partly in the formula for the specific stream power through the reference width (Equations 1 and 2). The material of which the streambanks consist is not considered, but does have a profound effect on the stream morphology. Streams in peatlands have highly resistant banks that prevent them from active meandering. They can, however, show a sinuous planform similar to that of a meandering stream due to other processes such as oblique aggradation (Candel et al., 2017). The overall texture of the streambank determines to a certain extent the erodibility of the bank. The silt-plus-clay content of the bank material influences the critical shear stress and thereby bank strength. Another factor is the vegetation cover as roots decrease the erodibility by keeping the soil together (Julian and Torres, 2006; Micheli and Kirchner, 2002).

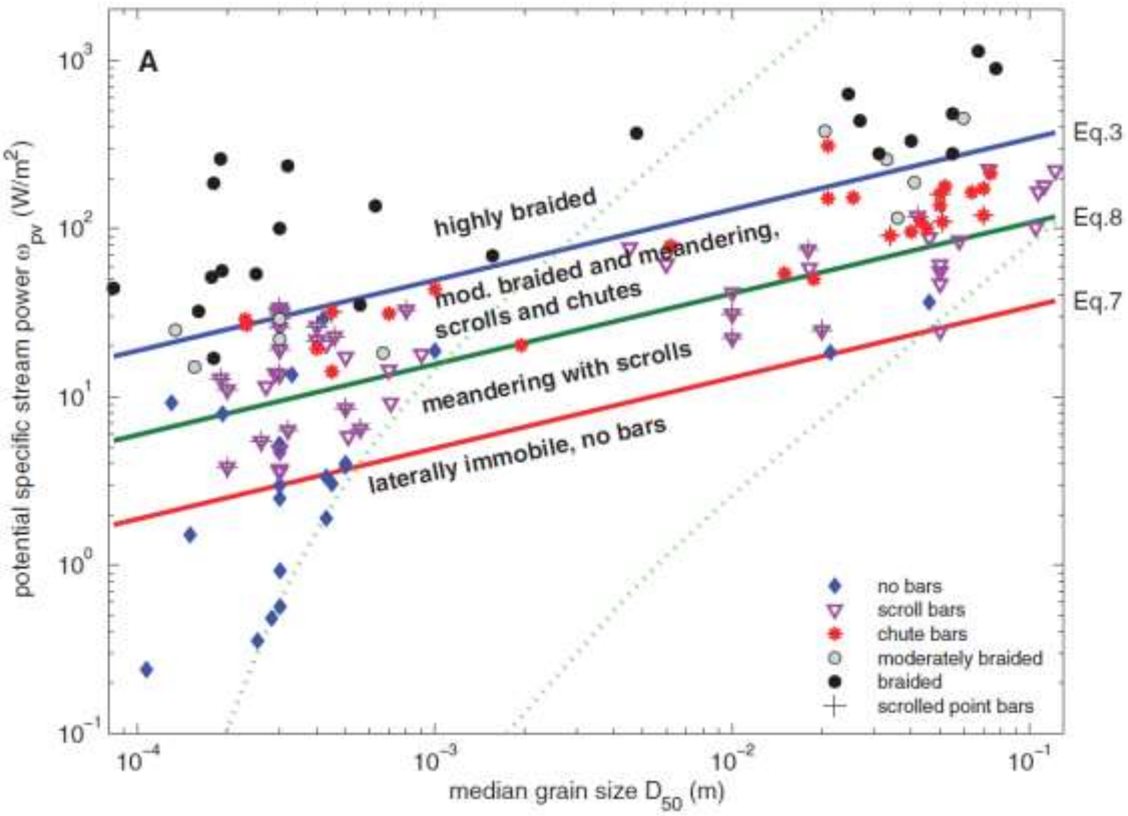

Figure 1. Stability diagram retrieved from Kleinhans and Van den Berg (2011); it shows the potential specific stream power on the y-axis calculated by equation 1 and the median grain size of the bed load on the x-axis.

1.1 Objective and research question

The objective of this research is to get a better understanding of processes and factors that influence the lateral stability in lowland streams. The first objective therefore is to determine whether the streams are laterally active or whether they are laterally stable. After determining the lateral activity, the streams can be plotted in the stability diagram from Kleinhans and Van den Berg (2011) to check whether the lateral activity of the streams matches its position within the diagram. Finally, a bank erodibility proxy as a third parameter/axis can be introduced to the stability diagram, to test if the predictive capabilities of the diagram for channel patterns could be increased. The research questions that follow from this objective are:

- Are the investigated streams laterally active or stable and how could this be deduced?

- Could the stability diagram be used as a predictor for channel patterns in Dutch lowland streams?
- Should a bank erodibility parameter be included in the stability diagram to increase the predictive capabilities of the diagram?

The hypothesis here is that the lateral activity of the streams can be deduced using a combination of field observations and digital elevation model analysis. These findings can be tested using historical map analysis of the last century and by dating the point bar material to check whether the lateral activity is recent.

The hypothesis regarding the use of the stability diagram is that the stability diagram functions similarly for the lowland streams as for the larger rivers used by Kleinhans and Van den Berg (2011). It has some predictive capabilities, but can mostly be used to indicate the discriminators above which certain channel patterns start to occur (Van den Berg, 1995). Focus will mainly be put on the discriminator between meandering and laterally immobile since most streams plot in the lower fields of the stability diagram.

The final hypothesis is that the predictive capabilities of the diagram will indeed increase with the addition of the bank erodibility parameter. The erodibility of the bank plays an important role in the morphodynamics of the stream and cannot be excluded if a prediction is to be made. It will be unlikely that the addition of the erodibility factor will result in a perfect predictor for channel patterns since many smaller factors are at play, influencing the stream morphology. This will, however, be a step in the direction of a better understanding of stream morphology and possibly towards a usable predictor for channel patterns.

2. Theory

2.1 Stability Diagram

The stability diagram (Fig. 1) as retrieved from Kleinhans and van den Berg (2011) plots the bedload of a river against its potential specific stream power in order to relate these features to the morphodynamics of the river. These morphodynamics are a result of the balance between driving forces of erosion, such as those caused by the channel gradient and discharge, and erosion resisting forces, such as bed and bank resistance to transport (Makaske and Maas, 2015). Stream power is a measure of these main driving forces and is closely related to the ability of a river to perform geomorphic work. It has been widely used to assess channel geomorphic patterns and (sediment) transport (Bizzi and Lerner, 2015; Ferguson, 2005). Resisting forces are on the other hand mainly related to the sediment diameter (D_{50}), floodplain and channel characteristics that determine bank stability, such as the nature of the bank material and the presence of cohesive material. Variations within these driving and resisting forces result in various river patterns and morphologies that form a continuum (Robert, 2003). This continuum is partly plotted in the stability diagram, only the largest contributors to the driving (channel gradient and discharge) and the resisting forces (D_{50}) are plotted.

The potential specific stream power (ω_{pv}) that is used in the stability diagram is calculated by the following formula:

$$\omega_{pv} = \frac{\rho\, g\, Q\, S_v}{W_r} \tag{1}$$

Where:

ω_{pv}	= potential specific stream power	[W/m^2]
ρ	= water density	[kg/m^3]
g	= gravitational constant	[m/s^2]
Q	= channel forming discharge	[m^3/s]
S_v	= valley slope	[-]
W_r	= width of the reference channel	[m]

The water density is kept constant at 1000 kg m^{-3} and the gravitational constant at 9.81 m s^{-2}. The channel forming discharge is either the mean annual flood or, if this is not available, the bankfull discharge. If both discharges are available the, priority is given to the mean annual flood since it is less dependent on the channel pattern and for its reliability compared to the bankfull discharge (Kleinhans and Van den Berg, 2011).

The width of the reference channel is predicted to remain independent of the actual river width, which is affected by the river pattern. The width of the reference channel can be calculated using the following formula:

$$W_r = \alpha\, Q^b \tag{2}$$

Where α = 4.7 $\sqrt{s\ m^{-1}}$ for sandy rivers with a D_{50} that is smaller than 2 mm and α = 3.0 $\sqrt{s\ m^{-1}}$ for gravel bed rivers with a D_{50} that is larger than 2 mm. The exponent of the channel forming discharge (*b*) shows little variation and is typically equal to 0.5 according to Van den Berg (1995). This can be deduced using the hydraulic geometry equations which will not be explained in this thesis, but can found for further detail in the paper of Leopold and Maddock (1953).

Within the stability diagram three main types of river patterns are mentioned: laterally immobile, or stable rivers (Fig. 2A and B), meandering rivers (Fig. 2C) and braided rivers (Fig. 2D). Patterns of stable rivers can be rather similar to those of meandering rivers since they can be quite sinuous and are therefore hard to distinguish by merely looking at the river pattern. Laterally stable rivers often have a relatively deep channel compared to the width and can usually be found in flat regions where the small channel gradient results in a small stream power (Makaske and Maas, 2015). Meandering rivers are characterised by a regular pattern of bends that migrate laterally by erosion of the outer bank and sedimentation on the inner bank causing the formation of point bars, which are lacking in stable rivers(Kleinhans and Van den Berg, 2011). Usually these rivers are wider and more shallow than stable rivers (Makaske and Maas, 2015). Both the stable rivers and the meandering rivers often only have one channel (unless they are anabranching as seen in Figure 2), braided rivers, however, are characterised by more (sub-)channels. These sub-channels are divided by sand and gravel banks that slowly grow, causing the channels to migrate. This type of river is relatively shallow compared to its width and requires a very large potential stream power (Makaske and Maas, 2015).

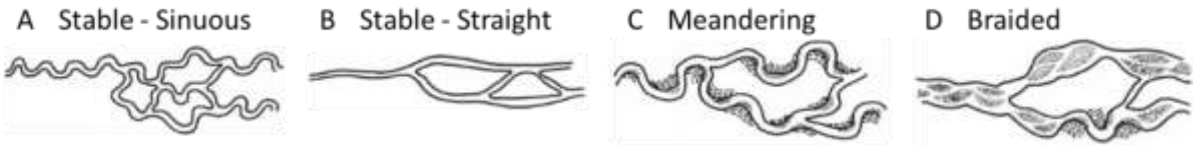

Figure 2. Channel patterns in both single channel and anabranching forms (where they split into multiple channels). As adapted from Nanson and Knighton (1996).

Within the stability diagram, no distinction is made between the different types of stable rivers. However, within the diagram as taken from Kleinhans and Van den Berg (2011) there is a separate field in the diagram that distinguishes between braided and meandering systems, an intermediate field. All fields above the laterally immobile field are those of laterally active rivers. The distinction between laterally active and laterally stable is where the focus of this study lies.

For a river to be able to be plotted in the original stability diagram it has to comply with several conditions. The river has to be in equilibrium, it should not be actively incising, nor should it be rapidly aggrading, and the flow should be perennial. Furthermore, the bankfull or mean annual discharge should be above 10 $m^3\ s^{-1}$ and the D_{50} should be between 0.1 and 100 mm (Van den Berg, 1995). It was, however, assumed by Makaske et al. (2016) that the diagram also applies to smaller rivers and streams (< 10 $m^3\ s^{-1}$). Finally, the rivers should be in a natural state and should not be affected by anthropogenic activities (groynes, dams, roads, etc.).

2.2 Critical shear stress

Within the stability diagram, the driving forces of lateral movement (channel gradient and discharge) are represented by the potential specific stream power and the resisting forces (bed and bank resistance to transport) are partly represented by the D_{50}. The bank strength is left out of the diagram, while this strength has a significant effect on the ability of a river to move laterally (Julian and Torres, 2006). There are several factors that influence the strength, or erosion resistance, of a river bank. Vegetation can increase the bank strength (Thorne, 1990) and should therefore be taken into account. Cohesive materials such as silt and clay increase the bank stability (Julian and Torres, 2006). The presence of organic material can also cause an increase in bank strength as is the case with peat banks, which are highly erosion resistant (Candel et al., 2017; Nanson et al., 2010). The critical shear stress (τ_c) is a measure of the minimum shear stress required for sediment movement and is often used as a measure for the bank strength. This is also the parameter that is used in the paper of Julian and Torres (2006), which combines the silt-plus-clay content (fraction < 63 µm) and vegetation cover of the banks to calculate the critical shear stress.

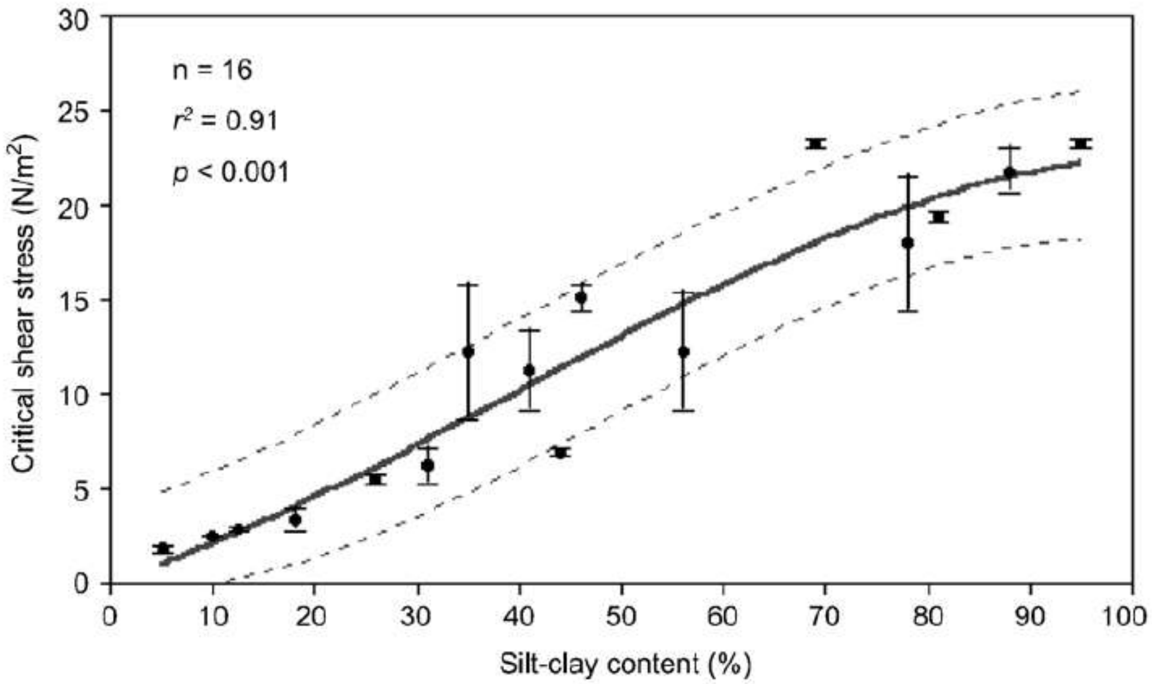

Figure 3. Critical shear stress estimate from the silt-clay content (Julian and Torres, 2006).

The relation between the silt-plus-clay (or silt-clay in Figure 3) content and the critical shear stress as seen in Figure 3 is based on work by Vanoni (2006) and data from Dunn (1959). A third-order polynomial trend line is applied to these data under the assumption that a maximum τ_c value is reached at a silt-plus-clay content of 100% and a minimum τ_c value at 0%. At 0% silt-plus-clay the corresponding τ_c value is 0.1 N/m^2, since this is the lower limit of the Shields curve (Julian and Torres, 2006; Shields, 1936). The resulting equation that is used in Figure 3 is:

$$\tau_c = 0.1 + 0.1779 * SC\% + 0.0028 * SC\%^2 - 2.34 * 10^{-5} * SC\%^3 \qquad (3)$$

Where SC% is the silt-plus-clay content (< 63 μm) of the bank in percentages. To account for the vegetation on the banks, coefficients were used to indicate the increase in τ_c per type of vegetation cover (Table 1). This τ_c coefficient for vegetation can be included in Equation 3 by multiplying the right hand side of the equation by the coefficient. Only four main vegetation covers were used in the paper of Julian and Torres (2006), a fifth one was added based on research on river dike vegetation communities by Vannoppen et al., (2016). Dikes with nettle communities were on average twice as susceptible to erosion as those solely containing grass. The τ_c coefficient for nettle vegetation is therefore set at 1.49 (Table 1). The organic matter content is not directly taken into account within this equation, while it is still a source of soil cohesion that grants the river banks extra strength (Daniels, 1971; Zhang and Hartge, 1990).

Table 1. Critical shear stress coefficients to account for vegetation (adapted from Julian and Torres, 2006)

Bank Vegetation	τ_c Coefficient
None	1.00
Nettles	1.49
Grassy	1.97
Sparse Trees	5.40
Dense Trees	19.20

2.3 Optically Stimulated Luminescence

Optically Stimulated Luminesce, also known as OSL, dating is a relatively new technique that allows age determination of sediments that are usually hard or impossible to be dated using other dating techniques (Wallinga, 2002). OSL has already been widely applied to determine the age of deposition in fluvial deposits (e.g. Candel et al., 2018; Quik and Wallinga, 2018) as well as aeolian (e.g. Bateman and Van Huissteden, 1999; Yang et al., 2018) and colluvial deposits (e.g. Poreba et al., 2015; Preusser et al., 2011). For fluvial deposits the most precise dating technique is still radiocarbon dating, but in-situ organic material, which is needed for ^{14}C dating, is often lacking and the organic material that is present in fluvial sediments is often reworked (Stanley and Hait, 2000; Wallinga, 2002). The sand sized mineral grains, needed for an age determination through OSL, are typically present in fluvial sediments.

OSL dating relies on the measurement of a low intensity light signal that is released from feldspar and quartz minerals upon exposure to light or heat. This light signal originates from energy trapped in defects in the crystal lattice of the minerals. The energy is accumulated over time as the minerals are exposed to natural ionising radiation from radionuclides that are naturally occurring (such as ^{40}K and constituents of the uranium and thorium decay chains) and cosmic radiation from space (Preusser et al., 2008). The energy in the mineral grains slowly accumulates as long as they remain buried and are not heated above the threshold of a couple of hundred degrees centigrade. Once the mineral grain is exposed to heat or light (e.g. during transport or erosion) the accumulated energy is released as a luminescence signal (Cunningham and Wallinga, 2012). The intensity of this signal can be measured and is known as the paleodose. If the mineral grains are exposed to enough light or heat the grains will be bleached and their luminescence signal will reduce to a base level (bleaching) often close to zero. If the mineral grain is buried after bleaching, energy can accumulate again as the process is repeated (Fig. 4). The paleodose is therefore a measure for the total amount of ionising radiation that the mineral grain was exposed to since its last (full) exposure to daylight, which is the age of burial (Wallinga, 2002).

One of the most common problems for dating sediments through OSL is partial bleaching, especially for dating fluvial sediments (Preusser et al., 2008; Wallinga, 2002). The relatively short transport times and often murky water can cause the OSL signal to not be completely reset in all grains, leading to an age overestimation (Fig. 4). This is especially a problem in young sediments as the overestimation can be considerable. Fluvial sediments often consist of a mixture of poorly and well bleached grains, resulting in a wide range of ages. By limiting the size of the aliquots, the individual luminescence signals of grains will become more apparent, instead of the averaged signal of multiple grains. The individual signals can be separated, ideally resulting in a bimodal distribution of the ages. A bootstrapped minimum age model can be applied, which assigns more weight to lower values as it assumes that these are more representative for the actual age (Galbraith et al., 1999).

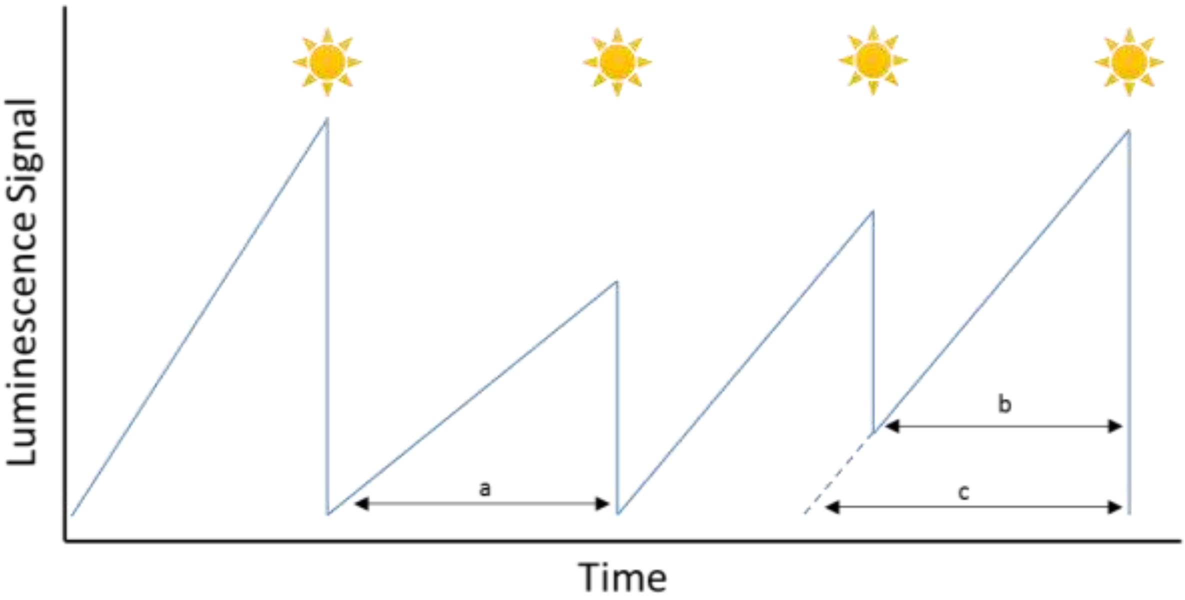

Figure 4. The build-up of a luminescence signal of a single quartz grain over time, slowly building up until it is exposed to sunlight. The signal is completely bleached for situation (a), where span (a) represents the actual age and the luminescence age. Situation (b) represents a situation where the signal is poorly bleached. The span (b) represents the actual age and span (c) represents the luminescence age.

The rate at which the paleodose is accumulated over time, is also known as the (environmental) dose rate. This dose rate consists of three different components: cosmic radiation, external radiation and internal radiation. The magnitude of cosmic radiation depends on the location and altitude due to the variation in Earth's magnetic field and absorption by the atmosphere. The magnitude of the cosmic radiation also depends on the overburden on the sample by both sediments and water, which can shield the sample from the radiation (Preusser et al., 2008). In order to estimate the contribution of the cosmic radiation it is essential to know whether the sample was gradually buried by sedimentation until it reached the depth at which it was sampled, or whether the burial was "instant". For the point bar deposits the burial was assumed to be instant because point bars have lateral accretion surfaces and are deposited approximately at the same depth as they are sampled. The external radiation comprises all radiation from surrounding sediments within a radius of approximately 30 cm that may contain radionuclides such as ^{40}K and constituents of the uranium and thorium decay chains. The moisture content of the sediment is of great importance for the calculation of the external dose rate since the attenuation of radiation is greater in water than in air. The internal radiation is radiation that originates from radioactive elements within the crystal lattice of the mineral grain, which is assumed to be negligible in quartz grains compared to the other components of the environmental dose rate (Preusser et al., 2008).

In order to calculate the age of the sediment since its burial, the following equation should be used:

$$Luminescence\ age\ [yr] = Paleodose\ [Gy]/Dose\ rate\ [Gy/yr] \quad (4)$$

The paleodose can be calculated by exposing the mineral grains to blue LEDs and heating them simultaneously. Once exposed to the blue light the stored energy will be released and a luminescence signal can be measured, the natural luminescence signal. The mineral grains will be bleached after exposure to the blue light and a test dose can be given to the mineral grains by exposing them to a Strontium/Yttrium Beta source. Energy is accumulated in the grains at a much higher rate than in nature. At a certain time interval the exposure can be stopped and a new luminescence signal can be measured by exposing the grains to heat and the blue LEDs. This generated luminescence signal is also known as the test dose luminescence signal. This process can be repeated a multitude of times and the duration of the exposure can be regulated, thereby creating luminescence signals of different magnitudes. This includes one recuperation measurement, where the mineral grains are bleached and are not exposed to the Beta source. No charge should be accumulated, therefore the luminescence values here should be close to zero. The process is repeated until the test dose luminescence signal exceeds the natural luminescence signal. The natural signal can then be compared to the test dose signals and the paleodose can be interpolated from these data.

2.4 Study Area

All sampled streams were picked from a lowland stream database that was gathered for the STW funded RiverCare project. The streams are considered to be natural in at least part of their course, usually in a nature reserve where the natural course remained unaltered. These streams were selected because their discharge data were readily available and because they satisfy the conditions posed by Kleinhans and Van der Berg (2011) for streams and rivers to be plotted in the stability diagram. These natural stretches of the stream course are also the locations where the streams were sampled (Fig. 5A). Many of these streams have been canalised in other parts of their course. Most streams are also bordered by areas where water drainage is managed through ditches (Table 2).

All except one of the streams are located in the Dutch physical geographical zone of higher sand areas, landscapes that are dominated by coversands (Fig. 5B). Only the Geul, located in the province of Limburg, can be found in a different physical geographical zone: hilly land, a zone that is dominated by loess and exhibits larger variations in altitude than other parts of the Netherlands (Fig. 5B). Even though most streams are located within the same geographical zone, they are mostly different as to stream valley fill (peat or clastic fluvial material), length and their surrounding geomorphological features (Table 2). Some of these features are explained in the following section, where all streams are shortly introduced. Information on the surrounding geomorphological features and the valley fill of the streams was gathered from the 1:50.000 Dutch Geomorphological Map. Digital Elevation Models (DEMs) of every sample location of the streams can be found in Appendix III.

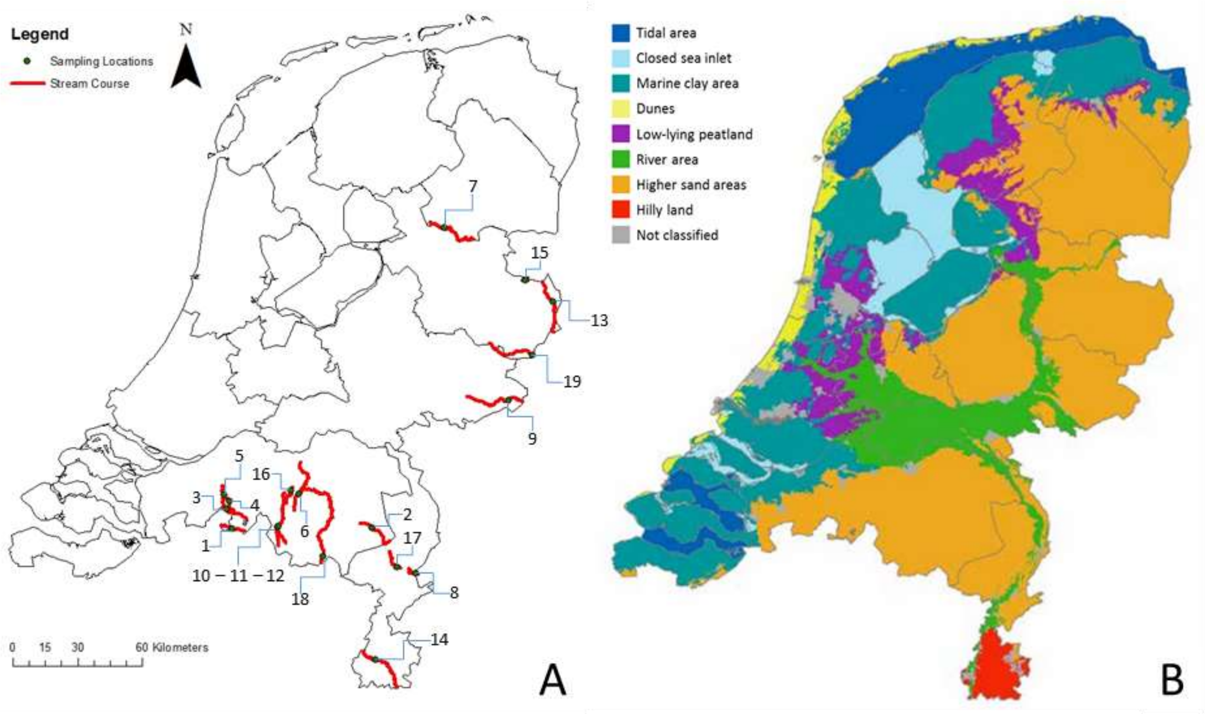

Figure 5. A: Locations of the sampled streams and their stream courses within the Netherlands. The streams are numbered, the numbers remain constant throughout this thesis. B: The physical geographical zones of the Netherlands (adapted from Makaske and Maas, 2015).

Het Merkske (1)
Het Merkske makes up part of the national border of the Netherlands and Belgium, it is located partly in the provinces of Antwerp and North Brabant. Most of the stream valley is filled or covered with peat and surrounded by coversand ridges. The stream has never been canalised and shows a sinuous planform. Some old oxbows can still be distinguished on the DEM. After about 17 km the stream eventually discharges into the river Mark.

Astense Aa (2)
The stream valley of the Astense Aa is located between coversand ridges in the north of the province of Limburg. Most of this stream was canalized in the 1960s, but a limited reach of the stream is located in a nature reserve where the stream remained unaltered and still retains its highly sinuous planform. Old oxbows can still be distinguished on the DEM. The stream is approximately 20 km long and discharges in the canal South Willemsvaart.

Strijbeekse Beek (3)
This is another stream that makes up the border between the Netherlands and Belgium, located in the provinces of Antwerp and North Brabant. The stream valley is filled with peat and the surrounding area is quite marshy. Coversand ridges border the stream valley on both sides. Multiple smaller and some

larger fens can be found in close proximity to the stream. The stream discharges into the river Mark after about 14 km.

Chaamse Beek (4)

The Chaamse Beek is located in the west of the province of North Brabant and discharges into the river Mark. The stream is approximately 10 km long and flows through an area with large stretches of coversand and coversand ridges. Parts of the stream course have been canalised, but recent efforts have been made to restore the original sinuous course. Old oxbows can still be distinguished on the DEM along the current channel.

Bovenmark (5)

The Bovenmark has largely been canalised in the last century, many old meanders are however still intact and are located close to the new river channel. The surrounding area is mainly dominated by coversand (ridges) and the stream valley still clearly retains characteristics of the old sinuous character of the river with both point bar deposits and peat infill. The Bovenmark is about 21 km long and streams through the city of Breda, after which it is called the Mark.

Beerze (6)

The Beerze originates at the convergence of the Grote and Kleine Beerze and flows through North Brabant for approximately 14 km where it eventually discharges into the river Dommel. The area surrounding the Beerze shows large influences of (peat) reclamation. The stream valley of the Beerze is surrounded by plains and ridges of coversand. The stream itself has been canalised over large parts of its course and some bypass canals have been constructed, yet some original sinuous parts still remain. Efforts already have been made to restore the original (sinuous) course of the river.

Reest (7)

The Reest is a stream that makes up part of the boundary between the provinces of Drenthe and Overijssel. Due to difficulties with the planological effects of canalisation, this stream has never been canalised. It flows through a peat filled stream valley and environment that is only flanked by coversand ridges halfway downstream. The stream course is around 37 km long, it discharges into the canal Meppelerdiep.

Swalm (8)

The Swalm is a tributary of the Meuse River that originates in Germany, but also flows through the province of Limburg over its course of approximately 45 km. It has largely maintained its natural sinuous character in the Dutch part of its course. The Dutch part of the stream valley is still characterised by meander ridges, oxbow remnants and local peat infill (of the oxbow remnants). The area surrounding the Swalm stream valley can be characterised by terrace deposits of the Meuse River.

Bovenslinge (9)

The Bovenslinge is a stream that has its origin in Germany and crosses the Dutch border into Gelderland where it eventually discharges into the Oude IJssel as the Bielheimerbeek. Some parts of the 55 km long course have been canalised, but some natural parts of the river course can still be found in nature reserves. The natural river valley is characterised by meander ridges and is bordered by large stretches of coversand.

Reusel (10)

The Reusel is located in the south of the province of North Brabant, most of its 10 km course has been canalised apart from the last kilometre. Here it enters a nature reserve where it has remained mostly unaltered, but is surrounded by ditches used for land reclamation. The stream valley is surrounded by areas of cover sand and coversand ridges.

Raamsloop (11)

The Raamsloop is a stream located slightly eastward of the Reusel, of which it is a tributary. Like the Reusel, the Raamsloop is also mostly canalised apart from the last kilometre of its 12 km course. The Raamsloop is also surrounded by ditches used for land reclamation. The stream valley of the Raamsloop is quite broad, especially in the region close to the conversion point with the Reusel. The valley is surrounded by areas of coversand and coversand ridges.

Reusel + Raamsloop (12)

This stream is also called the Reusel, however this lower part of the stream is investigated separately. After about 18 km the Reusel discharges into the Achterse Stroom, which eventually discharges into the river Dommel. Once the Reusel and the Raamsloop merge, the width of the stream valley decreases. The stream valley shows signs of lateral activity as oxbows and meander ridges that can be easily distinguished on the DEM.

Dinkel (13)

The Dinkel is an 89 km long tributary of the river Vecht that originates in Germany and crosses the border with the Netherlands to the province of Overijssel. The river valley is enveloped in areas of coversand, including coversand ridges. The river valley clearly shows signs of lateral migration with multiple oxbows and meander ridges scattered in the valley. Recent lateral activity can be found in the area of the nature reserve Lutterzand. A bypass canal has been constructed just downstream of Lutterzand.

Geul (14)

The Geul originates in Belgium, but crosses the border in the south of Limburg where it discharges in the Meuse River after 56 km. It is the only investigated river that is not found in the physical geographical zone of higher sand areas, but in the hilly land. The sediments in the stream valley of the Geul are mainly clay and loam, while the river bed consists mainly of gravel. The stream valley is bordered by steep walls and terrace plateaus of the Meuse River. Parts of the Geul have been canalised in the past, but some river restoration projects have already taken place. Oxbows can be distinguished on the DEM along some stretches of the river. Lateral migration is actively taking place at most parts of the river course.

Mosbeek (15)

The Mosbeek is a somewhat smaller stream, with a total stream course of only 2 km, that flows down the ice-pushed ridge of Ootmarsum in the east of Overijssel near the German border. The stream valley in which it flows is most likely a remnant of melt water incision, as the valley is very wide relative to the stream. The material surrounding the stream is a mix between coversand and coarser material from the ice-pushed ridge.

Rosep (16)

The Rosep is a stream that is located in the province of North Brabant, where it is canalised in the upstream area. Downstream it flows through nature reserve Kampina where it has maintained a natural course. After 10 km it discharges into the Essche stroom, a tributary of river the Dommel. The stream valley is located between some large coversand ridges and is quite wide in nature reserve Kampina, where it is mostly filled with peat.

Roggelse Beek (17)

The Roggelse Beek (also known as the Zelsterbeek) is a 12 km long stream located in the province of Limburg. It merges with the Leubeek to create the Neerbeek, a tributary of the river Meuse. It has largely been canalised in the past, but the natural course has been maintained in the nature reserve Leudal. Here some oxbows can still be distinguished in the river valley that is bordered by steep coversand ridges in the south.

Dommel (18)

The Dommel is a river that has its origin in Belgium, but mainly flows in the province of North Brabant. It discharges into the Dieze, a tributary of the river Meuse, after 120 km. The Dommel streams through multiple nature reserves, one of which is the Malpie (the area of focus for this research). Here the Dommel flows in a river valley consisting of a mix of peat, loam and coversands. The stream valley is bordered on both sides by coversands. Large parts of the course of the river Dommel have been altered or canalised over the years.

Buurserbeek (19)

The Buurserbeek, also known as the Ahauser Aa in Germany and the Schipbeek further downstream is a tributary of the river IJssel. The Buurserbeek has a stream course of approximately 81 km of which large parts have been canalised in the past. However, for some parts of the river the original course of the river is being restored. Near the border with Germany the stream flows down an ice-pushed ridge that has been covered with coversands.

Table 2. Summary table of all streams and characteristics of the area surrounding the sampling point. Stream valley fill and geomorphology are based on the PDOK geomorphological map (1:50.000) of the Netherlands.

Name	Oxbow Remnants	Surrounding drainage	Stream length (km)	Stream valley fill	Geomorphology of surrounding area
Het Merkske	Yes	Yes	17	Covered or filled with peat	Curved terrace deposits with coversand (ridges)
Astense Aa	Yes	Yes	20	Filled with fluvial sediments	Coversand (ridges)
Strijbeekse Beek	No	Yes	14	Covered or filled with peat	Curved terrace deposits with coversand (ridges)
Chaamse Beek	Yes	Yes	10	Filled with fluvial sediments	Plain of terrace deposits, filled or covered by coversand (ridges).
Bovenmark	Yes	Some	21	Meander ridges and gullies	Curved terrace deposits (E) with coversand (ridges) (W)
Beerze	No	Yes	14	Filled with fluvial sediments	Curved coversand deposits and ridges
Reest	No	Yes	37	Covered or filled with peat	Coversand (ridges) (S) and plains of meltwater deposits (N)
Swalm	Yes	Close to river	45	Meander ridges and gullies	Fan like structure and terraces, covered with sandy loess or coversand
Bovenslinge	Yes	Little	55	Meander ridges and gullies	Coversand (ridges)
Reusel	No	Yes	10	Filled with fluvial sediments	Curved terrace deposits with coversand (ridges)
Raamsloop	No	Yes	12	Filled with fluvial sediments	Curved terrace deposits with coversand (ridges)
Reusel + Raamsloop	Yes	Yes	18	Filled with fluvial sediments	Curved terrace deposits with coversand (ridges)
Dinkel	Yes	Little	89	Meander ridges and gullies	Coversand (ridges)
Geul	Yes	Very little	56	Filled with fluvial sediments	Overall loess cover and rocky valley sides with gullies
Mosbeek	Too small	Very little	2	Sediments of the ice-pushed ridge	Ice-pushed ridge covered with coversand (ridges)
Rosep	No	Yes	10	Covered or filled with peat	Coversand (ridges)
Roggelse Beek	Yes	Yes	12	Filled with fluvial sediments	Coversand ridges and valley terrace plain deposits covered with coversand
Dommel	Some	Yes	120	Covered or filled with peat	Curved terrace deposits with coversand (ridges)
Buurserbeek	Some	Some	81	Filled with fluvial sediments	Ice-pushed ridge covered with coversand (ridges)

3. Methodology

3.1 Lateral Activity Determination

In order to answer the first research question on whether the investigated streams are laterally active or inactive, several features had to be studied. First of all, fieldwork was conducted to check for indicators of lateral activity. A Digital Elevation Model (DEM) of every stream was analysed for the presence of oxbows and clear point bars. All information found during the fieldwork and the analysis of the DEMs was combined into a decision table where the lateral activity of the streams was determined. The results of the decision table were then checked by dating some of the point bar sediments using Optically Stimulated Luminescence (OSL) and by studying historical maps from the past century. All these methods, needed to answer the first research question, are elaborated on in the following sections.

3.1.1 General Field Description

Before heading into the field, sampling locations or areas were chosen based on accessibility. Geomorphological maps and soil maps were studied to gain a better understanding of the area and to get a slight grasp of what to expect in the field. These findings were later checked with the actual findings in the field. In general, the sampling locations were chosen to be at a stream bend that had a chance of being laterally active, while still being representative for the entire stream.

At each sampling location a general description of the area around the stream was made using a special field form (Appendix I). Any features that could indicate lateral migration of the stream were noted down, such as difference in bank height, erosion along the streambanks, and exposed tree roots along the streambanks. The dominant soil type (sand, clay or peat) and the vegetation cover were noted down for both sides of the stream, as well as the dimensions of the stream itself. The vegetation cover categories are similar to those suggested in the paper by Julian and Torres (2002), either no vegetation, grassy, sparse trees, or dense trees. Additional information about the vegetation type and the abundance of nettles was also added. The stream width was measured from bank to bank, the stream depth was measured in the middle of the stream from streambed to the height of the bank. The height of the water level was also noted down at this location.

On both sides of the stream along the apex of the bend (Fig. 6), a detailed description of the soil was made. For coring, two types of instruments were used. An Edelman auger with a set of extension pieces was used for coring above the groundwater level. Additionally a Van der Staay suction corer (Van der Meene et al., 1979) was used to core beneath the groundwater level to a maximum depth of 4.20 m. Due to the sheer length of the Van der Staay suction corer, it could not be brought to all sampling locations. In these cases, the Edelman auger was also used for coring beneath the groundwater level. In peat-rich soils a gouge auger was used. A detailed soil description was made of the top 1.20 m of the soil at the indicated soil description locations (Fig. 6). The soil description was made using the field form (Appendix I) and the soil classification was made according to the Dutch Soil Classification system (Ten Cate et al., 1995). This description mainly focussed on the soil formation on either side of the stream. For every soil horizon the following information was noted down on the soil description form:

- Soil horizon according to the Dutch Soil Classification system, this includes the presence of iron oxidation and reduction mottles as well as presence of organic matter.
- The dominant soil texture
- Colour of the soil in moist condition according to the Munsell Soil Colour booklet (Munsell Color, 2009).
- Additional information such as the presence of layering, fibres, charcoal, etc.

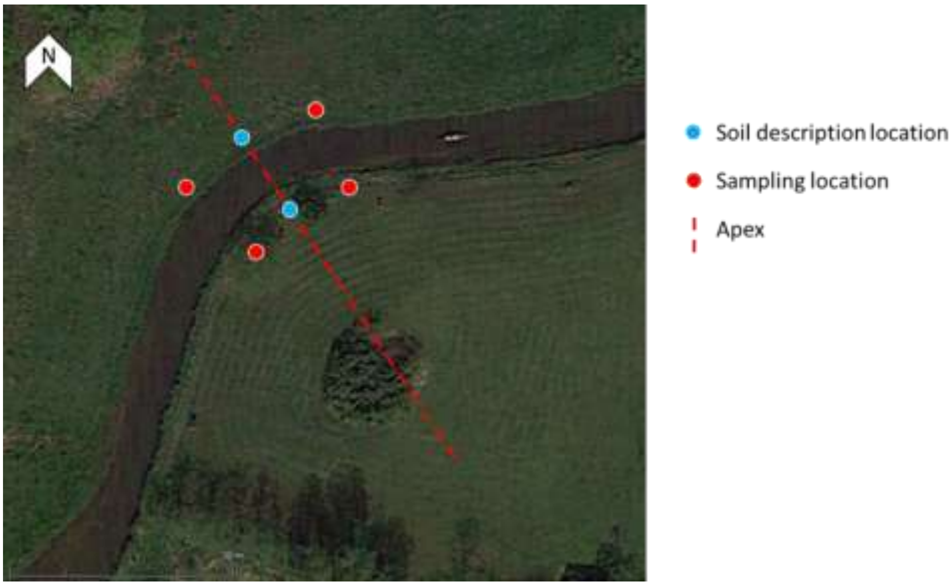

Figure 6. Sampling locations for texture measurements; example is from the Dommel.

Apart from the soil description per horizon also a description of the sediment per 10 cm was made following Berendsen and Stouthamer (2001). This description mainly focussed on the texture of the material and the presence of thin layers of differently textured material and thin organic layers. The sediment was described to a depth that was ideally greater than the stream depth. For every 10 cm of soil the following information was noted down on the soil texture form (Appendix I):

- The dominant texture
- The type and amount of organic material
- The colour (not as precise as done before with the Munsell Soil Colour booklet)
- The percentage of gravel, if this was present
- The presence of iron oxidation or reduction mottles
- The highest level of groundwater that was reached in recent years (GHG), and the lowest level of groundwater reached in recent years (GLG), deduced from zones of iron oxidation and reduction
- Additional information such as the presence of layering, fibres, charcoal, etc.

All texture descriptions were done using the Dutch classification system as used in the soil description program Low Land Genesis (LLG), the approximate matching USDA terminology as provided by LLG is used in this paper. Using a sand ruler the median of the sand fraction was determined as one of the categories: extremely fine sand (50 µm – 105 µm), very fine sand (105 µm – 150 µm), fine sand (150 µm – 210 µm), medium sand (210 µm – 420 µm) and (very) coarse sand (420 µm – 2000 µm) (De Bakker and Schelling, 1989). In the field the other texture classes (these can be found in Figure 7) were determined by comparison of relative loam content with known textures. The texture triangles (Fig. 7A and B) as found on the help page of LLG 2012, based on the texture triangles as originally defined by De Bakker and Schelling (1989), were used to check the categorisation that was made in the field.

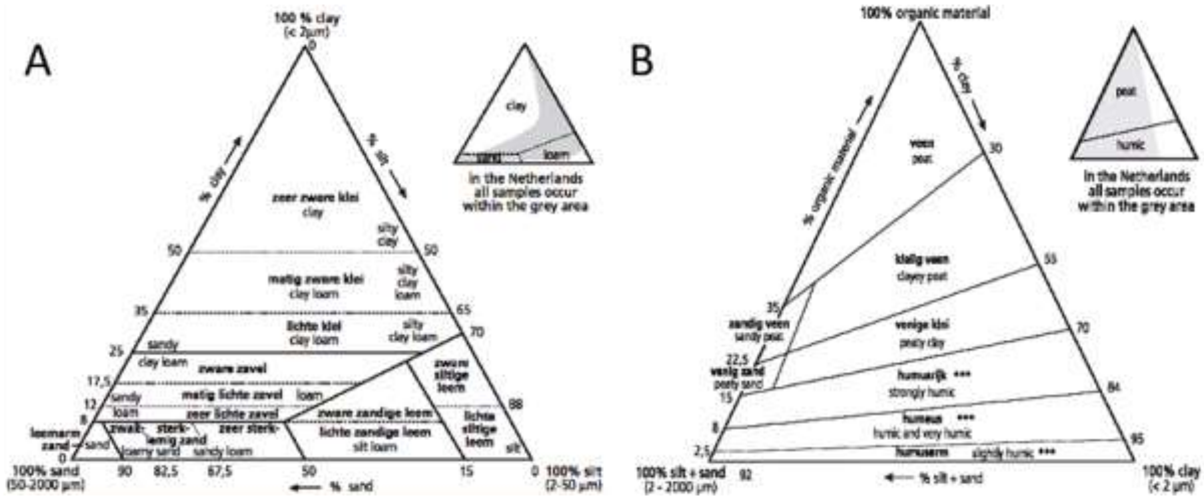

Figure 7.Texture triangles used during the fieldwork. A. Clastic material dominated and B. Organic material dominated. Adapted from the LLG 2012 help page (De Bakker en Schelling, 1989)

Regarding organic material in the soil, a distinction was made between mineral soils containing organic matter and organic soils containing a mineral component. The latter was categorised in one of five classes based on the relative abundance of a mineral component in the peat. These categories are peat, peaty clay, peaty sand, sandy peat and clayey peat (Fig. 7B). In cases where the dominant texture was mineral, the organic component was categorised as a certain degree of humic content, ranging from strongly humic to slightly humic (Fig. 7B). Based on the findings in the field and the visualisation of the data in LLG, a relative ranking of the organic matter in the outer bends was made to see if there is a relation between stream activity and organic matter content (Section 3.2.3). All data that were gathered through the coring and soil description were entered into LLG to visualise the soil columns.

3.1.2 Decision Table

The activity estimation is based on the six characteristic features: erosional features, organic layering, oxbow remnants, a fining upward sequence, peat in the outer bank and cross-sectional asymmetry. The presence or absence of these features was determined for every stream and summarized in the decision table. All features and the used methods to inspect them will be shortly introduced in the following paragraphs. The different features are all given a weight in the decision table based on how predictive they are considered to be for current lateral activity. The weights are elaborated on after the introduction of the features.

Erosional features

During the fieldwork campaign all streams were checked for erosional features such as exposed tree roots, fallen trees or bank undercutting. Erosion is mostly affecting the outer bank of the river where a steep scarp surface can be created. Of all features that may give indications of lateral activity, this is the most indicative of current lateral migration and therefore carries the largest weight in the decision table. Without erosion, it is very unlikely that a stream is currently laterally active. In the decision table the presence of erosional features per stream is indicated, the degree of active erosion is however not indicated.

Organic layering

Organic layering within the soil can be an indication of Holocene point bar deposits, where the deposition of clastic material is alternated with formation of organic material on the inner bend resulting in lateral accretion surfaces (Kamstra, 2018; Kijm, 2018). Often these types of sediments contain reworked (and intact) plant remains throughout the deposit. The layering can be hard to distinguish while using an Edelman auger, since the structure of the soil is affected by the auger. Ideally the Van der Staay suction corer was used, because then the layering of the deposit remains mostly unaffected. It was not possible to bring the van der Staay corer to every stream due to logistical reasons, in these cases a gouge was used to distinguish the organic layers within the deposit. Within the decision table the presence of organic layering on the inner bank is indicated. Cases where organic layers can only be found on the outer bank are also indicated in the table. In these cases the organic layering is taken out of consideration for the activity reasoning, since it is present, but not where it is expected.

Organic layering found within the banks is a good indication of the presence of lateral activity of the streams. This layering, in combination with a fining upward sequence, could indicate the presence of a point bar. However, the presence of these layers does not directly indicate current lateral activity, as the deposit could be old. These were therefore the layers that were dated using the OSL technique (Section 3.1.3) to get an indication of the recentness of the formation of the "point bar".

Oxbow remnants

The 0.5 m resolution DEM was studied closely to distinguish potential oxbows near the sampling points. The locations of some of these oxbows were checked within the field for naturalness since it can be hard to distinguish oxbows created by natural lateral migration from oxbows created by anthropogenic alterations such as canalisation or artificial bend cut-off.

Some streams show clear signs of migration throughout their stream valley with multiple abandoned channels on either side of the current channel. The topography within the valley and especially the inside of the bends is often undulating, indicating the existence of a point bar. This type of stream valley topography clearly indicates lateral activity in the past and, combined with more information, potentially current activity. On the geomorphological map of the Netherlands, the valleys of these streams and rivers are indicated as: "River valley with meander ridges and channels".

Not all stream valleys are characterised by meander ridges and channels. Stream valleys can often be rather smooth and lack clear undulations. Here the oxbows are less common and are concentrated in certain stretches of the stream, often containing just a single oxbow. In these cases, it is harder to distinguish natural oxbows from those created by anthropogenic alterations. Historical maps of these areas can help determine which of the two processes is at play here. Bonnebladen and RD025 maps can be accessed at Topotijdreis and are fairly accurate after the 1900's (Het Kadaster, 2019; "HisGIS," 2019)

Fining upward sequence

As stated before, the classic point bar in small streams exhibits a combination of organic layering (at a slight angle) and a fining upward sequence. The fining upward sequence is, however, more difficult to distinguish in the field if the difference in grain size within the profile is limited. All but one of the streams flow through the higher sand areas (Fig. 5), areas that are mainly affected by coversands that range from fine sand to very fine sand. Within this region it is often hard to distinguish the fining upward sequence. In some cases however, the fining upward sequence within the point bar is very clear. The presence of a fining upward sequence was determined using the texture analysis conducted during fieldwork (Section 3.1.1).

Peat in the outer bank

Similar to a high silt-plus-clay content, a high organic content of the soil increases the erosion-resistance of a soil. Peat banks are extremely rich in organic material and are therefore hard to erode (Candel et al., 2017; Micheli and Kirchner, 2002; Nanson et al., 2010), limiting the lateral activity of a stream. The presence of peat does not necessarily mean that a stream is laterally inactive, but does give a fairly good estimation. Peat tends to form in environments where the organic matter can accumulate, environments with low to no energy and low sediment input such as abandoned channels. Peat therefore most likely formed due to absence of energy within the system and stream (Cameron et al., 1989). As stated before, peat banks are relatively erosion-resistant so the streams within these peat-filled valleys remain largely laterally restricted, even if their stream regime changes and more energy becomes available. In meandering systems, the peat can be more localised as it is formed in abandoned channels. The peat can still restrict the lateral movement of the stream locally in one direction, but overall the stream remains laterally active.

The presence of peat was determined using the texture analysis conducted during fieldwork (Section 3.1.1). No distinction was made between the different types of peat-infill in the valleys that were encountered during fieldwork, since point measurements were done for pre-selected river bends. Using only these point measurements, one cannot accurately indicate the infill of the entire valley.

Steep outer bank and a gentle inner bank

In a typical meander bend, the cross-section of the bend along the apex shows a steep outer bank and a more gentle sloping inner part of the bend (Fig. 8). In these cases the outer bank can also be slightly elevated above the inner bank. A cross-sectional asymmetry within the river or stream is hereby formed, where the river is deeper on the outside of the bend and the flow velocity is higher. Erosion of the outer bank can therefore occur, while sedimentation happens on the inside of the bend where the river is shallower. Cross-sectional asymmetry enables lateral migration of rivers and is therefore a feature that can be used to asses activity in the field.

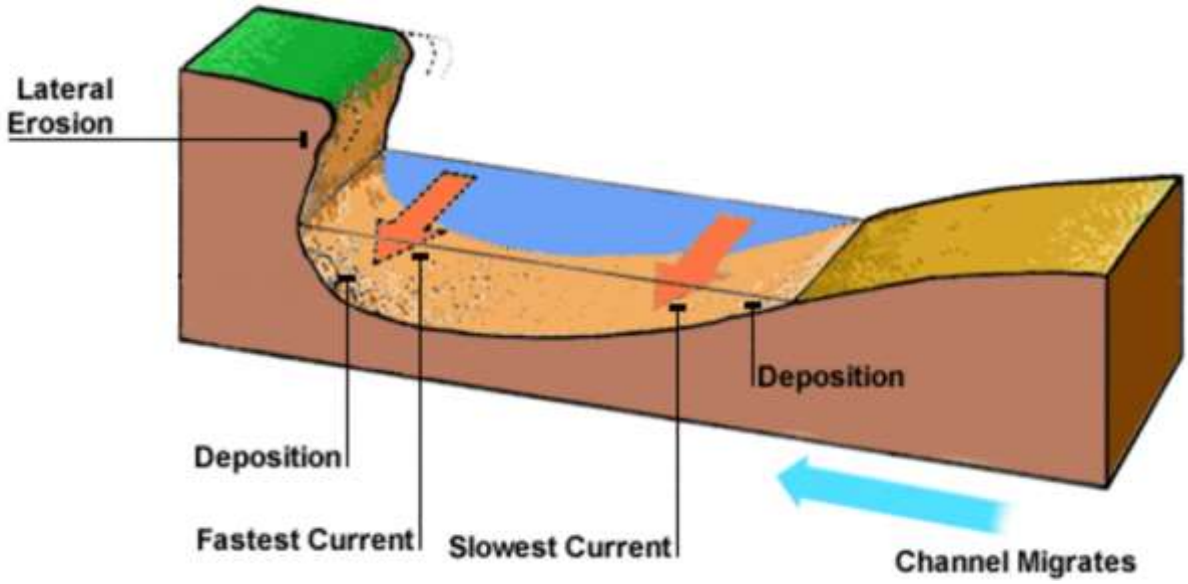

Figure 8. Typical cross-section of a meander bend. Adapted from: (Anonymous, 2019).

No cross-sections of the investigated rivers were available, fieldwork was therefore necessary. The goal of the fieldwork was however not to construct cross-sections of these streams. In cases where the stream was shallow or small enough to enter with waders, an approximation was made by wading through the water. In the other cases an approximation was made from the side, mainly focussing on the banks, often wading through part of the stream. Because the largest difference within the cross-section is the bank slope, this method was deemed sufficient.

Within the decision table, only the streams where the morphology strongly resembles the typical cross-section are indicated with a check mark. This feature also carries a relatively low weight because the streambed morphology is closely related to erosional features that are already represented within the decision table.

Weights of the decision table

All features carry a certain weight to the decision on whether a stream is considered to be active or not. The features are divided into three weight classes, the first of which is the most predictive and only consists of erosional features. This class is most predictive because it gives an indication whether lateral migration processes are currently happening. Without active erosion the process of meandering cannot take place. The second class consists of the presence of organic layering and oxbow remnants. These are also very predictive as they indicate past lateral activity, but do not give further insight into current activity. The final class, consisting of fining upward sequences, peat in the outer banks and the cross-sectional shape of the channel, carries the least amount of weight due to various reasons. They are already partly covered by other more descriptive and more recognisable features such as in the case of the fining upward sequence in contrast to the organic layering and the channel shape which is partly covered by the erosional features. In the case of peat there is ambiguity, it limits the lateral movement but on itself the presence can both indicate (past) activity (oxbow infill) and non-activity (complete valley infill).

The feature in the first class was given a base weight value of 1, the features in the second class were given a value of 0.75 and those of the last class a value of 0.5. Based on these weights a score was calculated for each stream indicating the likelihood of lateral activity. If all features were present for a stream, a total score of 4 out of 4 (100%) was achieved. The threshold score between streams that are considered laterally active and laterally stable was determined after comparison with the OSL data.

3.1.3 Optically Stimulated Luminesence

Optically Stimulated Luminescence (OSL) is used in this thesis as a tool to check the ages of point bar sediments of certain streams. These ages in combination with historical map analysis (Section 3.1.4) are used to verify and check the findings of the decision diagram. It is also possible to determine to a certain extent how recent the lateral activity was.

Sampling method

Nine streams ranging from a 0% to a 100% score regarding the activity features were selected to both check the current decision diagram and to give clarification in cases where doubt existed. The ages that were gained by OSL are used as definitive activity indications as the ages are absolute.

The selected streams were revisited and for each stream one sediment sample was collected for OSL dating. The samples were taken on the inner bend along the apex approximately 5 metres from the stream channel. The previously gathered texture data were used to locate the depth of the point bar deposits. All samples were taken below the groundwater level to ensure that the samples were saturated. The assumption was made that the sediments have been water-saturated ever since the moment of deposition. This reduces some uncertainty later in the process of calculating the environmental dose rate (Quik and Wallinga, 2018). Sampling was done using a PVC sampling pipe of approximately 30 cm long and a diameter of 7 cm which could be mounted on an Edelman auger. This PVC pipe was inserted into an auger hole that was made beforehand using a regular Edelman auger until the sampling depth. The pipe was then pushed further into the hole until it was filled with sediment. The pipe was carefully removed from the auger hole, limiting the loss of soil from the pipe as well as the amount of light exposure. The pipe was quickly sealed with lids and tape and carefully transported to avoid further light exposure and unwanted movement of the sediment within the tube.

Laboratory method

The measurements and preparation of the OSL samples that were gathered at various streams for this research were done at the Netherlands Centre of Luminescence dating or NCL in Wageningen. The tubes containing the samples were carefully opened under amber safelight conditions and the outer 5 cm of the light exposed soil on each end of the tube was separated. The light exposed outer material was prepared for dose rate estimation while the inner, still unexposed, material was further prepared for the paleodose measurements. For every sample a description was made of the material within the tube, an estimation was made of the organic and water content and the texture of the material. The material used for the paleodose measurements was sieved to get the 180 – 212 µm grain fraction, the other grain fractions were stored for possible further research. The samples were subsequently treated with hydrochloric acid (HCL 10%) to remove any calcium carbonates and with hydrogen peroxide (H_2O_2 10%) to remove the organic material. The samples were then treated with hydrofluoric acid (HF 40%) for 45 minutes to remove feldspars and etch the quartz grains. Any salts that could have been formed during the etching were removed by adding more hydrochloric acid (10%) and rinsing the grains in water.

For each sample multiple small aliquots were prepared by coating stainless steel discs with a layer of silicon spray to ensure that the grains would stick. The mask size used here was 2 mm in diameter, enough to hold approximately 100 grains. Measurements were conducted using a slightly altered Single-Aliquot Regenerative dose (SAR) protocol (Wintle and Murray, 2006) on a Risø TL/OSL DA20 reader (Bøtter-Jensen et al., 2003). The test dose and natural dose measurements for all samples are shown step by step in Table 3. The process is repeated at least five times, with the natural dose, a regenerative dose (50 s), a recuperation dose (0 s), a recycling dose (50 s) and a purity test (50 s) where the sample is checked for feldspar contamination. For further explanation of these doses and tests, please turn to the paper of Wintle and Murray (2006), where the details of the SAR protocol are explained. The process was repeated with additional regenerative doses if the natural signal exceeded the signal created by the regenerated dose. In these cases the duration of exposure to the Beta source was doubled until the natural signal was exceeded.

Table 3. Steps taken during the OSL process.

	Step	Light	Temperature (ºC)	Duration (s)
1.	Beta or natural dose	-	-	Variable
2.	Pre-heat	-	200	10
3. *	Feldspar signal measurement	Infra-Red LED's	30	40
4.	Quartz signal measurement	Blue LED's	125	20
5.	Beta test dose	-	-	50
6.	Cut-heat	-	180	10
7.	Quartz signal measurement	Blue LED's	125	20
8.	Bleaching	Blue LED's	210	40
9.	Repeat steps 1 – 8			

* This step is only applicable in the final measurement where the aliquot is checked for feldspar contamination.

The pre-heat (before natural dose) and the cut-heat (before test dose) are done before the measuring steps in order to remove any unstable electrons from shallow traps. When the grains are preheated, some electrons can shift from shallow light insensitive traps to deeper light sensitive traps, thereby leading to an age overestimation. This phenomenon of is called thermal transfer, to which young samples are especially sensitive to thermal transfer and need to be checked prior to the luminescence measurements (Madsen and Murray, 2009). The height of the pre- and cut-heat used in step 2 and 6, respectively, were determined using a thermal transfer test. The sample started to show a luminescence signal caused by thermal transfer around 220 to 240 ºC, therefore the pre- and cut-heat were kept at 200 ºC and 180 ºC respectively. Using the selected pre- and cut-heat a dose recovery test was done for all samples to determine whether the samples were suitable for the SAR protocol.

For the initial analysis of the OSL data the Risø Luminescence Analyst software was used. Further analysis was done using RStudio and scripts provided by NCL. A maximum test dose error of 15% was used for the analysis and the integration limits (in 1/100 s) used were 1 – 25 for the signal and 26 – 88 for the background based on earlier research on similar sediments by Kamstra (2018). An early-background methodology is therefore used as proposed by Cunningham and Wallinga (2010). All discs were checked for recycling ratio, fast component ratio and feldspar contamination before they were accepted. No extra recuperation check was done due to the expected young nature of these sediments. The luminescence of every sample was measured at least twice with aliquot sizes of 24 discs, until enough discs were accepted (around 30).

The bootstrapped minimal age model (MAM) (Galbraith et al., 1999) was applied in RStudio using the Luminescence package provided there. The overdispersion that was used for the MAM was 0.20 ± 0.05. Overdispersion is the presence of a variability in a dataset that cannot be explained based on a statistical model. One of the explanations for this greater variability is the previously mentioned poor bleaching of fluvial sediments. Using a bootstrapped MAM improves the age estimate in these types of sediments. Further analysis and recombination of the paleodose calculated by the MAM and the dose rate for the eventual age calculation were done in Excel using a spreadsheet provided by NCL.

3.1.4 Historical Map Analysis

For every OSL sampled stream, the historical maps of the area and stream channel surrounding the sampling point were investigated for lateral activity of the streams. Bonnebladen and RD025 maps were accessed through the Topotijdreis webpage. These maps are fairly accurate after the 1900's and can be used to study general trends in the courses of the streams (Het Kadaster, 2019; "HisGIS," 2019). The maps were also studied to inspect the representativeness of the sampling locations for the entire stream. At least three maps per stream (ideally from the early 20th century, the late 20th century and the most recent map) were selected and the course of the streams was traced. A simplified version of the method of Quik and Wallinga (2018) was used for georeferencing. High quality ground control points, such as road crossings and edges of arable fields were selected and used to overlay the maps of different ages. The overlay was done by hand due to time constraints, matching the ground control points for the different maps as close as possible. This method was deemed sufficient because the focus was to look at general trends in lateral migration and not a detailed look at the exact location of the stream course. Once the overlay was complete, the trends of lateral migration for the stream courses could be studied.

3.2 Stability Diagram

In order to answer the second and third research question on the predictive capabilities of the stability diagram, the streams needed to be plotted in the diagram. To plot streams in the stability diagram, the stream power and the D50 of the bed material had to be determined. Additionally, the texture or silt-plus-clay content of the streambanks, the vegetation cover and the organic content of the banks needed to be determined, because they contribute to the erodibility of the streambanks. The methods used to find the answers to the second and third research question are elaborated upon in the following sections.

3.2.1 Texture Analysis

A similar method was used for determining the D50 of the bed material of the streams and the silt-plus-clay content of the streambanks, because both rely on a texture analysis. A Van Veen sediment grabber (around 1 dm^3) was lowered in the middle of each stream to sample the bed material. Samples of the bank material were taken using an Edelman auger at three locations on each side of the stream. These samples were taken at approximately 2/3 of the depth of the stream and within 1 – 3 m from the stream channel. One sample was taken at the apex of the bend at the same location as the soil description. The two other samples were taken on either side of the apex within 5 – 10 m (Fig. 6). Approximately one drill head of sediment was sampled per point (around 0.5 dm^3), resulting in three drill heads worth of sediment per side of the stream. These samples were put into one sample bag and mixed together in order to deal with small-scale spatial variability in the sediment. In cases where the gathered sediment was visually significantly different, the samples were kept separate in different sample bags. Further analysis on these different samples was then also done separately.

To determine the grain size of the streambank and bed material a laser diffraction particle size analyser was used. The analyser used for these measurements was the Beckman Coulter grain size analyser, LS 230. It measures particle size distributions by measuring the light scattered by the particles in the sample. The scatter pattern created by the particle is formed by light intensity as a function of scattering angle, each particle's scattering pattern is therefore characteristic of its size (Beckman Coulter Inc., 2011).

Prior to the measurement the material had to be dried and sieved for material larger than 2 mm. The samples were left in an oven for approximately 24 hours at 105 ºC to remove all water. The material larger than 2 mm was collected separately and saved for later correction of the D_{50} and silt-plus-clay content. The sieved material was then homogenised and between 0.5 and 6 grams was weighted and used for the measurements. The amount of material that was used depended on the clay content of the sample. Only 0.5 gram was needed in the case of clayey material while up to 5 grams should be used for sandy material. The amount of sample that was used determined the total obscuration that would be achieved during the measurement, which affected the accuracy of the measurement. The weighted material was then treated with 10 ml of 1M hydrochloric acid (HCl) to remove any calcium carbonate. The beaker glasses containing the samples were filled with 20 ml of water and put on a boiling water bath. The samples were further treated three times with 10 ml of 30% hydrogen peroxide (H_2O_2) for 30 minutes, to remove the organic material. In order to get accurate measurements, the electrical conductivity (EC) within the sample has to be below a value of 1 mS/cm. To ensure that the sample was clean it was left to settle. Most of the water was drained from the beaker after it had settled and fresh demineralised water was added. This process of refreshing the sample was repeated at least twice after which the sample EC was measured. If the sample's EC was still too high the process had to be repeated.

A mixture of sodium carbonate (Na_2CO_3) and sodium polyphosphate $(NaPO_3)_n$ was added as a dispersion agent. The samples were then given a treatment of sonication, in order to separate any grain aggregates left in the samples. After the sonication, the samples could be inserted in the particle size analyser for the measurement. Accurate measurements could be obtained if the obscuration of the sample was between 6% and 14%. Measurements (slightly) outside of the ideal obscuration range can still be used but are slightly less accurate. Other than the obscuration, the Polarization Intensity Differential Scattering or PIDS should also have a value below 85%, this value is especially important in clay rich samples, since the PIDS is used to measure particles between 0 and 0.4 µm. Data from samples that did not fall within the ideal ranges for obscuration and PIDS could still be used, but it should be noted that these data are slightly less accurate. The output of the particle size analyser is a list of particle diameters ranging from 0.04 µm to 2000 µm and the cumulative volumetric percentage of the sample that is smaller than that particle diameter.

The particles that were larger than 2 mm, which were sieved and separated from the sample, were weighted. For each sample the gravel was roughly separated in up to three size categories (small, medium and large) depending on size variation and the intermediate axis of the grain was measured, this was assumed to be similar to the grain size (Buscombe et al., 2010). The average grain size was then calculated for all three categories and all categories were weighted. The assumption was made that the particle density for the fraction < 2 mm and the fraction > 2 mm is similar, since both consist mostly of quartz and feldspar and will thus have a particle density close to 2.65 g/cm^3 (Alden, 2019). Under this assumption the weight ratios and volume ratios of the fractions should be similar and the weight ratio can be used as a proxy for the volume ratio. The three size categories of the gravel can therefore be added to the output of the particle size analyser with their mean particle diameter and their (corrected) cumulative volumetric percentage. The D_{50} was calculated by interpolation between the two points closest to the 50% cumulative volumetric percentage. The silt-plus-clay content was calculated as the cumulative volumetric percentage of particles that were smaller than 63 µm.

3.2.2 Stream Power

Most information regarding the calculation of the stream power as seen in Equation 1 was readily available. The discharge data were provided by various water boards and gathered in a dataset for Project RiverCare, this dataset was used for this thesis. If both the bankfull discharge as well as the mean annual flood were available, the priority was given to the latter, similar to the method used by Kleinhans and Van den Berg (2011). The average valley slope was also provided in the dataset and was determined using a digital elevation model of the area. The width of the reference channel depends partly on the D_{50} of the bed material (Eq. 2), this was measured using the methods in Section 3.2.1.

3.2.3 Bank Erodibility

The critical shear stress is used as a proxy for the bank strength or erodibility. The relation used in the paper of Julian and Torres (2006) between the silt-plus-clay content and the critical shear stress (Eq. 3) is also applied for this thesis. The silt-plus-clay-content of the banks that was measured during the texture analysis (Section 3.2.1) could be used to calculate the critical shear stress. In the paper of Julian and Torres (2006) the additional effect of vegetation cover on the critical shear stress is also taken into account. During fieldwork, a description was made of the vegetation cover per bank. One of the five categories presented in Table 1 that best described the vegetation cover was selected per streambank and used to calculate the critical shear stress.

Due to time constraints it was unfortunately not possible to measure the organic matter content of the samples accurately using the loss on ignition method (LOI) (Heiri et al., 2001). A rough estimate of the organic matter content of the samples relative to each other was, however, made by eye, using the Munsell Color booklet as a guide (Munsell Color, 2009) and by looking at intact organics to distinguish peat. The streambanks were ranked relative to each other based on their organic matter content. The order of ranking was: peatbanks, organic banks with a mineral component, mineral banks with an organic component and mineral banks. Within these “categories” the ranking was based on the amount of organics (for organic banks) and the colour of the sediment (for mineral banks). Streams where there was little to no visible organic matter within the streambank ranked low, while streams with complete peatbanks ranked high. Since 19 streams were investigated, the ranking was out of 19. Using this method it is not possible to draw definitive conclusion regarding the effect of organic matter on the bank strength. However, it could give an indication whether this is a topic worth further investigating.

4. Results

4.1 Lateral Activity Determination

4.1.1 Decision Table

In the following sections a short summary is given of the findings for all activity features. The activity decision table (Table 4) can be found at the end, this can also function as an overall summary table for the activity features.

Figure 9. Erosional features in the field. A: Undercutting on the outer bank and exposure of tree roots at the Mosbeek. B: Sedimentation of (eroded) clastic material on the inside of the bend in the Mosbeek. C: Steep scarp surface on the outside of the river bend and formation of gravel banks in the river Geul.

Erosional features

In twelve out of nineteen streams the erosional features were observed. Among these were exposed tree roots, fallen trees and bank undercutting (Fig. 9A). The eroded material was often deposited on the inner bend of the stream (Fig. 9B). In the case of the Geul a steep scarp surface was created on the outer bank (Fig. 9C). Streams where these erosional features could be found are indicated by a check mark in the decision table (Table 4).

Organic layering

Organic layering could be found in the streambanks of fifteen out of nineteen streams. The Astense Aa, Reest, Reusel and Raamsloop did have organic layering, but this was only found in the outer bank. Organic layering is assumed to be a point bar deposit and is therefore not expected on the outer bank. In these cases the organic layering is left out of consideration for the decision table, this is indicated by a swung dash (~) in Table 4. Organic layering was clearly visible in most cases, especially when a Staay suction corer was used (Fig. 10A), however, when a gouge was used the organics could be hard to distinguish (Fig. 10B). The streams where organic layering was found on the inner bank are indicated by a checkmark in Table 4.

Figure 10. Organic layering in the subsoil. A. Clear layering from 80 cm and onward on the outer bank of the Chaamse Beek, taken with a van der Staay suction corer. B. Slightly distinguishable organic layering from 90-120 cm on the inner bank of the Reusel + Raamsloop stream, taken with a gouge.

Oxbow remnants

Oxbow remnants could be found in the DEM's of ten of the investigated streams. Four of these streams showed clear signs of multiple abandoned channels on either side of the current channel (Fig. 11A). These were the Swalm, Bovenmark, Dinkel and the Bovenslinge. Within the geomorphological map of the Netherlands the stream valleys of these streams are indicated as: "Stream valley with meander ridges and channels". The other stream valleys where oxbow remnants were found often contained a single or a small cluster of oxbows (Fig. 11B). These stream valleys overall showed less undulations and were smoother. Within Table 4 the presence of both of these types of oxbow remnants are indicated by a checkmark.

Oxbows in two streams, the Buurserbeek and the Dommel, were found to be anthropogenic after the historical maps of these regions were checked. For these streams the presence or absence of oxbows is taken out of consideration for the activity reasoning of the rivers. It is unknown whether the oxbows might also have formed under natural circumstances. These streams are therefore indicated by a swung dash (~) in Table 4.

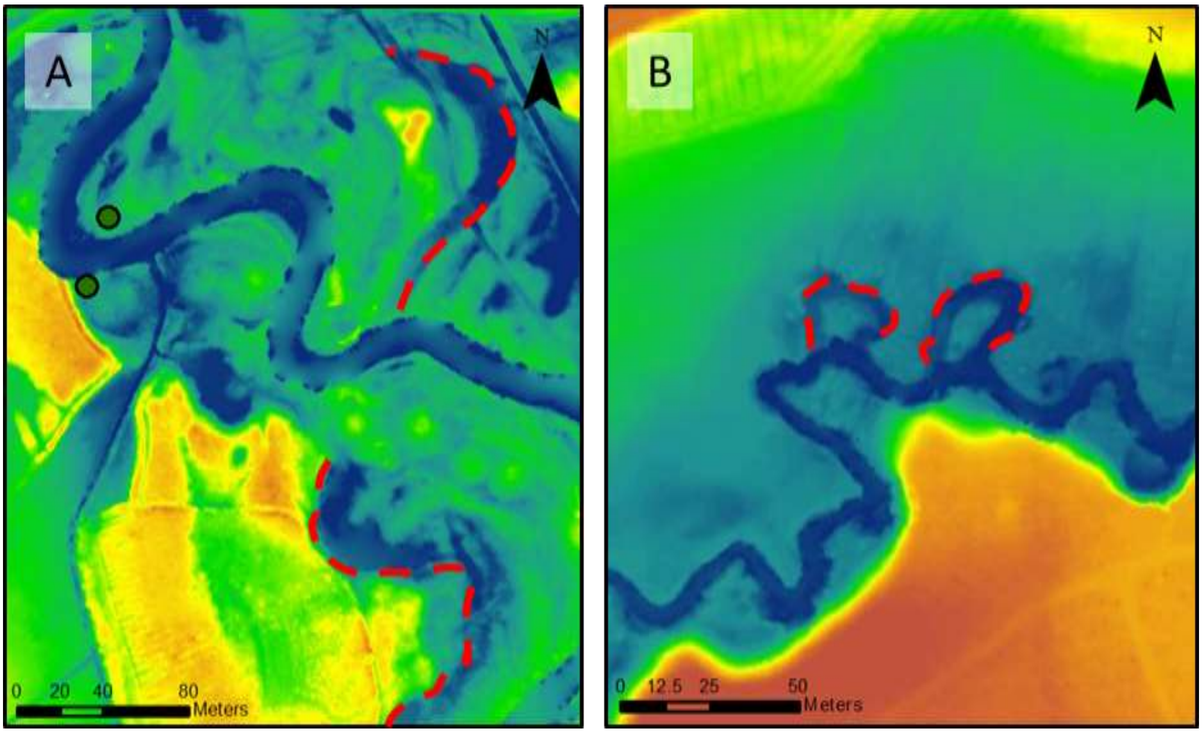

Figure 11. DEM with the stream course of the Dinkel (A) and the Roggelse Beek (B), oxbows are indicated with a red dashed line. The sampling locations for the Dinkel are indicated with green dots.

Fining upward sequence

A clear fining upward sequence could be found in nine of the investigated streams. This is perhaps most clear in for the inner bend of the Swalm (Fig. 12), where both organic layering and a fining upward sequence can be found. The fining upward sequence gradually changes from a mixture of (very) coarse sand and gravel at 130 cm depth to fine sand at 30 cm depth. Not all streambanks showed such a clear fining upward sequence, as the difference in grain size was often hard to distinguish in the field. The fining upward sequence, if present, was indicated by a checkmark in Table 4.

Peat in the outer bank

Ten out of the nineteen streams that were investigated had peat in their outer banks. Multiple degrees of peat presence were found during the fieldwork campaign. Streams like the Reest and Rosep were dominated by peat on both sides dominated by peat that filled the entire stream valley, little to no clastic material was found indicating very little to no lateral activity. Streams like Merkske and Strijbeekse Beek are also located in valleys that are filled with peat but also contain sections with more clastic material. The outer bank of the Swalm (Fig. 12) also contains peat, or very organic material, that was most likely formed in a former stream course of the river itself, this is therefore characterised as channel fill. Within the activity decision table, streams that are not laterally limited by peat or very organic banks are indicated by a checkmark in Table 4.

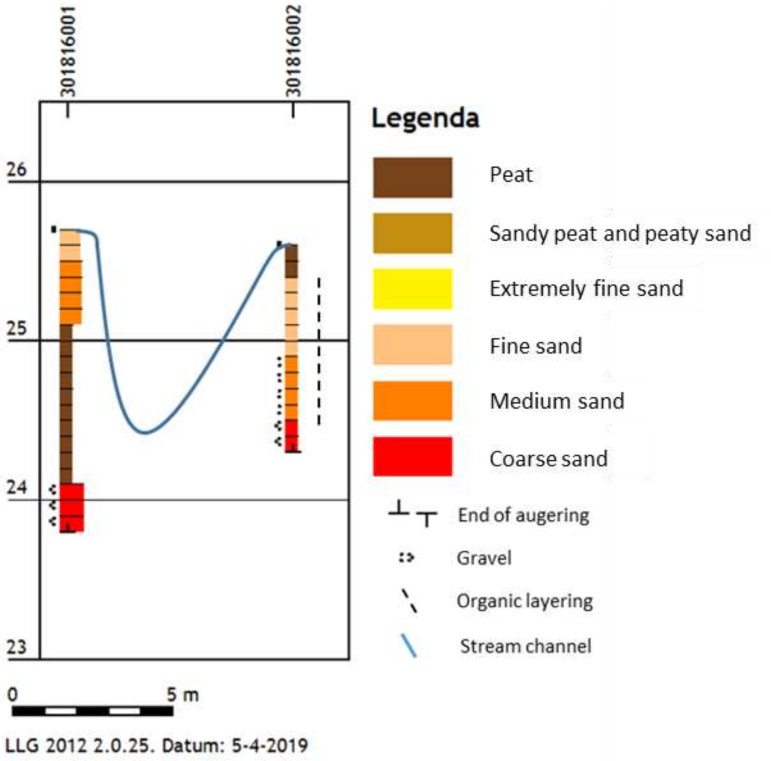

Figure 12. LLG plot of the subsoil of the inner (right) and outer (left) bank of the Swalm.

Steep outer bank and gentle inner bank

Ten of the investigated streams had a clear cross-sectional asymmetry where the outer bank was steeper than the inner bank. This feature was clearly found in streams such as the Swalm and the Geul, however, these streams have higher stream powers. The difference between the inner and the outer bend tends to become less prominent, if present at all, in streams with lower stream powers. It is therefore hard to distinguish between those streams that only slightly exhibit these features and those that do not. Especially if there is no available cross-section of the stream and the size of the river does not allow closer inspection of the streambed morphology.

Explanation of the decision table

The presence or absence of the various activity features are indicated in Table 4. The classes of activity features are grouped. Based on these features an activity score was calculated following the method in Section 3.1.2. Streams that scored over 60% in the decision table are deemed to be active. This was based on comparisons with the OSL data and historical map analysis, this will be elaborated on further in Sections 4.1.2 and 4.1.3. The activity estimation is made in the final column, where streams that are deemed laterally active are indicated by a checkmark (✓). The streams that are not deemed laterally active are indicated by a cross symbol (X). The estimation is purely based on the decision table, the final activity estimation can still be adjusted using the OSL ages from Section 4.1.2. The activity estimation for the Bovenmark and the Buurserbeek are both left out of the, as they are definitely not active at this moment due to human interference. This is due to canalisation in the Bovenmark and recent placement of stone bank protection for the Buurserbeek.

The decision table shows that all the activity features can be found for the Chaamse Beek, Reusel + Raamsloop and Geul. There are also the Reest, Reusel and Rosep, three streams where none of the activity features can be found. Apart from these streams, no two other streams to have the same combination of activity features.

Table 4. Decision table based on activity features found during fieldwork, literature study and OSL measurements for every stream. Explanatory text can be found underneath the table.

Name	EF	OL	OR	FU	PFO	SOB & GIB	Activity Score (%)	Activity Estimation
Het Merkske	✗	✓	✓	✓	✗	✗	50	✗
Astense Aa	✓	~	✓	✗	✗	✗	54	✗
Strijbeekse Beek	✗	✓	✗	✗	✗	✓	31	✗
Chaamse Beek	✓	✓	✓	✓	✓	✓	100	✓
Bovenmark	✗	✗	✓	✗	✗	✗	19	n/a
Beerze	✓	✓	✗	✓	✓	✓	81	✓
Reest	✗	~	✗	✗	✗	✗	0	✗
Swalm	✓	✓	✓	✓	✗	✓	88	✓
Bovenslinge	✓	✓	✓	✓	✓	✗	88	✓
Reusel	✗	~	✗	✗	✗	✗	0	✗
Raamsloop	✗	~	✗	✓	✗	✓	31	✗
Reusel + Raamsloop	✓	✓	✓	✓	✓	✓	100	✓
Dinkel	✓	✓	✓	✗	✓	✓	88	✓
Geul	✓	✓	✓	✓	✓	✓	100	✓
Mosbeek	✓	✗	✗	✓	✓	✓	63	✓
Rosep	✗	✗	✗	✗	✗	✗	0	✗
Roggelse Beek	✓	✓	✓	✗	✓	✗	75	✓
Dommel	✓	✓	~	✗	✗	✗	54	✗
Buurserbeek	✓	✗	~	✗	✓	✓	62	n/a

EF = Erosional features, OL = Organic Layering (Point bar sediments), OR = Oxbow Remnants, FU = Fining Upward, PFO = Peat-Free Outer bank, SOB & GIB = Steep Outer Bank and Gentle Inner Bank. ✓ = The feature in question is applicable to the stream, ~ = The feature in question is not taken into consideration within the decision table due to (see explanation in text), ✗ = The feature is question is NOT applicable to the stream.

4.1.2 Optically Stimulated Luminescence

All nine samples that were taken for OSL measurements were adequate for age estimations. However, some samples showed more spread in the equivalent dose (ED) than others. The spread of the measured ED for two samples is represented in abanico plots (Fig. 13A and B), for a detailed description of these type of plots please turn to Dietze et al. (2016). These plots show a relatively well bleached sample (A: Reusel + Raamsloop) and a poorly bleached sample (B: The Beerze). For the Reusel + Raamsloop 89.3% of the measured ED's are within a 2σ range of the central value line and only one peak can be distinguished in the KDE plot (Fig. 13A) . Therefore, the Central Age Model (CAM) already gives an adequate estimate for the ED and will not differ greatly from the ED obtained through a Minimum Age Model (MAM). The Beerze however, has a larger spread with only 2.9% of the measured ED's within a 2σ range of the central value line. Multiple peaks can also be distinguished in the KDE plot of the Beerze (Fig. 13B). Here the ED's obtained through either a CAM or MAM will differ greatly.

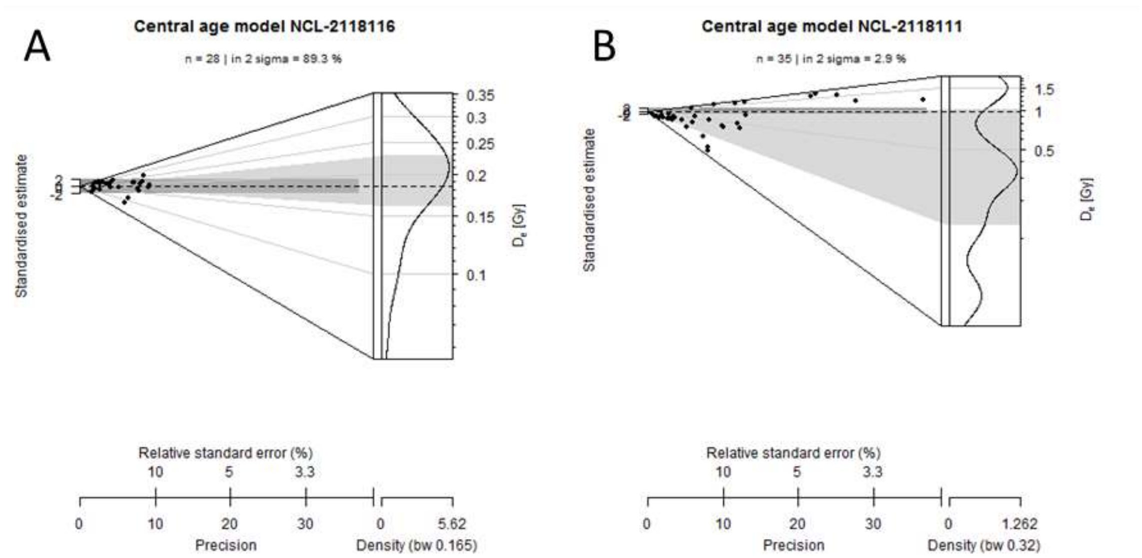

Figure 13. Abanico plots of the equivalent dose distribution of the Reusel + Raamsloop (A) and the Beerze (B). An alternative of the standard radial plot (left of the graph) is combined with a KDE plot (right of the graph).

Another parameter that can be used to express the magnitude of the spread within a sample is the overdispersion. There is a clear relation between the overdispersion within a sample and the age difference that is estimated using either a CAM or a MAM (Fig. 14). The poorly bleached sample of the Beerze (red circle) has a large overdispersion and will benefit most from the MAM, the estimated age of the well bleached Reusel + Raamsloop sample (green circle) is barely affected. The base overdispersion of the well bleached samples seems to be around 20%, this is therefore also the value of overdispersion (or sigma b as it is called in the R function) that is used for all samples in the bootstrapped MAM.

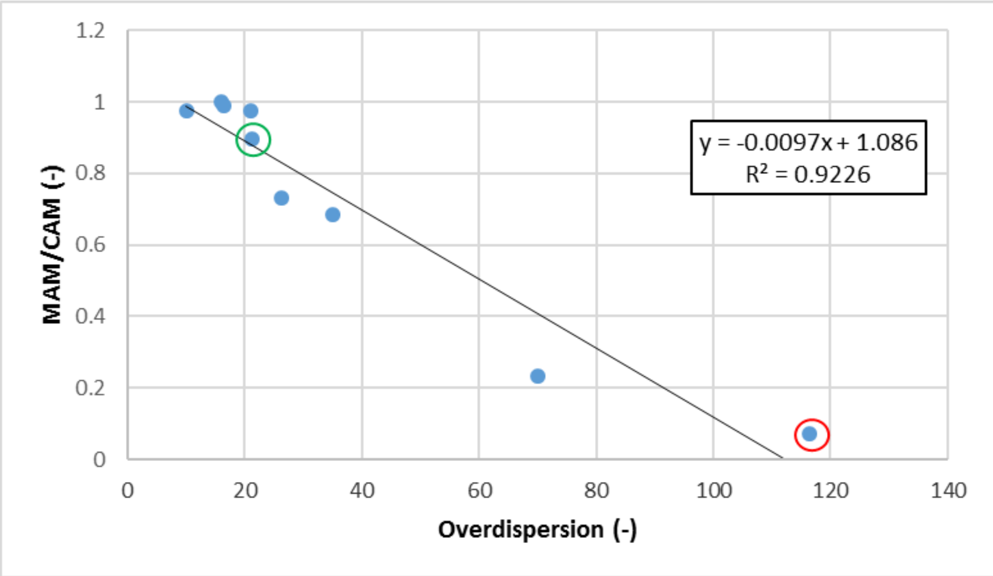

Figure 14. Ratio of equivalent dose calculated by the bootstrapped minimum age model over equivalent dose calculated by a central age model plotted against the overdispersion of the data. The data point within the green circle is that of the Reusel + Raamsloop, the point encircled by the red circle indicates the Beerze.

The workings of the MAM for both well and poorly bleached samples is even more evident in ED distribution plots of the Reusel + Raamsloop and that of the Beerze (Fig. 15A and B respectively). The bootstrapped likelihood area of MAM is relatively close to the centre of the ED distribution for the well bleached sample and it closely resembles the Gaussian fit. This is not the case for the poorly bleached Beerze where the bootstrap likelihood completely moves towards the younger part of the distribution and does not resemble the Gaussian fit as much.

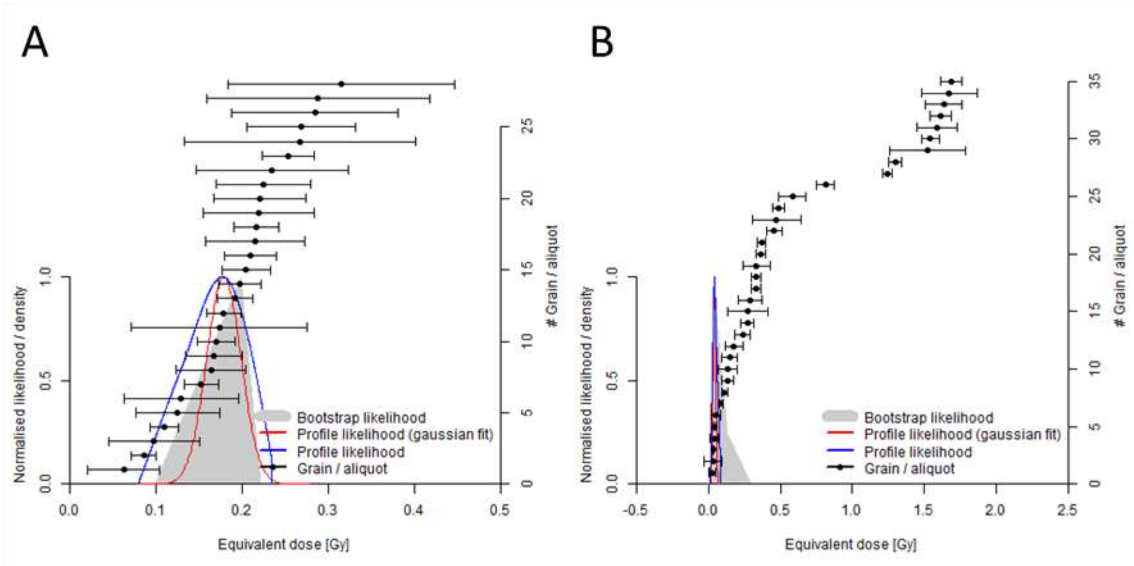

Figure 15. Plot of the Minimum Age Model for the equivalent dose distribution of the Reusel + Raamsloop (A) and the Beerze (B).

The other samples taken for OSL measurements were all further analysed using the MAM. This resulted in the estimated ages that can be found in Table 5. Striking about these ages is that about half of these samples are estimated to be very close to 300 years old. A relatively young sample within the set is the

Beerze that is estimated to be less than a century old, which matches a description of the river made by a bystander in the field. On the other hand there are two samples, Reusel and Merkske, that are estimated to be much older than all other samples. Samples from Roggelse Beek and the river Dommel are estimated to be somewhat older than the bulk of the other samples. These samples are both close to the “activity threshold” of 500 years determined by historical map analysis (Section 4.1.3), with the Roggelse Beek just young enough and the Dommel slightly too old. Note that the error margins also differ greatly between samples. The trend in error margins mostly follows the overdispersion in the samples, where samples with large error margins also have a high overdispersion. The highest error percentage margin is 22.4% and it can be found for the Beerze which is additionally the youngest sample. The lowest error percentage margin on the other hand is just 5.3% which is found for the oldest sample: Merkske. The error margins in other samples do not seem to be related to their age, as would seem regarding only the two extremes. The sample from the Chaamse Beek as well as that of the Raamsloop are both relatively young whilst also having a low error percentage margin of 7.1% and 7.9% respectively.

Table 5. Results of the OSL dating based on the bootstrapped Minimum Age Model. Location expressed in the Dutch Coordinate system Rijksdriehoekstelsel.

Sample		**Location (RD coordinates)**		**Sample Depth**	**Paleodose**	**Dose rate**	**Age estimate**
NCL Code	Name	x	y	[cm]	[Gy]	[Gy ka^{-1}]	[ka]
2118110	Bovenslinge	245386	440221	130 – 160	0.36 ± 0.07	1.30 ± 0.04	0.27 ± 0.06
2118111	Beerze	148356	397026	60 – 90	0.04 ± 0.01	0.63 ± 0.02	0.06 ± 0.01
2118112	Merkske	117401	380920	135 – 165	1.59 ± 0.06	0.46 ± 0.02	3.47 ± 0.18
2118113	Roggelse Beek	193712	363012	90 – 120	0.37 ± 0.05	0.85 ± 0.03	0.43 ± 0.06
2118114	Chaamse Beek	116212	393651	120 – 150	0.15 ± 0.01	0.52 ± 0.02	0.29 ± 0.02
2118115	Raamsloop	138811	381993	90 – 120	0.29 ± 0.02	0.96 ± 0.03	0.31 ± 0.02
2118116	Reusel + Raamsloop	138800	382194	100 – 130	0.18 ± 0.02	0.69 ± 0.02	0.26 ± 0.03
2118117	Dommel	159613	368175	100 – 130	0.58 ± 0.08	0.95 ± 0.04	0.61 ± 0.09
2118118	Reusel	138473	381793	120 – 150	1.79 ± 0.15	0.98 ± 0.04	1.82 ± 0.17

Using the 500 year activity threshold this means that of the nine OSL sampled streams, only the Dommel, Reusel and Merkske are not active. All six other OSL sampled streams are deemed to be laterally active. Since the ages gained by OSL are absolute, this is also seen as final lateral activity estimation. Comparing these activities to the scores in the decision table it seems that there is no possible score threshold possible where the activity estimation of OSL and the decision table match completely. Both the Dommel (score of 54%) and the Merkske (score of 50%) are deemed inactive by OSL, the threshold should therefore logically be higher. The threshold is set at 60% for the decision table because the Mosbeek (score of 63%) shows very strong signs of current erosion of the outer bank and formation of (small) point bars on the inner bend (see Fig. 9A and 9B). Using this threshold of 60%, the eight out of nine OSL activity estimations match the activity estimations made by the decision table. Only the activity estimations of the Raamsloop do not match, where the OSL deems it laterally active and the decision table does not. The activity determined by the OSL is kept as absolute here. Therefore the activity estimations made by the decision table are all accepted apart from the Raamsloop, which is changed to laterally active.

4.1.3 Historical Map Analysis

Lateral activity of the Roggelse Beek can be spotted by looking at historical maps (Fig. 16). The accuracy of the maps is not as perfect as that of the DEM which will function here as the "true" course of the river. However, signs of lateral activity can be seen in stretches A, B and C. In stretch A, the process of oxbow formation can be seen at the location of the sampling (indicated by the red arrow on the DEM in Figure 16). The stream course slowly moves eastwards while forming a new river bend. Meanwhile the left-hand bend was cut off between 1979 and 2011 and the right-hand bend is in the process of being cut off, the latter was confirmed in the field. In stretch B, only one bend can be seen facing north on the 1938 map. Both on the right and the left-hand side of the initial north facing bend two new north facing bends are formed that become more sinuous over time, while the initial bend is cut off. Finally, for stretch C the stream channel gradually evolves from meandering mainly in a north – south direction to an east – west direction, gradually becoming more sinuous.

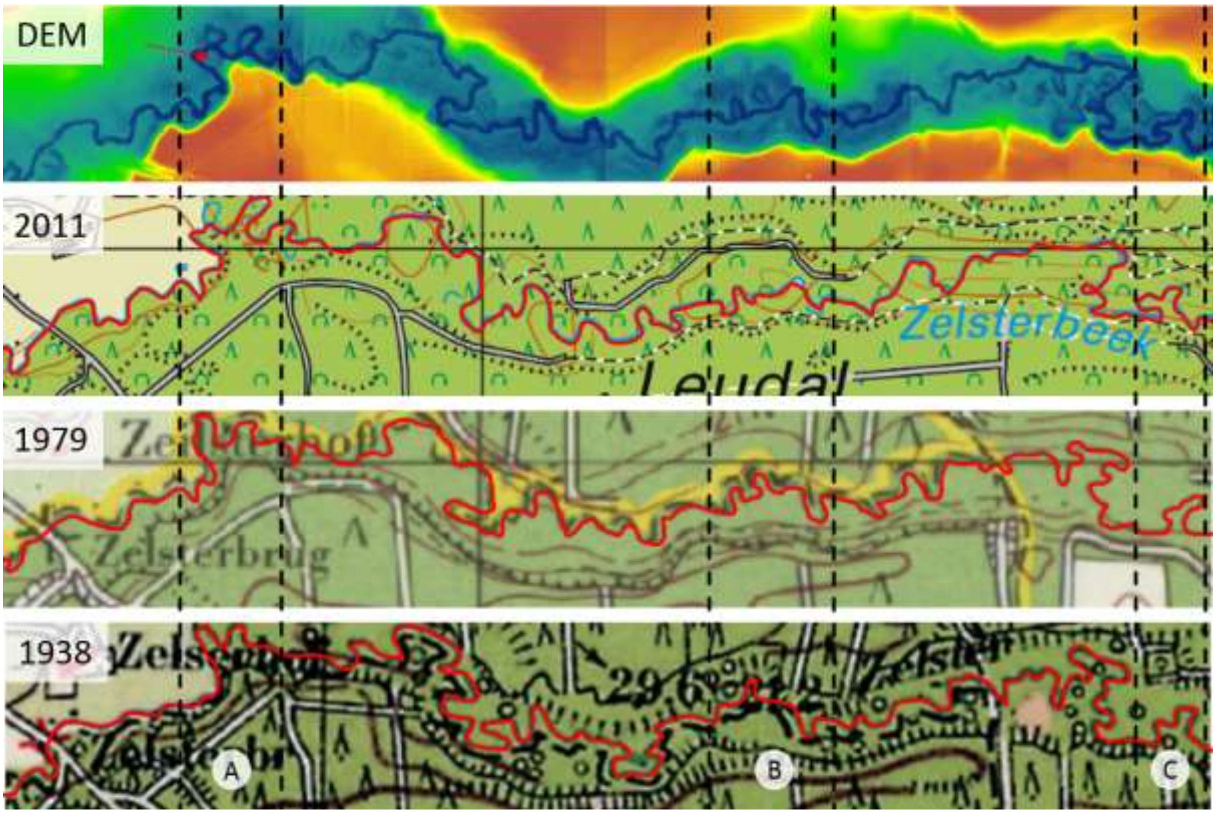

Figure 16. Historical maps of the same stretch of the Roggelse Beek through the ages, accompanied by the DEM where the OSL sampling location has been indicated by a red arrow. Stream courses are indicated by the red line.

For the Dommel (Fig. 17), not as much lateral activity has been seen since at least the 1930's. Within the shown stretch of the river only two major bends have changed, these are indicated by orange circles on the map of 1930. It is very likely that these particular bends have been artificially cut off, remnants of these former courses can still be seen in the DEM. Other river bends have not changed very drastically, not enough to accurately point it out on historical maps. When comparing the courses closely over time there are both indications of the bends becoming sharper and some becoming less so. These (already) sharp bends becoming sharper over time can be an indication of flow separation occurring and causing localised bank erosion, as similar effects were observed in the paper of Kleinhans et al. (2009). It might also be caused by the canalisation that happened, followed by a period in which the river was in disequilibrium and changed its course only slightly.

The OSL sample for the Roggelse Beek was dated at 0.43 ± 0.06 ka while the sample of the Dommel was dated at 0.61 ± 0.09 ka. The activity threshold for the OSL sampled streams should be somewhere between these two streams. For convenience's sake the rounded off age of 500 years is chosen here as the activity threshold. Historical maps for the past 90 years of other OSL sampled streams have also been studied, such as the Chaamse Beek (0.29 ± 0.02), the Beerze (0.06 ± 0.01) and the Merkske (3.47 ± 0.18) and they seem to follow the same pattern (Appendix IV). Little to no lateral movement is seen for the streams where the samples are older than 500 years, while the streams that are younger do tend to show more movement on the historical maps. These streams show more movement than can be explained by inaccuracies in the maps. The only streams where an in depth historical map analysis is lacking are the Reusel, Raamsloop and Reusel + Raamsloop since not enough detail was used in the older maps due to the small size of the streams.

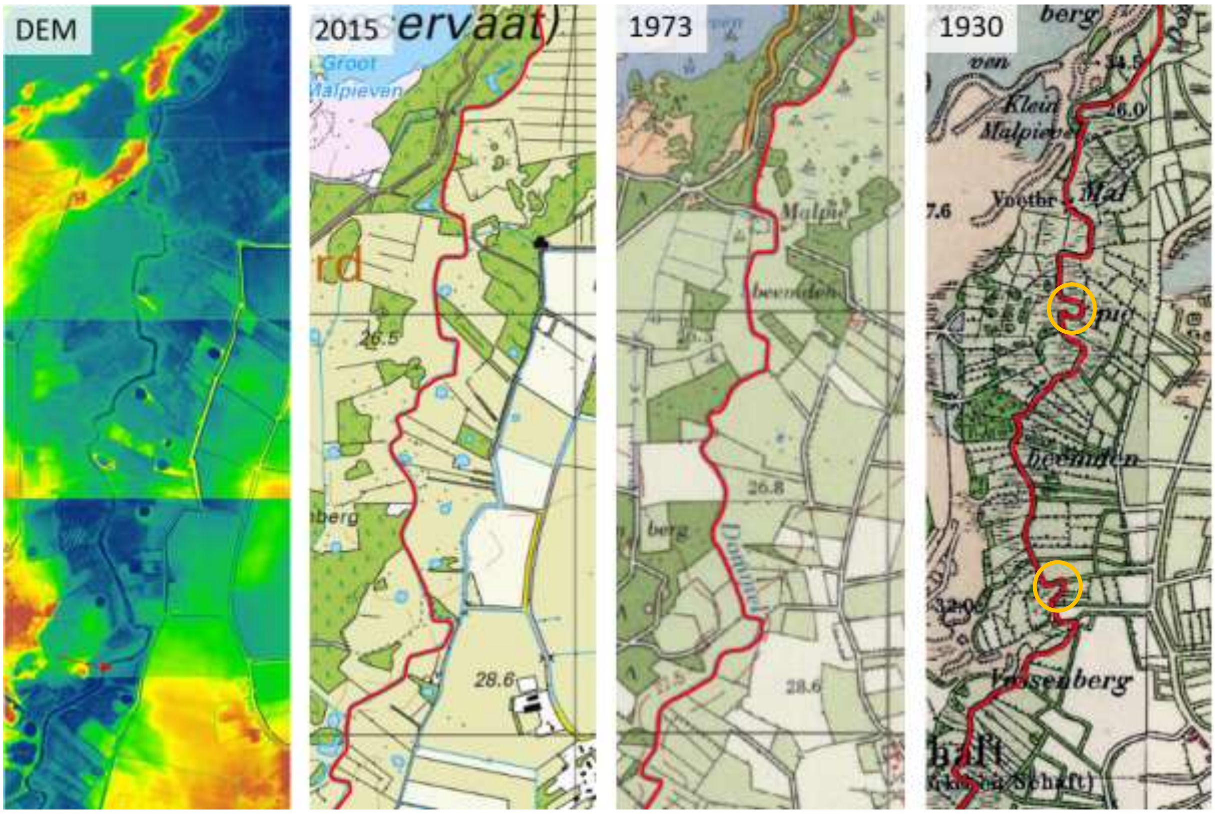

Figure 17. Historical maps of the same stretch of the Dommel through the ages, accompanied by the DEM where the OSL sampling location has been indicated by a red arrow. Stream courses are indicated by the red line.

4.2 Stability Diagram

4.2.1 Texture Analysis

The grain size analysis of the bed material for all rivers resulted in two groups of streams with a bed of clastic material. The gravel bed streams, which included the Swalm and the Geul, the sand-bed streams which included the remaining analysed streams. Texture analysis for the bed material was not done for the Rosep and the Reest since the material for these streams is too organic to be measured accurately using a particle size analyser. In total, five (out of 17) of the D_{50} samples had to be corrected to some extent for their gravel content (Appendix II).

For the bank material, both the D_{50} and the silt-plus-clay content were calculated. Less samples than those of the streambed had to be corrected for gravel content since the gravel, if it was present in the bank, was located at a depth greater than the channel depth. Still five (out of 35) of these samples had to be corrected for their gravel content (Appendix II).

For most streams, the material in the bed and the banks is rather similar in size and size distribution, mostly dominated by fine sand. This only differs in the cases of the gravel-bed streams. The bed of the Geul consists mostly of gravel, while the surrounding area is dominated by clay and loam. The Swalm also has a gravel bed, but is surrounded by coversand, which can also be found in the banks.

Overall, considering only the sand bed streams the D_{50} of the inner bank seems to be slightly higher than that of the outer bend (Fig. 18A). The D_{50} of the bed material is overall coarser than that of both the inner and the outer bank (Fig. 18B). This is to be expected, considering the fining upward sequence usually found in point bar sediments. The coarsest material can be found on the streambed and at the lowest parts of the point bar. The inner bank in the cases where it is an (old) point bar has a fining upward sequence. Since the bank samples were taken at about 2/3 of the stream depth, the inner bank sample should be somewhat finer than the bed material. The outer bank, however, mostly consists of unaltered surrounding sediments, in this case mostly coversand, which is rather fine.

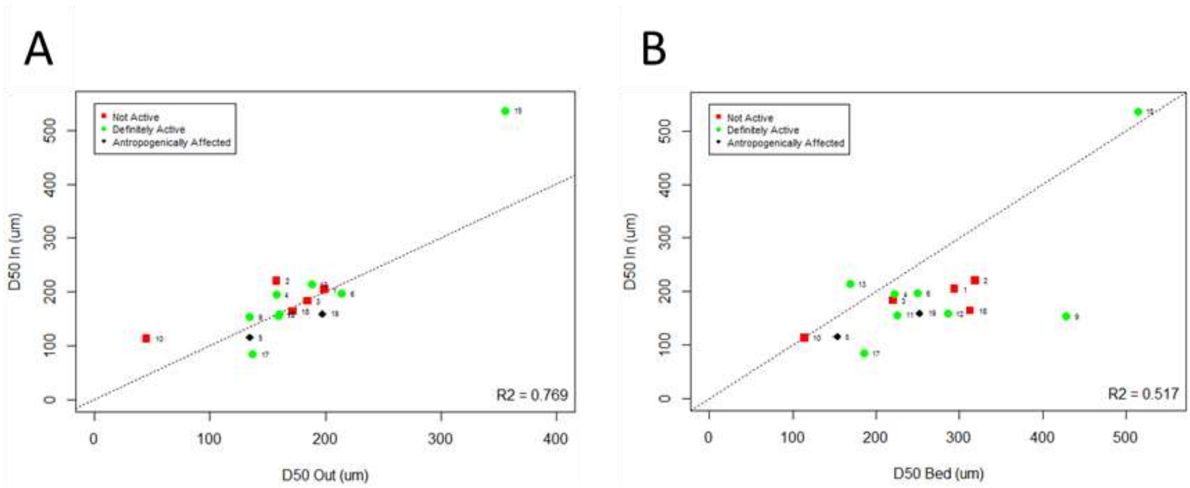

Figure 18. The D_{50} of the material found in the inner bank plotted against that of the outer bank (A) and the D_{50} of the bed material (B). The dotted line is the 1:1 line and the R2 is the R-square value for the two plotted features.

4.2.2 Classic Diagram

Combining the D_{50} of the bed material and the stream power calculated using the data provided in the previously acquired dataset (see Section 2.1), the stability diagram can be constructed (Fig. 19). All 19 studied streams are plotted here with their respective lateral activity indicated by either a red square (inactive) or a green dot (active). The Buurserbeek and the Bovenmark are both indicated by a black diamond, as they are still influenced by anthropogenic activities such as canalisation in the case of the Bovenmark and recent stream restoration activities in the case of the Buurserbeek.

Looking at the diagram, the gravel-bed streams and the sand-bed streams can easily be distinguished. The gravel-bed streams, Geul and Swalm, have a significantly higher D_{50} than the other streams. The Reest and Rosep are two streams of which the sampled material was too organic to be analysed for texture. These two streams therefore do not have a D_{50} value that can be used to correctly plot them in the stability diagram. In order to still visualise these two rivers an assumption was made regarding the nature of the clastic material that might be in the stream. The material retrieved during sampling of both of these streams contained small amounts fine to medium sand which probably originated from the coversand areas surrounding these streams. The D_{50} for both of these streams is therefore set at 250 µm, which is approximately the average of the other D_{50} values of streams surrounded by coversand. An exact value is not necessary in this case, because the calculated stream powers are too low for the streams to rank in any other field of the diagram other than the laterally immobile one considering that the clastic material is indeed fine to medium sand.

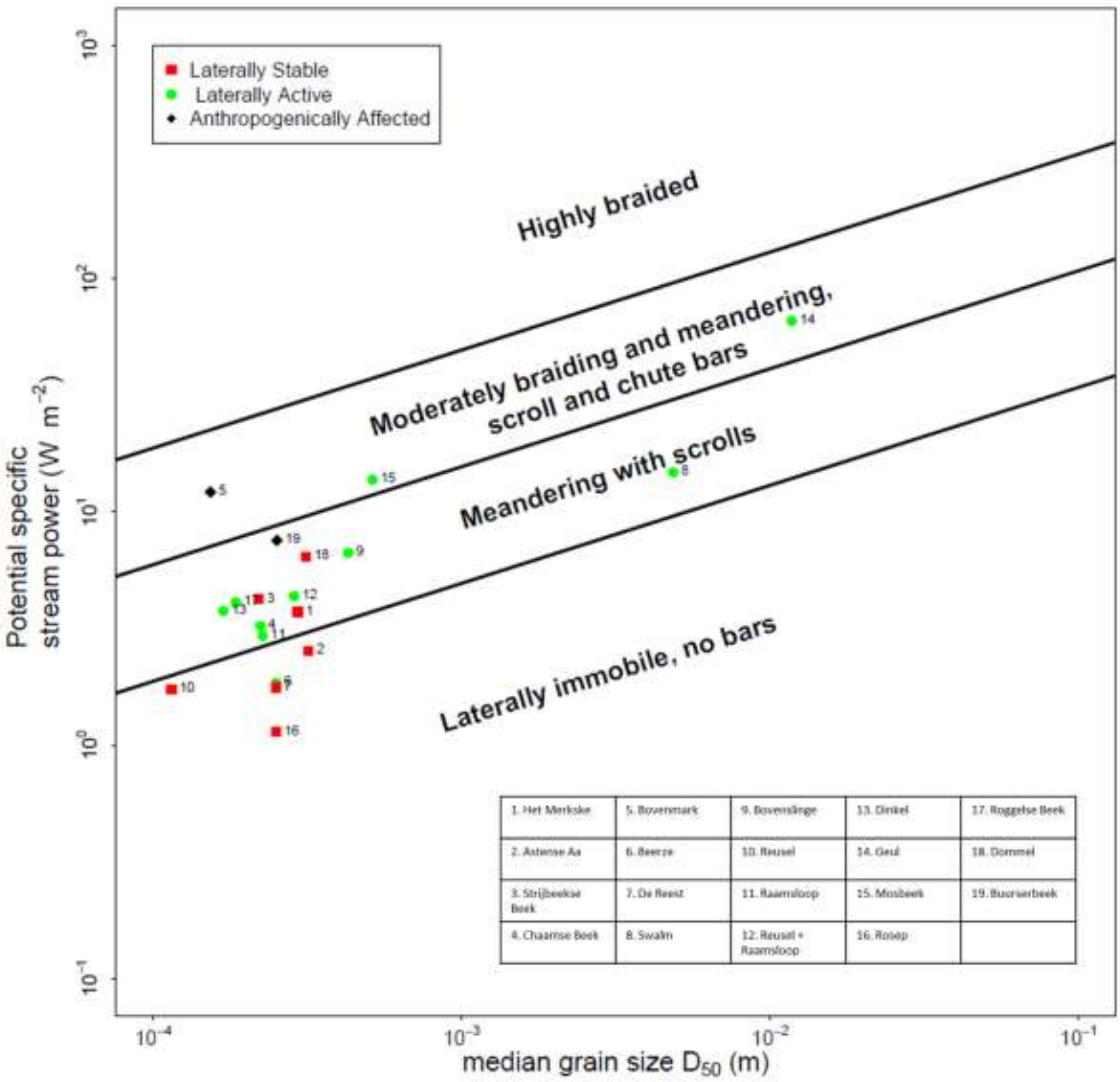

Figure 19. Stability diagram as used by Kleinhans and van den Berg (2011) *in Figure 1, with the investigated streams and their lateral activity plotted in the diagram.*

Overall, the stability diagram seems to have adequate "predictive" qualities for the investigated streams. Most of the streams that were investigated seem to plot in the correct field of the stability diagram, however still four streams plot in fields that do not match their activity. The Beerze is the only stream that is assumed to be laterally active while it plots in the laterally immobile field in the stability diagram. There is little doubt about the classification of the investigated bend as it scores quite high in the decision table and its point bar is dated at 0.06 ± 0.01 ka (Table 5).

The three other streams that do not plot in the field that matches with their presumed activity are the Dommel, the Strijbeekse Beek and Merkske. Both the Dommel and Merkske score slightly below the "threshold" in the decision table. Merkske is dated at 3.47 ± 0.18 ka, which is deemed too old to be laterally active. The Dommel is dated at 0.61 ± 0.09 ka, which is again rather close to the set "threshold" of 500 years. Kamstra (2018) and Kijm (2018), stated that for the Dommel minor lateral migration could be detected. However, the historical map analysis (Fig. 17) gives a more definitive indication to the lateral inactivity of the river. Finally, the Strijbeekse Beek is deemed inactive solely based on the decision table, where it scores quite low. Based on this score this stream was considered to be laterally inactive.

One thing that the latter three inactive streams have in common is the presence of some form of peat or very organic material in the outer bend at some depth. This seems to be a phenomenon that all laterally inactive streams have in common. This relation does not seem to go both ways, however. Two streams, Swalm and Raamsloop, do have an abundance of peat in their outer bend, but are still deemed laterally active. The organic material in the outer bank increases the bank strength and thereby decreases the erodibility. The discriminators between the activity fields need to be adjusted to account for different levels of bank cohesion.

4.2.3 Bank Erodibility

Silt-plus-clay fraction and vegetation

A proxy of the discriminator between the laterally active and inactive fields in the stability diagram was created (Fig 20) (Courtesy of my supervisor Jasper Candel). The proxy serves as a way to visualise this discriminator if the silt-plus-clay fraction in the banks is added as a third axis. Using the relation between the silt-plus-clay content and the increase in critical shear stress as formulated by Julian and Torres (2006) (Fig. 3) the diagram can be extended. The discriminator between laterally stable and meandering streams is only affected in certain areas, mostly those with a low D_{50} value and a high silt-plus-clay fraction. The larger the D_{50} of the bed material, the less pronounced the effect of the silt-plus-clay fraction becomes, until it is no longer the factor limiting lateral migration. The effect of vegetation cover is not taken into account in this plot. The shape of the discriminator will, however, remain largely similar since the relation between vegetation cover and critical shear stress is linear (Eq. 3 and Table 1). The "affected" area (dashed lines in Fig. 20) will increase mostly in the z-direction (stream power) with an increase in vegetation cover since the critical shear stress will also increase (Eq. 3).

An exemplary 2D plot (Fig. 21) was made to show what the affected area would be if only additional critical shear stress caused by silt-plus-clay cohesion was taken into account at a D_{50} of 250 µm, which is approximately the mean of all non-gravel bed streams that were sampled. Within the plot, the Reest and Rosep are missing because no silt-plus-clay content could be measured due to the organic nature of their banks. Most streams plot in the field of the diagram (< 0.4 fraction of silt-plus-clay) that remains unaffected due to the relatively low levels of silt and clay. Only two streams plot outside of this field: Geul (14) and Reusel (10). Regarding the discriminator line between laterally active and inactive streams, the Geul is largely unaffected since the D_{50} is rather large as a gravel bed river. The stream power of the Geul is also out of range for its position to change regarding this exact discriminator, but might be changed for the other discriminators that are out of the scope of this thesis. The Reusel on the other hand plots rather close to the discriminator line in the original stability diagram (Fig. 19) while it plots lower if the silt-plus-clay fraction is taken into account (Fig. 21).

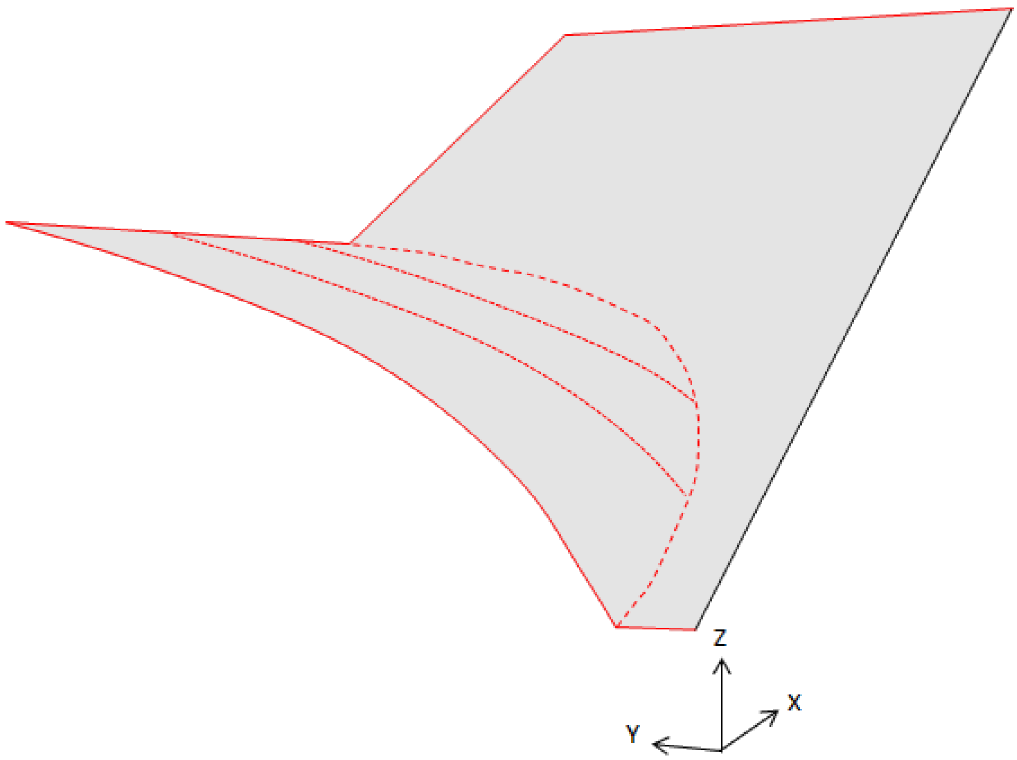

Figure 20. Example 3D plot of the stability diagram showing the shape of the discriminator field between laterally stable and meandering with scrolls. The black line corresponds to original discriminator line in the 2D plot (Fig. 19). Axis X plots the D_{50}, axis Y the silt-plus-clay fraction and axis Z the stream power.

If the vegetation of the outer bank is also taken into account according to the relation proposed by Julian and Torres (2006) (Fig. 3 and Table 1) a large spread in critical shear stress (τ_c) is found between all streams (Fig. 22). There does not seem to be a relation between the stream power and the τ_c, nor does there seem to be a clear relation between lateral activity and the τ_c. Laterally inactive streams can be found both at small τ_c values (Merkske and Dommel) and large τ_c values (Reusel and Strijbeekse Beek). This distribution does not explain the four streams that do not plot in their assumed activity fields. The lateral inactivity of the Merkske and the Dommel does not seem to be explained by their silt-plus-clay content, nor by the presence of vegetation on the outer bank. The Strijbeekse Beek does, however, have one of the largest τ_c values, if the vegetation on the outer bank is taken into account. This could be the explanation why this stream in particular is not laterally active. Another stream that has a high τ_c value is the Reusel + Raamsloop, a laterally active river that in plotted "correctly" in the 2D stability diagram (Fig. 19). If the vegetation cover and silt-plus-clay relation to the τ_c are taken into account as is this stream might now plot incorrectly under the discriminator. This would not increase the predictive power of the diagram, because the Strijbeekse Beek would potentially be correctly adjusted while the Reusel + Raamsloop is potentially incorrectly adjusted.

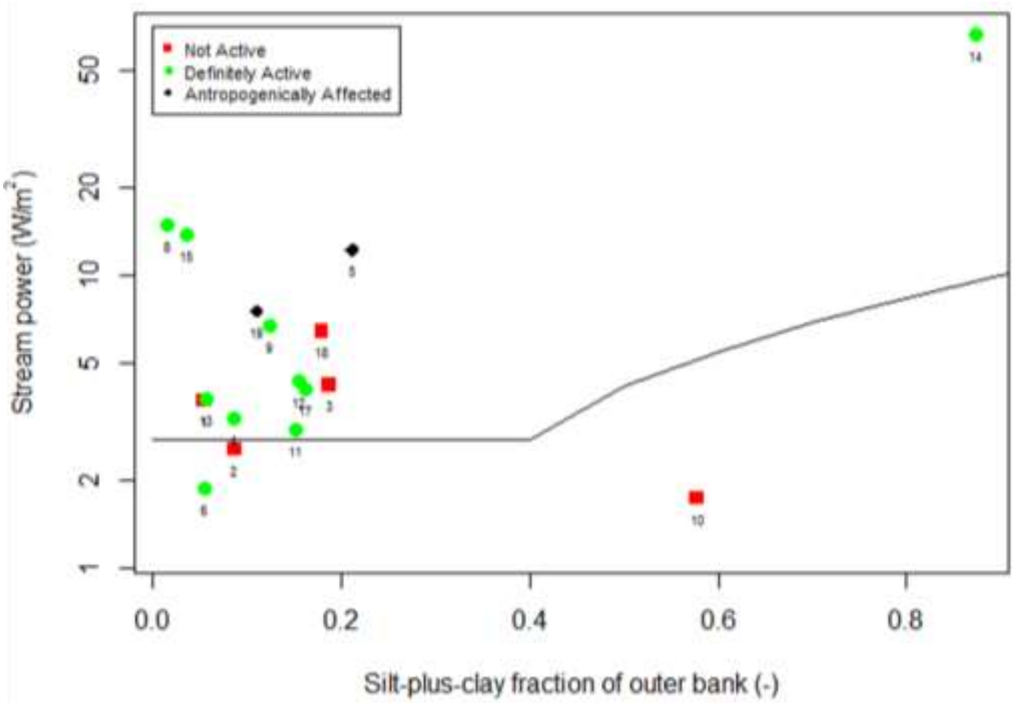

Figure 21. Cross-section of the stability diagram at a D_{50} value of 250 µm. The stream power plotted against the silt-plus-clay fraction of the outer bank. The line indicates the discriminator between laterally stable and meandering.

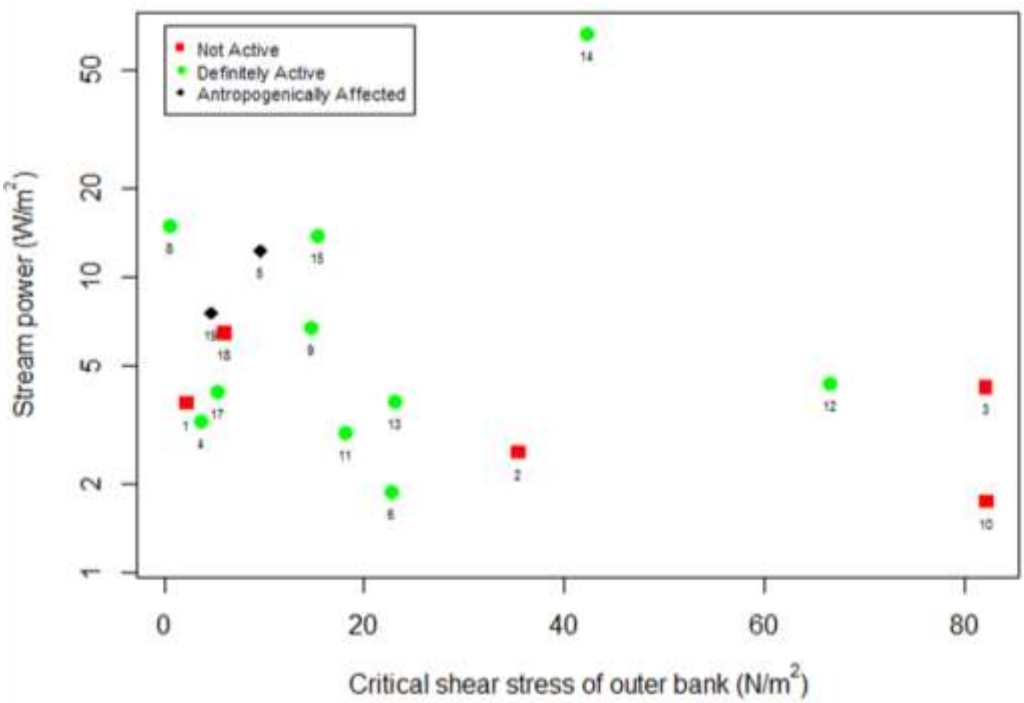

Figure 22. A plot of the critical shear stress of the streams based on silt-plus-clay content and vegetation cover, plotted against the stream power.

Organic content

As stated before, due to time constraints it was not possible to accurately determine the organic content of the bank samples using the loss on ignition method. The relative organic matter content of the outer banks was however estimated by analysing the coring data for fieldwork in LLG. Samples taken in the field for texture analysis were also inspected by hand, using the Munsell Color Booklet (Munsell Color, 2009) . After this analysis all streams were ranked, relative to each other, on the organic content in the outer bank and plotted against the stream power (Fig. 23).

Striking is that all laterally inactive streams are within the most organic half of the sampled streams. There also seems to be an inverse relation between the stream power and the relative organic matter content. However, since this is only a relative ranking and no exact organic content values can be assigned to the streambanks, little can be concluded about this potential relation.

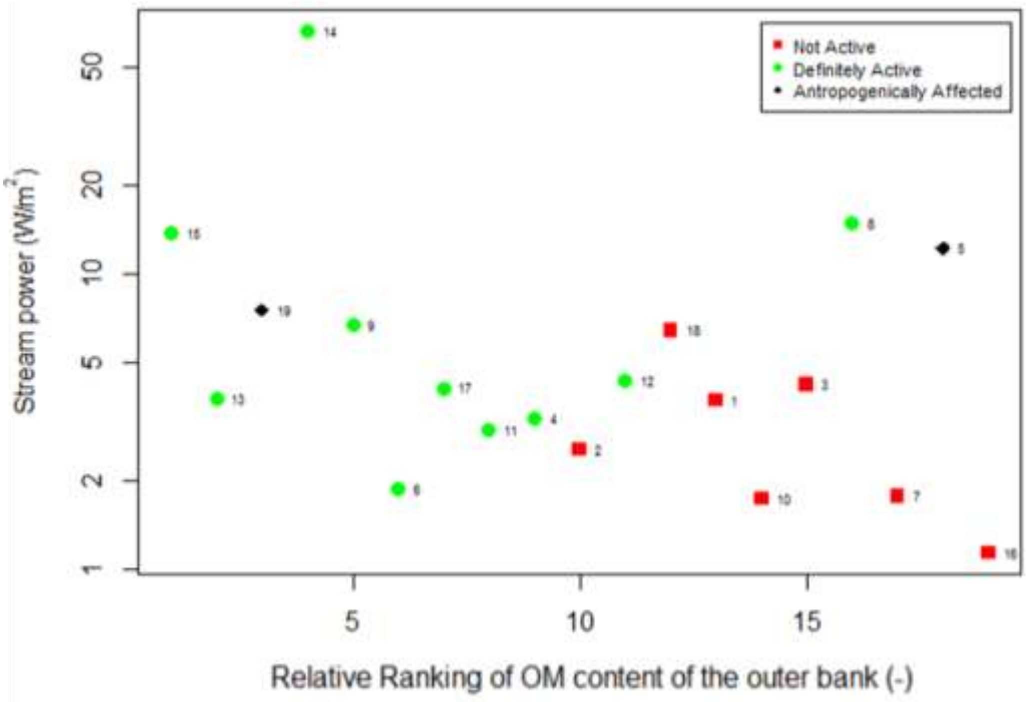

Figure 23. The relative ranking of organic matter content of the outer bank, based on the entire depth of the channel in LLG of all streams, plotted against the stream power.

5. Discussion

According to the findings presented in the decision table (Table 4) combined with the corrections of the OSL results, it can be stated that 10 out of the 19 streams are deemed to be laterally active. Often this lateral migration happens quite slowly, in the range of centimetres per year as could be deduced from the OSL dates (Table 5). It can therefore be hard to distinguish the lateral activity in streams since the indicators of erosion are not as strong as those in larger river systems. The image of a classic meandering river (Fig. 2B) as for instance posed in Kleinhans and Van den Berg (2011), does not seem to apply for these streams. The classic meandering river image has point bars of the inside of every river bend, this shows that every bend is also laterally active. This does not seem to be the case for most active lowland streams, where not every single bend is actively migrating as is shown in the historical maps of the Roggelse Beek (Fig. 16). The bends that are deemed laterally active, do show a lot of similarities with the classic meandering river bends. They have point bars and are actively eroding the outer bank. The lateral activity found in lowland streams should be considered as a type of meandering, but it should not be regarded as the classic type of meandering as posed in Figure 2B.

Overall the original (2D) stability diagram works rather well as a "predictor" for the lateral activity of the small streams that were investigated during the fieldwork. Since all but one of the investigated streams in the Netherlands can be found in fields that are dominated by coversands (Fig. 5) both the D_{50} value and the silt-plus-clay content of the banks differ only slightly. Therefore, these streams are comparable and plot within the same field of the stability diagram. The stream power is one of the variables that has a larger variation than the D_{50} and therefore causes a large part of the deviation in lateral activity between the streams. This is probably the reason why so many of the investigated streams plot correctly without the addition of another parameter. It therefore seems that streams with an average discharge < 10 $m^3\ s^{-1}$ are indeed plottable in the stability diagram, supporting the assumption made by Makaske et al. (2016). The decision table that was created to indicate the lateral activity of streams (Table 4) also appears to work, at least for the investigated streams. The findings are supported by the OSL data and the in-depth study of historical maps.

Another requirement posed by Kleinhans and Van den Berg (2011) is that a river has to be natural in order for it to be plotted in the stability diagram. All investigated streams were picked from the KWR dataset because they were stated to be unaltered in part of their course, the exception being the Bovenmark. After fieldwork the Buurserbeek was decided to be left out due to human intervention in its course. The other stream courses were (mostly) untouched by direct anthropogenic influence such as canalisation. Indirect anthropogenic influence was, however, found in most cases as drainage networks were set up in the area surrounding the streams (Table 2). The addition of drainage networks changes the hydrological character of an area, decreasing the average travel time of a water particle to the stream and thereby increasing the peak discharge of the stream. The intensity of a discharge peak is an important factor in erosion processes as the largest part of bank erosion happens during these peak events (Julian and Torres, 2006; Rinaldi et al., 2008). The amount of bank erosion and lateral activity has therefore increased ever since these water management through drainage networks was first introduced in the Middle ages (Kaijser, 2002), making the system not completely natural. There are however no "unaffected" area left within the Netherlands after the last part of Dutch wilderness disappeared in 1871 with the cutting of the Beekbergerwoud (Kwak and Kuiters, 2014). It is therefore quite unrealistic to only look at completely natural stretches of river, since the current courses of the investigated streams are probably as natural as they realistically can be. The semi-natural state of the streams is therefore deemed good enough for the plot in the stability diagram.

It still remains difficult to compare the lateral activity of these streams to that of larger rivers. Where large rivers such as the Mississippi migrate at rates of metres per year (Hudson and Kessel, 2000), these streams only migrate at rates of centimetres up to decimetres per year. Too little data were gathered to do an in-depth analysis of the migration rates of these streams and relate them to other features such as stream width or bend radius in order to find the relation between larger rivers and these streams. Also the streams that plot rather close to the discriminator can be hard to "predict" because the differences in stream power between the streams are quite small. In these cases it should be kept in mind that the difference here between active and inactive are in the order of a lateral migration rate of perhaps a few centimetres per year. It is also unknown whether the distance to the discriminator can be used as a proxy for the magnitude of lateral activity. Logically there should be some sort of relation since the discriminator roughly indicates the stream power required for a stream to become laterally active. If the stream power is higher than the discriminator, there should be larger driving forces of erosion than resisting forces, making more erosion and lateral migration possible.

Another thing that should be addressed, is the plot of the stream power and the relative organic content of the outer bank of the streams. All laterally inactive streams are within the most organic half of the sampled streams. There also seems to be a slight inverse relation between the stream power and the relative ranked organic matter content. Unfortunately this cannot be subjected to a correlation test since the organic matter content of these streambanks are ranked relative to each other. However, this relation would be expected. Organic matter can accumulate in areas with low energy (Cameron et al., 1989), it is therefore expected that the streams with the lowest energy also have the highest relative organic matter content. Organic matter in the soil has a stabilising effect on the soil, increasing the cohesion of both sandy and clay rich soils (Daniels, 1971; Zhang and Hartge, 1990). In cases where accumulation of organics is more extreme, such as in peatlands, the soil can become very hard to erode (Candel et al., 2017; Nanson et al., 2010). A higher amount of organic matter should therefore have a similar effect as a higher silt-plus-clay content on the stability diagram (Fig. 22). Because the organic matter is not taken up in the formula constructed by Julian and Torres (2006) and the exact organic matter contents of the streambanks is unknown, no relation between the τ_c and organic matter can be plotted yet.

Assuming that the critical shear stress for organic matter increases in a similar fashion as it does for the silt-plus-clay content, Figures 22 and 23 should show a similar shape for the lateral stability discriminator. It could be said that for the investigated streams the organic matter content of the outer bank is more predictive for lateral stability than the silt-plus-clay content and the vegetation cover combined. Ideally, all three of these factors should be taken into account because they are all constituents of the resisting forces of erosion. With the addition of organic matter to the stability diagram through shear stress, it is perhaps possible to explain the lateral inactivity of the Dommel, Merkske and Strijbeekse Beek as all of these have a relatively high organic matter content in their outer bank.

Apart from all the correctly plotted streams, there still remain four streams that do not plot in the field matching their activity. The Dommel, Merkske and Strijbeekse Beek all have in common that they are bordered by high levels of organic matter, which is likely to be the explanation for their lateral inactivity. On the other hand there is the Beerze, a stream that is deemed active, while it should not have the stream power to be active according to the original stability diagram (Fig. 19). It is supported by study of the historical maps that this bend of the Beerze is indeed laterally active. The historical maps also show that this bend is one of the few active river bends within this stretch of the river. Other bends do not show as much lateral activity, at least not significant enough to rule out the possibility of human error in the historical maps. Ideally, multiple river bends are inspected to determine lateral activity in a stream since not every bend can be laterally active, however this was not possible due to time and cost constraints. It might therefore be the case that the Beerze is overall laterally inactive, but that the sampled bend is an outlier. The reason as to why this might be the case for this particular bend is, however, unknown since no clear differences could be found between this bend and other ones.

The problem with the Beerze bend also raises the question whether there might have been a prejudice toward active bends whilst selecting the sampling locations for fieldwork. This probably was the case for some streams that were selected, however the overall analysis did not only focus on the selected bends in particular. By studying (historical) maps and the DEM of the area surrounding the selected field location it is possible to determine whether the sampled bend is representative enough for the area. This was deemed the case for all streams apart from the Beerze, where it only became apparent because it was studied more closely due to its position in the stability diagram.

Overall the stability diagram as presented by Kleinhans and Van den Berg (2011) with the initial dataset (Fig. 1), can be improved by the addition of the missing resisting force: the bank resistance. Especially for the lowest discriminator between laterally immobile and meandering rivers this addition can be useful. Rivers that plot around this discriminator can be constricted enough by organics in their surroundings to prevent them from being laterally active. Similar claims can be made about high concentrations of silt and clay in the surrounding area. Even though most of the studied streams did not contain enough silt and clay to be significantly affected, there should be more rivers throughout the world that are in clay-rich areas and are affected. No claims can be made about the higher discriminators, because only a couple of the studied streams plot in these fields. This was also outside of the scope of this research.

Focussing on these Dutch streams in particular the most important factor that influences the lateral activity of the streams, apart from the stream power, is the presence of organic matter in the area surrounding the stream. Because this feature was not the focus of this study this is unfortunately an assumption, it could not be checked by plotting it in a graph similar to Figure 21. However, the relative plots taken from the texture samples and the soil descriptions show promising results. With organic matter measurements of the streambanks, the stability diagram could be improved to even work better as a predictor for lateral activity in Dutch streams than it already is. For Dutch streams in valleys that are not (completely) filled with peat, the stability diagram should already be usable as lateral activity "predictor". The magnitude of the lateral activity or the migration rate can however not be deduced from the stability diagram, because this was not the intention of the stability diagram.

6. Conclusion

Overall the three research questions could be answered:

It was concluded that a significant amount of the Dutch lowland streams (10 out of 19) were considered to be laterally active. This could be deduced using the decision diagram that was produced for the identification of lateral activity in these streams. The decision diagram is not perfect, but correctly determined lateral activity in 8 out of 9 OSL sampled streams, which makes it good enough for further use.

For Dutch streams in particular, the stability diagram works rather well as "predictor" already. Since Dutch streams can mostly be found in areas consisting of coversands and therefore have relatively uniform bank material. Even though the stability diagram already works quite well still 4 out of 19 streams plot in a different field than their stream power would suggest.

The stability diagram can be improved by addition of the bank resistance. A large part of this resisting force is the presence of organic matter (either in the form of peat or otherwise). Silt-plus-clay and additional bank strength caused by vegetation could also be a source of bank resistance as well, but this could not be concluded using the streams investigated for this research. For Dutch lowland streams, the silt-plus-clay fraction and vegetation cover are less important compared to the presence of organic material. However, the inclusion of organic matter content in the stability diagram seems to be the best option for Dutch streams in particular since, many low energy streams are significantly influenced by peat and organic matter in the streambanks.

7. Recommendations

According to the findings of this thesis, it is possible for waterboards and other governing bodies to use the stability diagram to predict the lateral activity of streams. The stability diagram should give a fair estimation of the lateral activity, especially in cases where the streams are located in a sandy environment, as most streams in the Netherlands are. However, in cases where large amounts of organic matter are found close to the stream, the stability diagram might not give an accurate prediction. These streams might not be as laterally active as the stability diagram would indicate, this should be taken into account. If there is a wish to improve the stability diagram further for these cases, people should look into the relation between organic matter and the critical shear stress. This relation could eventually be implemented into the diagram to improve it further.

References

Alden, A., 2019. Densities of common rocks and minerals [WWW Document]. URL https://www.thoughtco.com/densities-of-common-rocks-and-minerals-1439119 (accessed 2.8.19).

Anonymous, 2019. Meanders & Associated Landforms [WWW Document]. URL https://www.geocaching.com/geocache/GC59WAY_meanders-associated-landforms?guid=edc1efe0-b44f-4071-bc6c-e0b832fa6c63 (accessed 11.3.19).

Bateman, M.D., Van Huissteden, J., 1999. The timing of last-glacial periglacial and aeolian events, Twente, eastern Netherlands. J. Quat. Sci. https://doi.org/10.1002/(SICI)1099-1417(199905)14:3<277::AID-JQS460>3.0.CO;2-W

Beckman Coulter Inc., 2011. LS 13 320 Laser diffraction particle size analyzer instructions for use [WWW Document]. URL https://www.beckmancoulter.com/wsrportal/techdocs?docname=B05577AB.pdf (accessed 7.12.19).

Berendsen, H.J.A., Stouthamer, E., 2002. Paleogeographic evolution and avulsion history of the Holocene Rhine-Meuse delta, The Netherlands. Geol. en Mijnbouw/Netherlands J. Geosci. https://doi.org/10.1017/S0016774600020606

Berendsen, H.J.A., Stouthamer, E., 2001. Palaeogeographic development of the Rhine-Meuse delta, the Netherlands. Koninklijke Van Gorcum.

Bizzi, S., Lerner, D.N., 2015. The use of stream power as an indicator of channel sensitivity to erosion and deposition processes. River Res. Appl. 31, 16–27. https://doi.org/10.1002/rra.2717

Bøtter-Jensen, L., Andersen, C.E., Duller, G.A.T., Murray, A.S., 2003. Developments in radiation, stimulation and observation facilities in luminescence measurements. Radiat. Meas. 37, 535–541. https://doi.org/10.1016/S1350-4487(03)00020-9

Buscombe, D., Rubin, D.M., Warrick, J.A., 2010. A universal approximation of grain size from images of noncohesive sediment. J. Geophys. Res. Earth Surf. 115, n/a-n/a. https://doi.org/10.1029/2009JF001477

Cameron, C.C., Esterle, J.S., Palmer, C.A., 1989. The geology, botany and chemistry of selected peat-forming environments from temperate and tropical latitudes. Int. J. Coal Geol. 12, 105–156. https://doi.org/10.1016/0166-5162(89)90049-9

Candel, J.H.J., Kleinhans, M.G., Makaske, B., Hoek, W.Z., Quik, C., Wallinga, J., 2018. Late Holocene channel pattern change from laterally stable to meandering – a palaeohydrological reconstruction. Earth Surf. Dyn. Discuss. (in Rev. 723–741. https://doi.org/10.5194/esurf-2018-31

Candel, J.H.J., Makaske, B., Storms, J.E.A., Wallinga, J., 2017. Oblique aggradation: a novel explanation for sinuosity of low-energy streams in peat-filled valley systems. Earth Surf. Process. Landforms 42, 2679–2696. https://doi.org/10.1002/esp.4100

Cunningham, A.C., Wallinga, J., 2012. Quaternary geochronology realizing the potential of fluvial archives using robust OSL chronologies. Quat. Geochronol. 12, 98–106. https://doi.org/10.1016/j.quageo.2012.05.007

Cunningham, A.C., Wallinga, J., 2010. Selection of integration time intervals for quartz OSL decay curves. Quat. Geochronol. 5, 657–666. https://doi.org/10.1016/j.quageo.2010.08.004

Daniels, D.E., 1971. Shear properties of an organic soil and the same soil with the organic matter removed (MSc Thesis), 1-89. University of Missouri, Columbia, MO.

De Bakker, H., Schelling, J., 1989. Systeem van bodemclassificatie voor Nederland; De hogere niveaus. Tweede gewijzigde druk, bewerkt door J. Brus en C. van Wallenburg. DLO Staring Centrum, Wageningen.

Dépret, T., Gautier, E., Hooke, J., Grancher, D., Virmoux, C., Brunstein, D., 2015. Hydrological controls on the morphogenesis of low-energy meanders (Cher River, France). J. Hydrol. 531, 877–891. https://doi.org/10.1016/j.jhydrol.2015.10.035

Dietze, M., Kreutzer, S., Burow, C., Fuchs, M.C., Fischer, M., Schmidt, C., 2016. The abanico plot: Visualising chronometric data with individual standard errors. Quat. Geochronol. 31, 12–18. https://doi.org/https://doi.org/10.1016/j.quageo.2015.09.003

Dunn, I.S., 1959. Tractive resistance of cohesive channels. J. Soil Mech. Found. Div. 85, 1–24.

Eekhout, J., Hoitink, T., 2014. Morfodynamiek van Nederlandse laaglandbeken. Stowa 15, 113.

Ferguson, R.I., 2005. Estimating critical stream power for bedload transport calculations in gravel-bed rivers. Geomorphology 70, 33–41. https://doi.org/10.1016/j.geomorph.2005.03.009

Galbraith, R.F., Roberts, R.G., Laslett, G.M., Yoshida, H., Olley, J.M., 1999. Optical dating of single and multiple grains of quartz from jinmium rock shelter, northern Australia: part I, Experimental design and statistical models. Archaeometry 2, 339–364. https://doi.org/10.1111/j.1475-4754 .1999.tb00987.x

Gouw, M.J.P., Erkens, G., 2007. Architecture of the Holocene Rhine-Meuse delta (the Netherlands) - A result of changing external controls. Geol. en Mijnbouw/Netherlands J. Geosci. 86, 23–54. https://doi.org/10.1017/S0016774600021302

Heiri, O., Lotter, A.F., Lemcke, G., 2001. Loss on ignition as a method for estimating organic and carbonate content in sediments: reproducibility and comparability of results. J. Paleolimnol. 25, 101–110. https://doi.org/10.1023/A:1008119611481

Het Kadaster, 2019. TopoTijdreis [WWW Document]. URL https://www.topotijdreis.nl/ (accessed 4.20.19).

HisGIS [WWW Document], 2019. URL https://hisgis.nl/ (accessed 4.20.19).

Hudson, P.F., Kessel, R.H., 2000. Channel migration and meander-bend curvature in the lower Mississippi River prior to major human modification. Geology.

Julian, J.P., Torres, R., 2006. Hydraulic erosion of cohesive riverbanks. Geomorphology 76, 193–206. https://doi.org/10.1016/j.geomorph.2005.11.003

Kaijser, A., 2002. System Building from Below: Institutional Change in Dutch Water Control Systems. Technol. Cult. 43, 521–548.

Kamstra, R., 2018. Duthmala (MSc Thesis), 1-104. Wageningen University & Research.

Kijm, N., 2018. The Late Glacial and Holocene morphodynamic evolution of the lowland stream the Dommel, southern Netherlands (MSc Thesis), 1-83. Wageningen University & Research.

Kleinhans, M.G., Cohen, K.M., Hoekstra, J., Ijmker, J.M., 2011. Evolution of a bifurcation in a meandering river with adjustable channel widths, Rhine delta apex, The Netherlands. Earth Surf. Process. Landforms 36, 2011–2027. https://doi.org/10.1002/esp.2222

Kleinhans, M.G., Schuurman, F., Bakx, W., Markies, H., 2009. Meandering channel dynamics in highly cohesive sediment on an intertidal mud flat in the Westerschelde estuary, the Netherlands. Geomorphology. https://doi.org/10.1016/j.geomorph.2008.10.005

Kleinhans, M.G., Van den Berg, J.H., 2011. River channel and bar patterns explained and predicted by an empirical and a physics-based method. Earth Surf. Process. Landforms 36, 721–738. https://doi.org/10.1002/esp.2090

Kwak, A., Kuiters, L., 2014. Wildernis in een getemd Europa, in: Janssen, J.A.M., Schaminée, J.H.J. (Eds.), Het Oude Continent. Beschouwingen over de Natuur in Europa. KNNV Uitgeverij, Zeist, pp. 161–176.

Leopold, L.B., Maddock, T.J., 1953. The Hydraulic Geometry of Stream Channels and Some Physiographic Implications, Geological Survey Professional Paper 252.

Madsen, A.T., Murray, A.S., 2009. Optically stimulated luminescence dating of young sediments: A review. Geomorphology. https://doi.org/10.1016/j.geomorph.2008.08.020

Makaske, B., Maas, G., 2015. Handboek geomorfologisch beekherstel. Stowa-rapport 2015-02 02, 188.

Makaske, B., Smith, D.G., Berendsen, H.J.A., de Boer, A.G., van Nielen-Kiezebrink, M.F., Locking, T., 2009. Hydraulic and sedimentary processes causing anastomosing morphology of the upper Columbia River, British Columbia, Canada. Geomorphology 111, 194–205. https://doi.org/10.1016/j.geomorph.2009.04.019

Makaske, B., Van der Deijl, E.C., Kleinhans, M.G., 2016. Het natuurlijke patroon van beken. Landschap 4.

Micheli, E.R., Kirchner, J.W., 2002. Effects of wet meadow riparian vegetation on streambank erosion. 2. Measurements of vegetated bank strength and consequences for failure mechanics. Earth Surf. Process. Landforms 27, 687–697. https://doi.org/10.1002/esp.340

Munsell Color, 2009. Munsell soil color charts: with genuine Munsell color chips. 2009 year revised. Grand Rapids, MI : Munsell Color, 2009.

Nanson, G.C., Knighton, A.D., 1996. Anabranching rivers: Their cause, character and classification. Earth Surf. Process. Landforms 21, 217–239. https://doi.org/10.1002/(SICI)1096-9837(199603)21:3<217::AID-ESP611>3.0.CO;2-U

Nanson, R.A., Nanson, G.C., Huang, H.Q., 2010. The hydraulic geometry of narrow and deep channels; evidence for flow optimisation and controlled peatland growth. Geomorphology 117, 143–154. https://doi.org/10.1016/j.geomorph.2009.11.021

Notebaert, B., Verstraeten, G., 2010. Sensitivity of West and Central European river systems to environmental changes during the Holocene: A review. Earth-Science Rev. 103, 163–182. https://doi.org/10.1016/j.earscirev.2010.09.009

Poreba, G.J., Śnieszko, Z., Moska, P., 2015. Application of OSL dating and ^{137}Cs measurements to reconstruct the history of water erosion: A case study of a Holocene colluvium in Świerklany, south Poland. Quat. Int. 374, 189–197. https://doi.org/10.1016/j.quaint.2015.04.004

Preusser, F., Degering, D., Fuchs, M., Hilger, A., Kadereit, A., Klasen, N., Krbetschek, M., Richter, D., Spencer, J., 2008. Luminescence dating: basics, methods and applications. Eiszeitalter und Gegenwart Quat. Sci. J. https://doi.org/http://dx.doi.org/10.3285/eg.57.1-2.5

Preusser, F., Schmitt, L., Delile, H., Grosprêtre, L., 2011. Optically stimulated luminescence (OSL) dating of the sedimentation history of the Yzeron Basin (Chaudanne sub-catchment), Rhône valley, France. Quaternaire 22, 73–83. https://doi.org/10.4000/quaternaire.5877

Quik, C., Wallinga, J., 2018. Reconstructing lateral migration rates in meandering systems; a novel Bayesian approach combining OSL dating and historical maps. Earth Surf. Dyn. Discuss. (in Rev. 705–721. https://doi.org/10.5194/esurf-2018-30

Rinaldi, M., Mengoni, B., Luppi, L., Darby, S.E., Mosselman, E., 2008. Numerical simulation of hydrodynamics and bank erosion in a river bend. Water Resour. Res. 44, 1–17. https://doi.org/10.1029/2008WR007008

Robert, A., 2003. River processes - An introduction to fluvial dynamics. Oxford University Press, Oxford. https://doi.org/https://doi.org/10.4324/9780203770481

Shields, A., 1936. Application of similarity principles and turbulence research to bed-load movement. Translated by W.P. Ott and J.C. Uchelen, Soil Conservation Service. Pasadena, CA.

Stanley, D.J., Hait, A.K., 2000. Deltas, radiocarbon dating, and measurements of sediment storage and subsidence. Geology 28, 295–298. https://doi.org/10.1130/0091-7613(2000)28<295:DRDAMO>2.0.CO;2

Ten Cate, J.A.M., Van Holst, A.F., Kleijer, H., Stolp, J., 1995. Handleiding bodemgeografisch onderzoek; richtlijnen en voorschriften. Deel B: Grondwater, Technisch document / DLO-Staring Centrum : 19-B. SC-DLO, Wageningen.

Thorne, C.R., 1990. Effects of vegetation on riverbank erosion and stability, in: Thornes, J.B., Group, B.G.R. (Eds.), Vegetation and Erosion: Processes and Environments. J. Wiley, Chichester, pp. 128–144.

Van den Berg, J.H., 1995. Prediction of alluvial channel pattern of perennial rivers. Geomorphology 12, 259–279. https://doi.org/10.1016/0169-555X(95)00014-V

Van der Meene, E.A., Van der Staay, J., Teoh, L.H., 1979. The Van der Staay suction-corer: a simple apparatus for drilling in sand below groundwater table. Rijks Geologische Dienst, Haarlem.

Vannoppen, W., Poesen, J., Peeters, P., De Baets, S., Vandevoorde, B., 2016. Root properties of vegetation communities and their impact on the erosion resistance of river dikes. Earth Surf. Process. Landforms 41, 2038–2046. https://doi.org/10.1002/esp.3970

Vanoni, V.A., 2006. Sedimentation engineering. American Society of Civil Engineers. https://doi.org/10.1061/9780784408230

Wallinga, J., 2002. Optically stimulated luminescence dating of fluvial deposits: A review. Boreas. https://doi.org/10.1080/030094802320942536

Wintle, A.G., Murray, A.S., 2006. A review of quartz optically stimulated luminescence characteristics and their relevance in single-aliquot regeneration dating protocols. Radiat. Meas. 41, 369–391. https://doi.org/https://doi.org/10.1016/j.radmeas.2005.11.001

Yang, L.H., Long, H., Cheng, H.Y., He, Z., Hu, G., 2018. OSL dating of a mega-dune in the eastern Lake Qinghai basin (northeastern Tibetan Plateau) and its implications for Holocene aeolian activities. Quat. Geochronol. 49, 165–171. https://doi.org/10.1016/j.quageo.2018.02.005

Zhang, H.Q., Hartge, K.H., 1990. Cohesion in unsaturated sandy soils and the influence of organic matter. Soil Technol. 3, 311–326. https://doi.org/10.1016/0933-3630(90)90013-S

Appendix I: Fieldforms

Name: Name of the river or stream that is investigated.

Date: Fill in the current date.

Site No: Indicate which location you are sampling using a unique number for each location. Starting with 1 at the first location.

Reference Location: Indicate where you are with reference to the river or stream. The inner or outer bend, also indicate if there is no bend.

Altitude/ Easting / Northing: Fill in the coordinates according to the RD new coordinate system.

KWR Streamtype: Indicate the streamtype of the stream or river following the diagram in the manual of geomorphological stream restoration of STOWA.

Vegetation cover: Give an indication of the total vegetation cover and the main type of vegetation (grass, bushes, and trees) and their respective cover percentages. Use an area of approximately 10 x 10 m on your side of the river or stream. Also indicate the vegetation cover on the streambank.

Migration indications: Indicate if there are any clear signs that the river or stream has been migration. This includes bank erosion, undulations in the inner bend, point bars, meandering. This also includes vertical migration such as clear signs of aggradation and incision.

Dominant soil type: Roughly note the dominant soil type in the area if this is easily visible. Possible answers could be: clay dominated, sand dominated, peat (OM) dominated. Also indicate is there is a variety of multiple soils types on a small scale. Use an area of approximately 10 x 10 m on your side of the stream.

Remarks: Note any aspects in the landscape and on the surface that are not yet covered by the form, but should be taken into account.

Texture Class: The main texture class of the horizon, texture type should be obtained through the soil texture triangle from the FAO.

Structure Class: The main structure class of the horizon, structure classes should be taken from the FAO.

Colour: The colour value and hue according to the Munsell colour book.

Classification: The soil classification according to the Dutch Soil Classification system.

Remarks: Note any aspects within the soil profile that are noteworthy, but have not been mentioned before such as clear layering, a fining upward sequence.

Symb: The letter combinations that indicate the type of soil horizon that is encountered in the soil profile. Letter codes according to the FAO soil classification system.

Depth: The minimum and maximum depth in cm where the horizon can be found.

Field form

MSc Thesis Tom Harkema

Name:	GPS-Reading (RD New)
Date:	RD New / Easting [m]:
Site No:	Altitude [m]: / Northing [m]:
Reference Location:	KWR Streamtype:

Site description

Vegetation cover:		Migration indications:
Dominant soil type:	Remarks:	

Soil profile description #1					**Soil profile description #2**				
Horizon		Texture	Structure	Colour	Horizon		Texture	Structure	Colour
Symb	Depth (cm)	Class	Class	Moist	Symb	Depth (cm)	Class	Class	Moist
Classification:					Classification:				

Remarks:

Appendix II: Grain size analysis

Name	Number	Bed			Inner Bank				Outer Bank			
		D10 (um)	D_{50} (um)	D90 (um)	SC (%)	D10 (um)	D_{50} (um)	D90 (um)	SC (%)	D10 (um)	D_{50} (um)	D90 (um)
Het Merkske	1	133	294	540	5	96	204	345	6	98	199	321
Astense Aa	2	144	319	738	6	104	220	367	9	68	158	275
Strijbeekse Beek	3	117	220	345	9	68	183	309	19	16	185	419
Chaamse Beek	4	102	223	399	6	93	195	322	9	70	157	270
Bovenmark	5	57	153	305	22	13	115	209	21*	12*	135*	295*
Beerze	6	147	250	387	7	88	196	345	6	88	214	370
De Reest	7	#N/A	#N/A	#N/A	#N/A	#N/A	#N/A	#N/A	#N/A	#N/A	#N/A	#N/A
Swalm	8	277*	4845*	15955*	8	106	249	407	2*	286*	842*	2357*
Bovenslinge	9	215*	428*	3127*	11	55	154	254	13	52	134	222
Reusel	10	21	114	293	27	12	113	251	58	3	45	270
Raamsloop	11	33*	226*	1013*	23	10	156	300	15	47	159	315
Reusel + Raamsloop	12	70	286	513	21	14	159	320	16	46	160	318
Dinkel	13	84	169	263	3	128	214	308	6	85	188	304
Geul	14	2693*	11764*	16593*	49	11	64	281	87	3	32	68
Mosbeek	15	232*	514*	1218*	2*	184*	537*	8181*	4*	139*	356*	2332*
Rosep	16	#N/A	#N/A	#N/A	#N/A	#N/A	#N/A	#N/A	#N/A	#N/A	#N/A	#N/A
Roggelse Beek	17	71	185	306	44	4	85	235	16	40	137	249
Dommel	18	155	313	646	21	15	164	282	18	18	172	440
Buurserbeek	19	121	252	476	15*	33*	160*	425*	11	56	197	374

*Samples where a correction was made because the sample contained gravel (>2 mm)

Appendix III: Digital Elevation Model of streams

Stream channels are clearly visible, they are coloured dark blue or white. Sampling locations of the inner and outer bank are indicated by red dots.

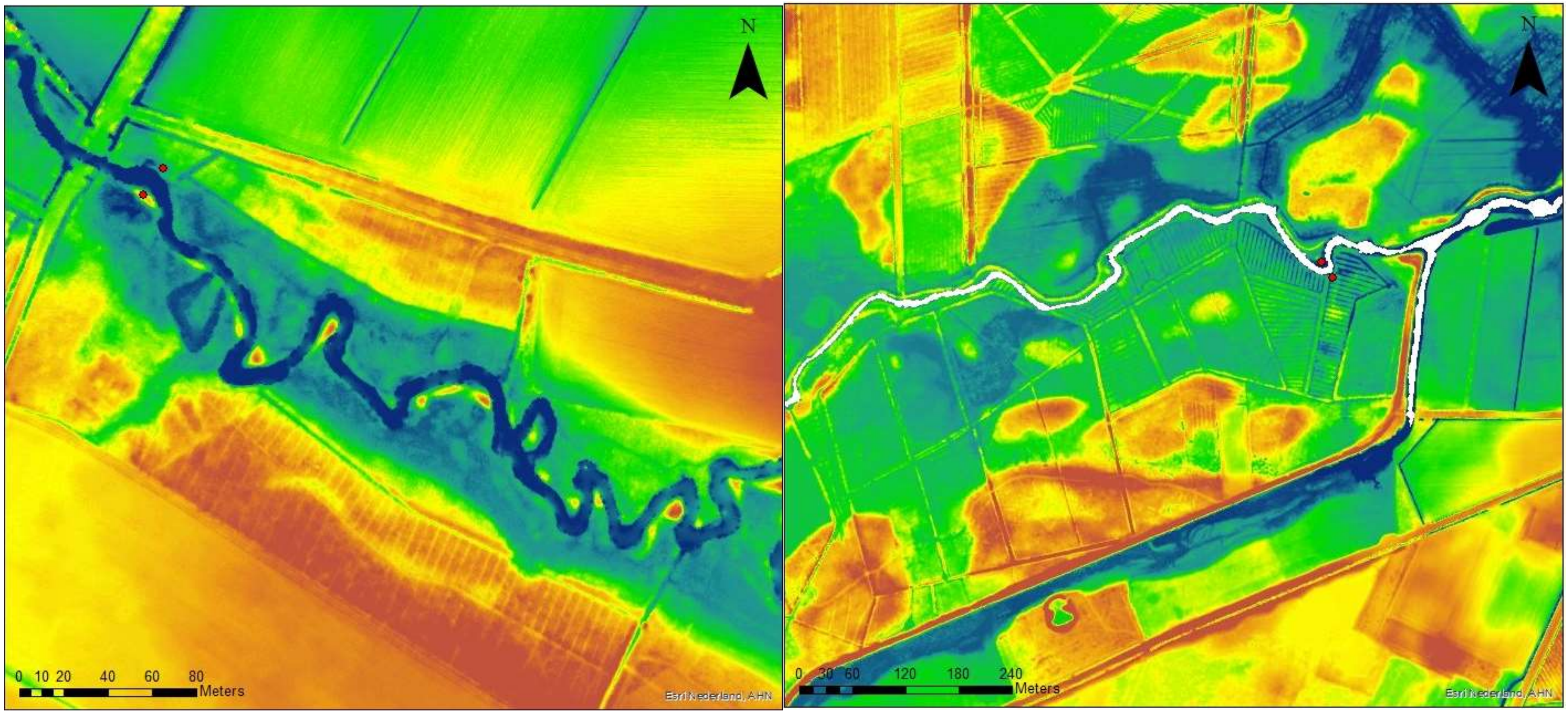

Left: *Astense Aa*
Right: *Beerze*

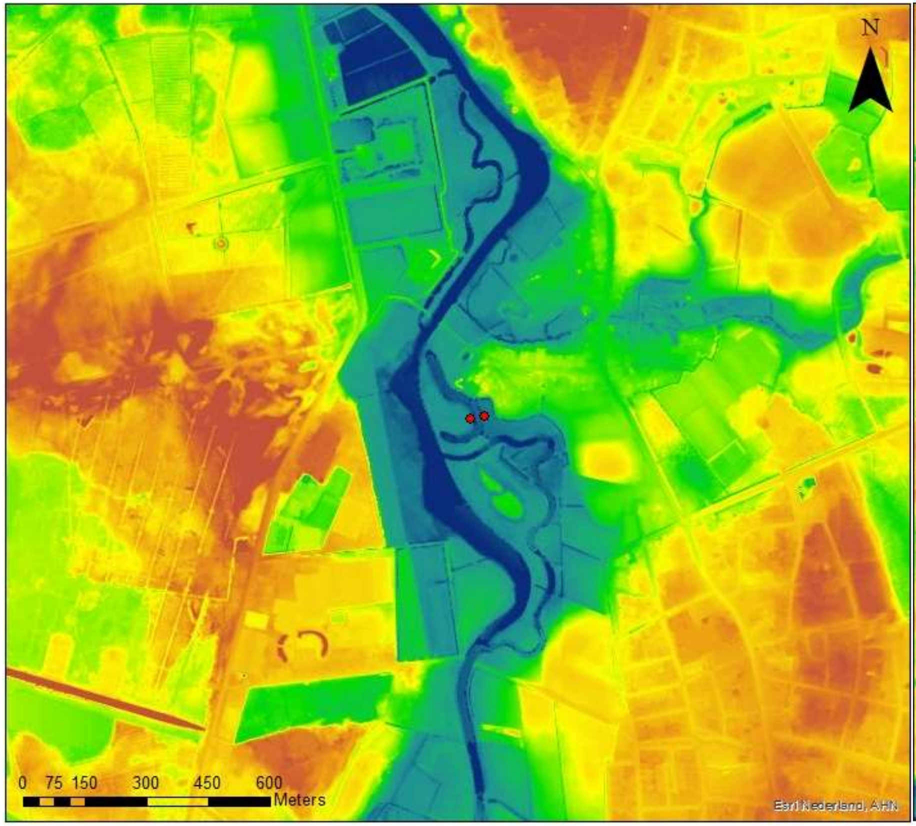

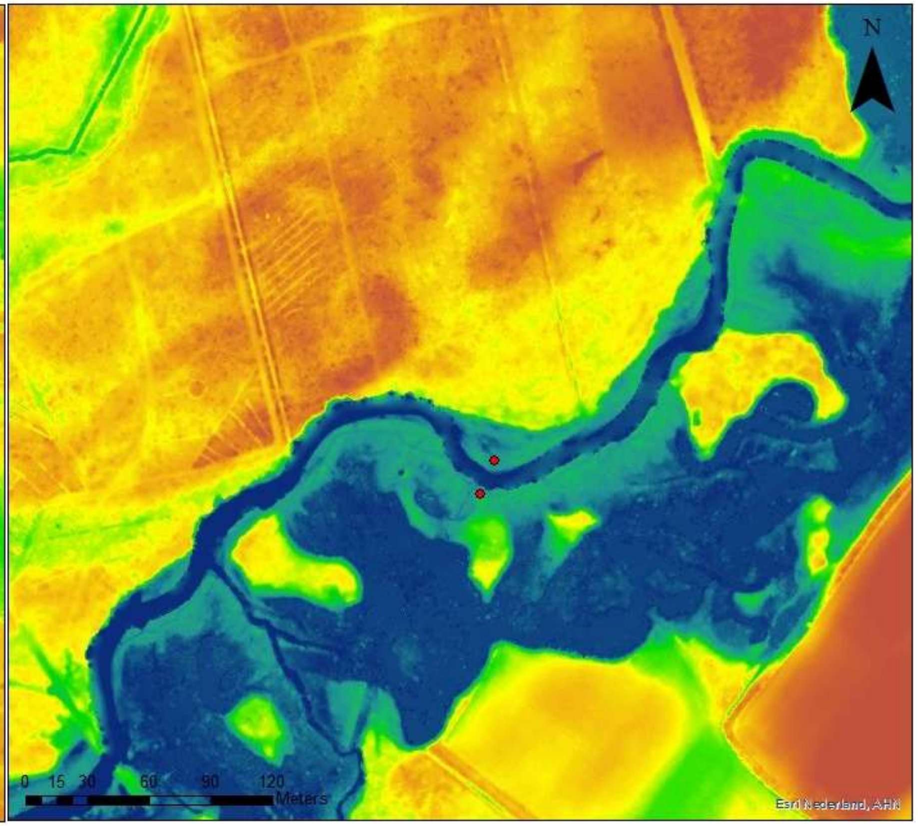

Left: *Bovenmark*
Right: *Bovenslinge*

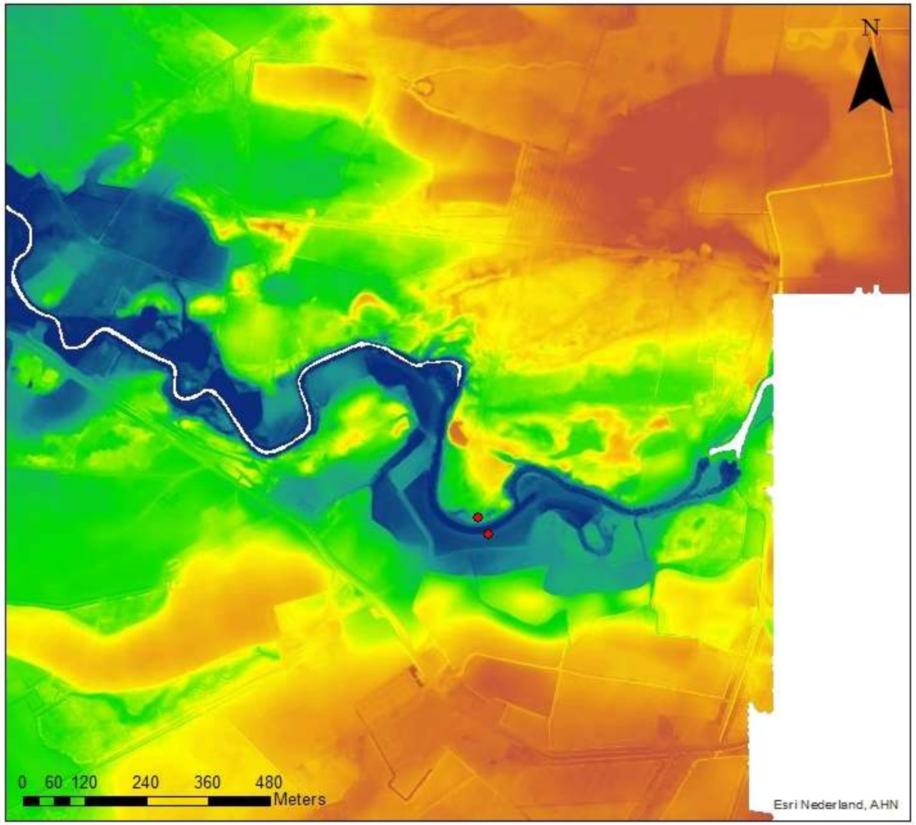

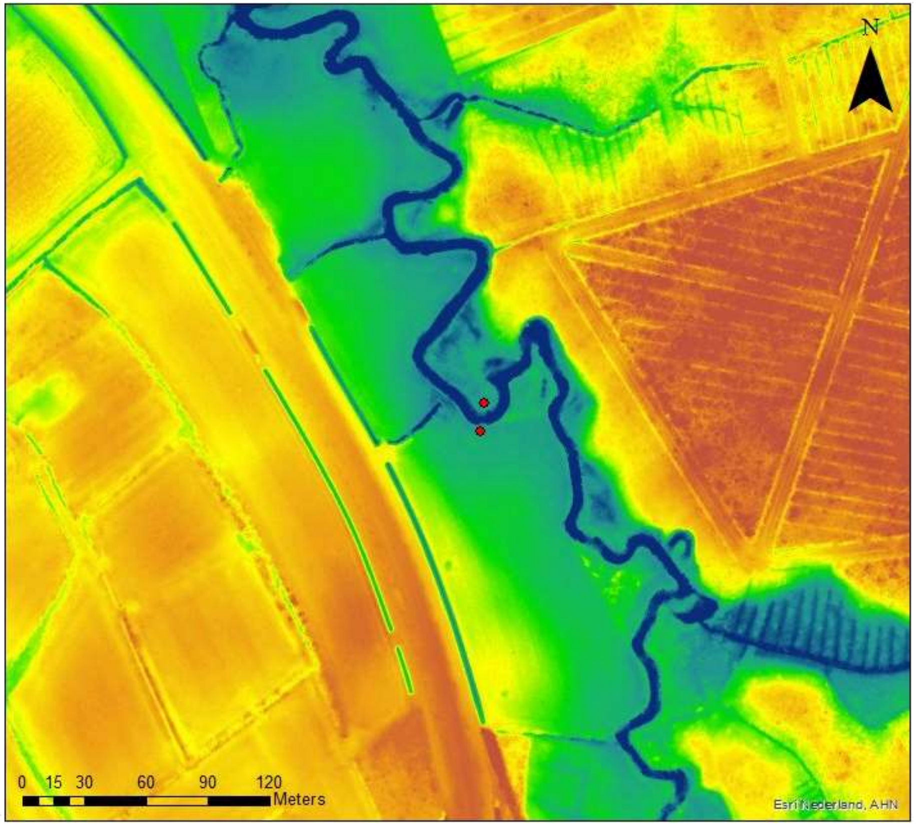

Left: *Buurserbeek (white area in the figure is Germany, no DEM data of this area were available)*
Right: *Chaamse Beek*

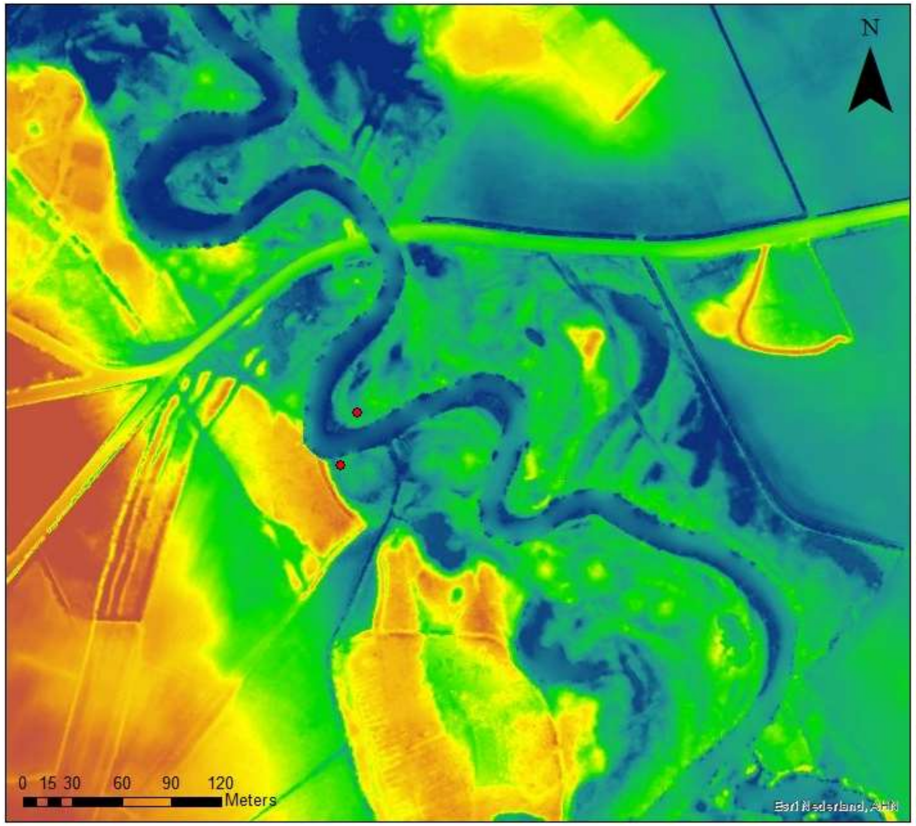

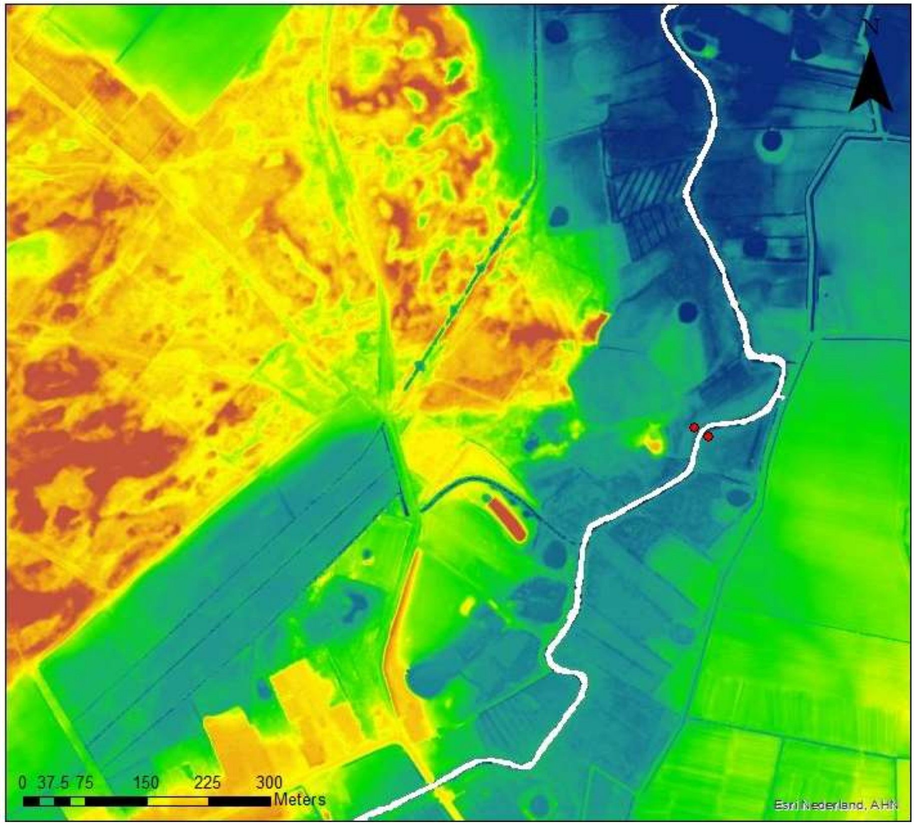

***Left**: Dinkel*
***Right:** Dommel*

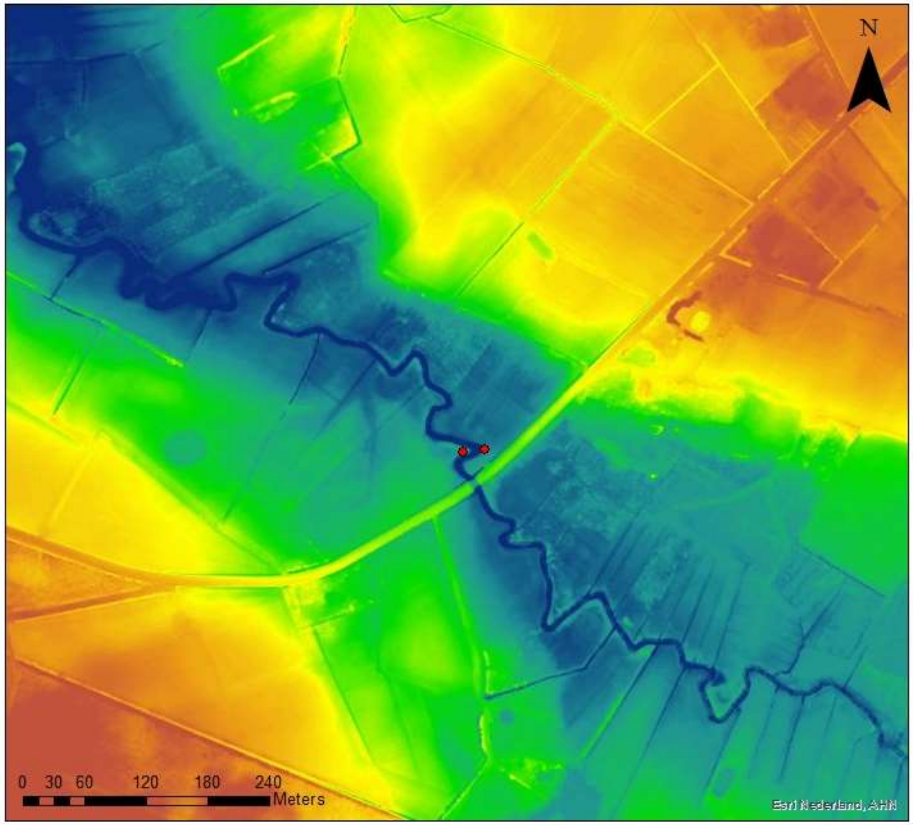

Left: *Geul*
Right: *Merkske*

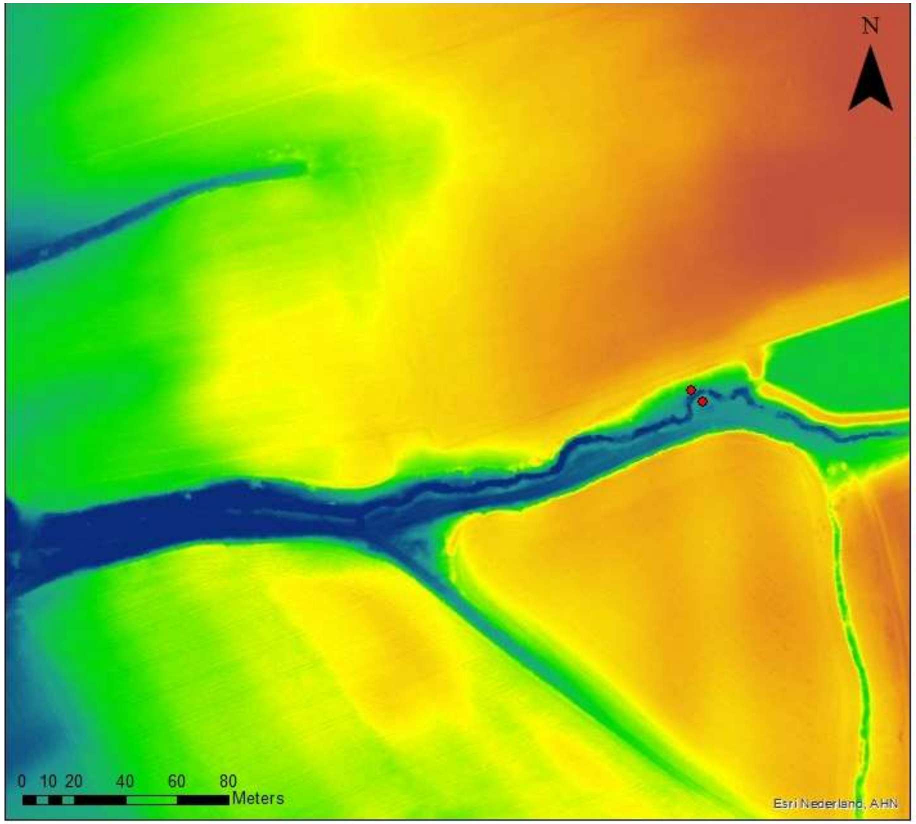

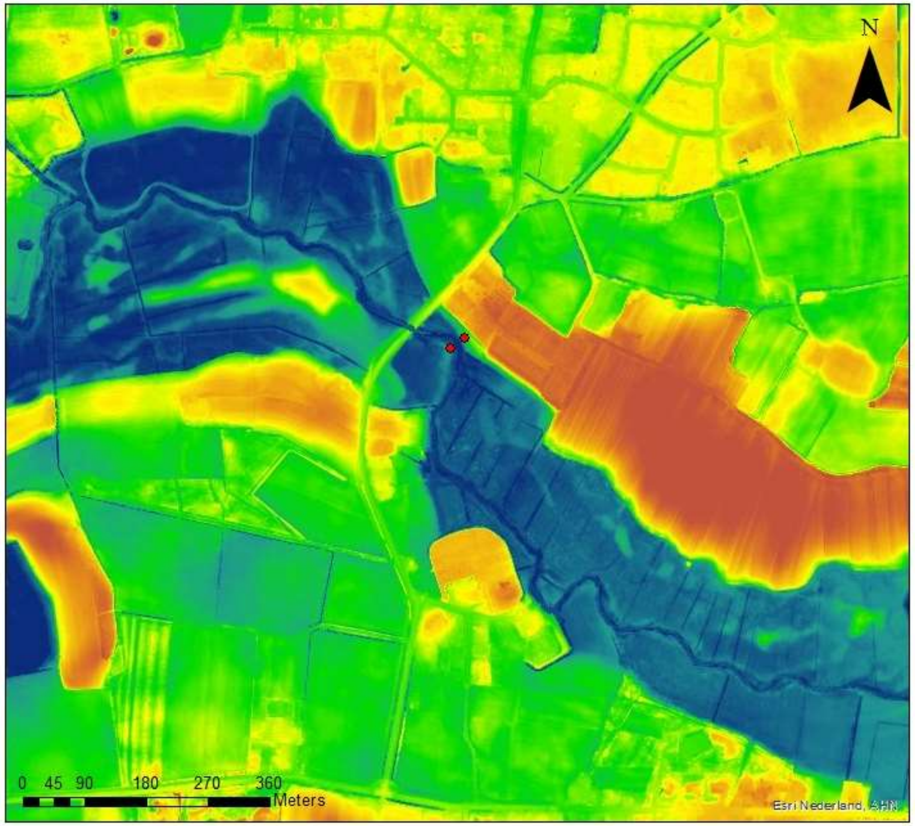

Left: *Mosbeek*
Right: *Reest*

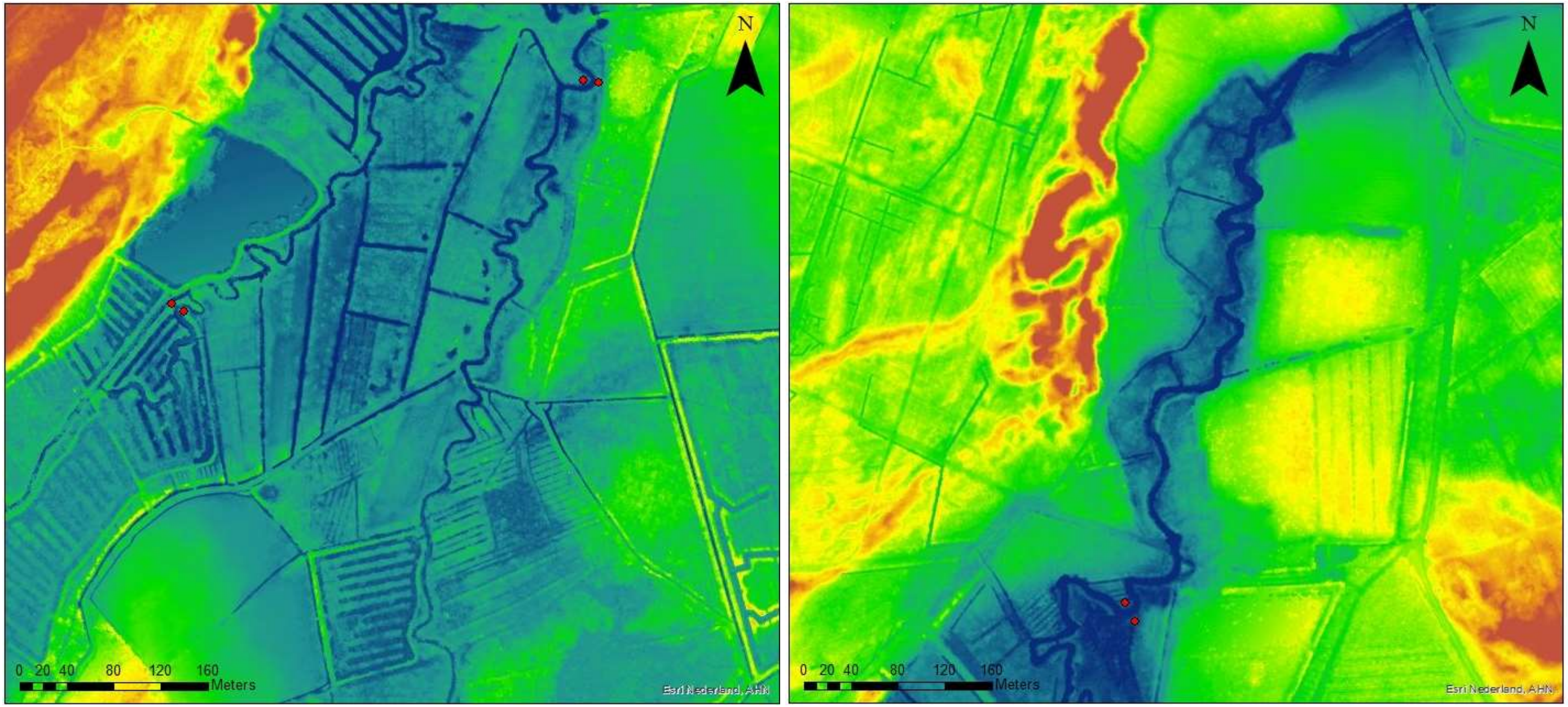

Left: *Reusel (left stream within the figure) and the Raamsloop (right stream within the figure)*
Right: *Reusel + Raamsloop*

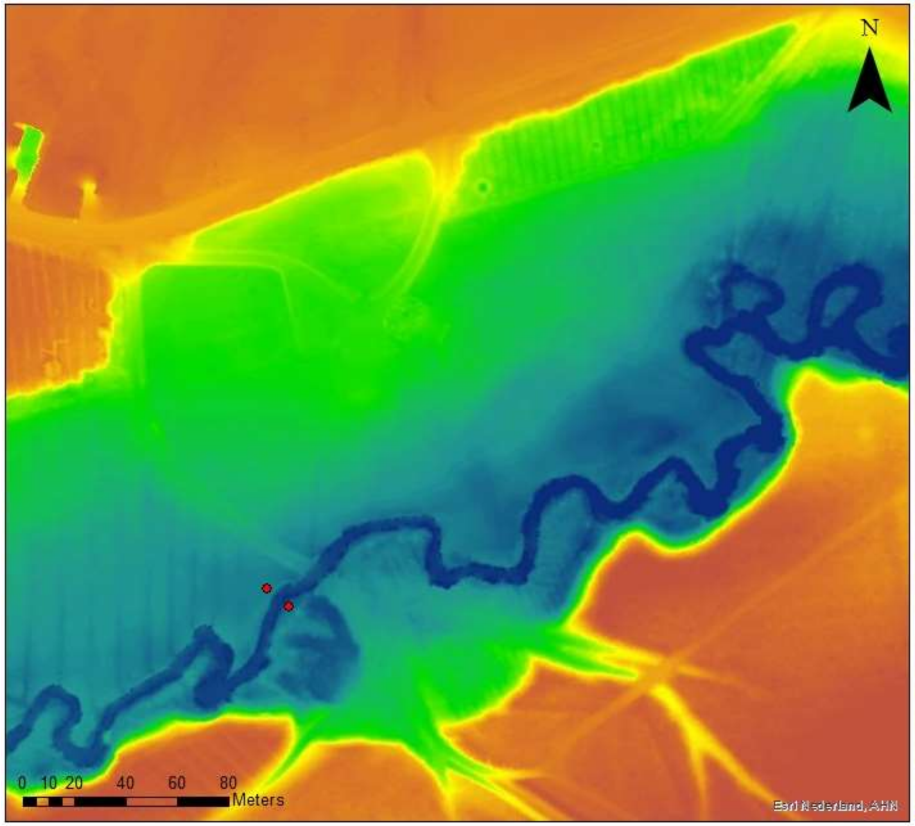

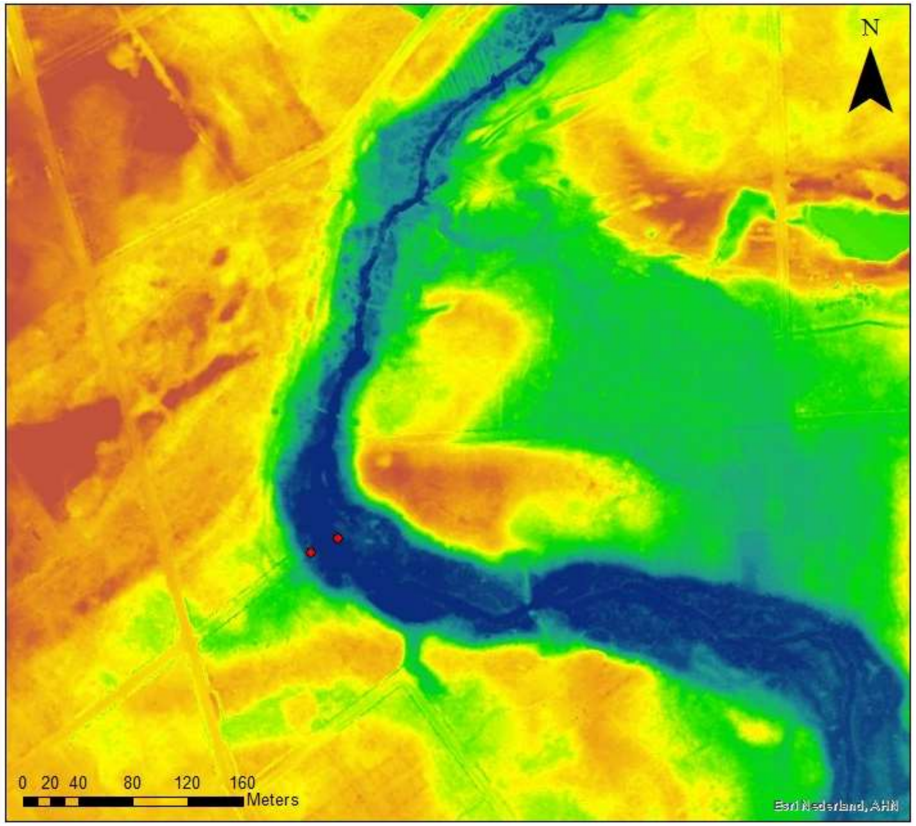

***Left**: Roggelse Beek*
***Right:** Rosep*

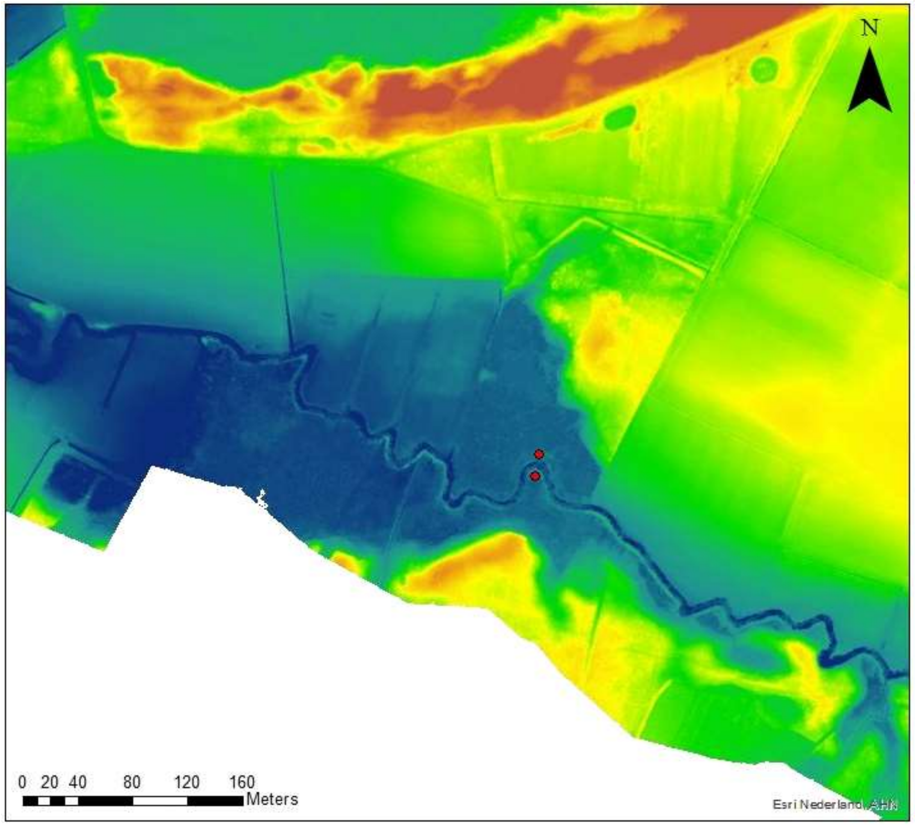

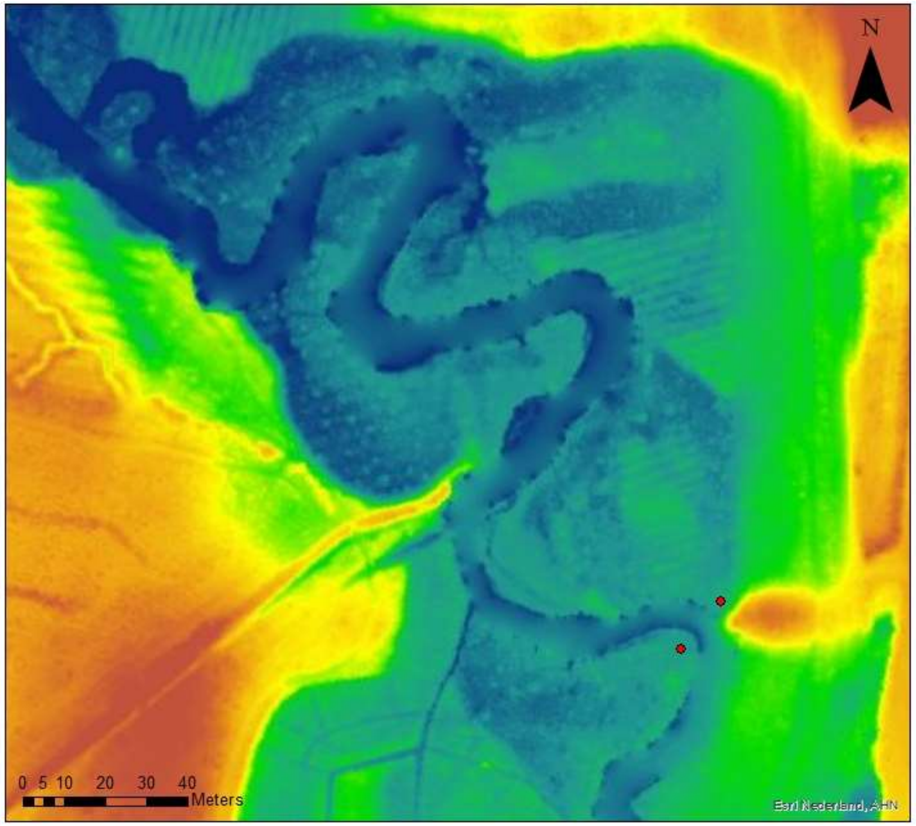

Left: *Strijbeekse Beek (white area in the figure is Belgium, no DEM data of this area were available)*
Right: *Swalm*

Appendix IV: Historical maps

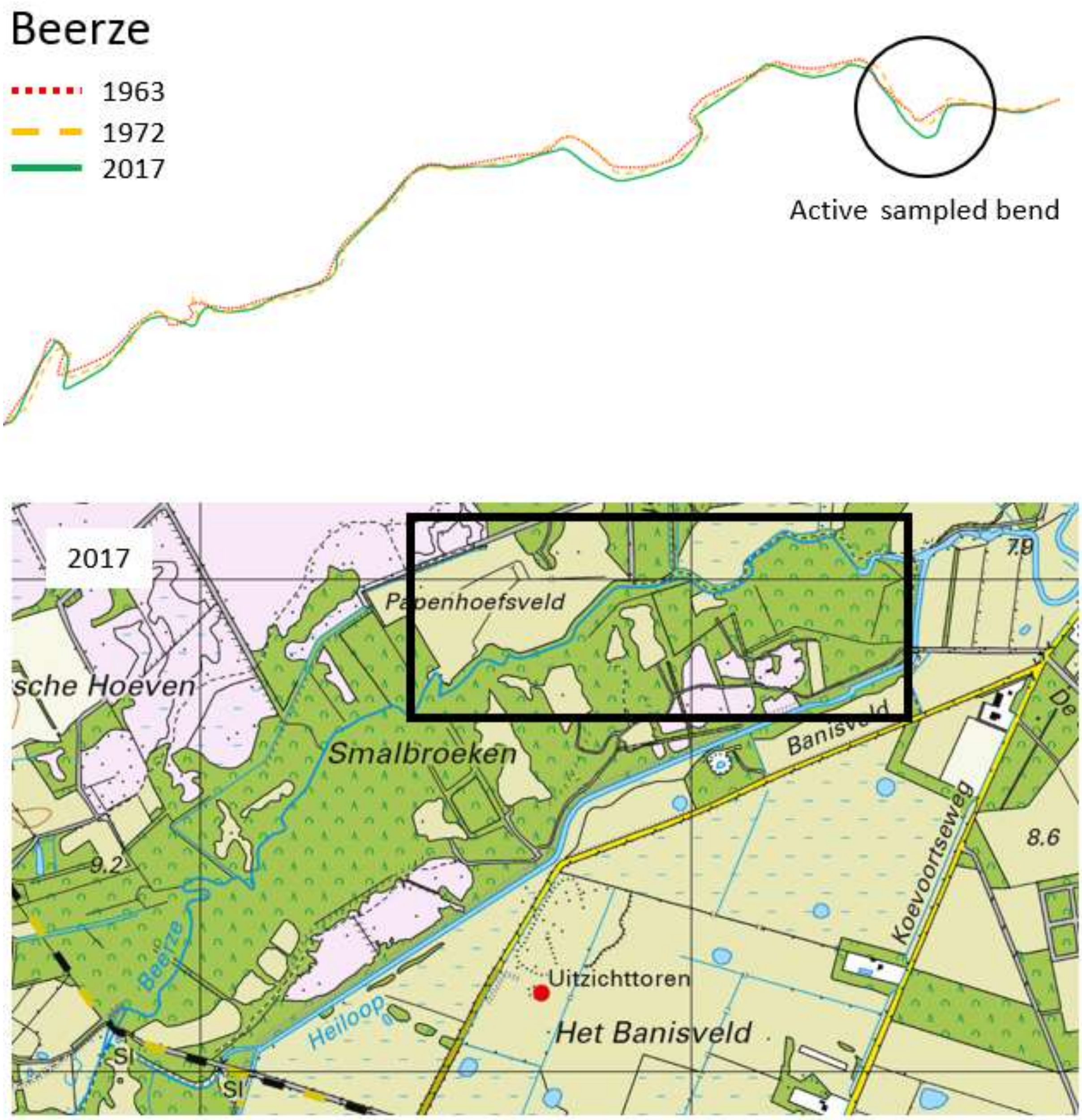

The historical map of the Beerze from 2017 with the stream courses from older maps visualized on the top of the figure. Focus of the stream courses was put in the area mark by the black box in the 2017 map of the Beerze. Overall the stream course is rather stable. The sampled bend is indicated by the circle.

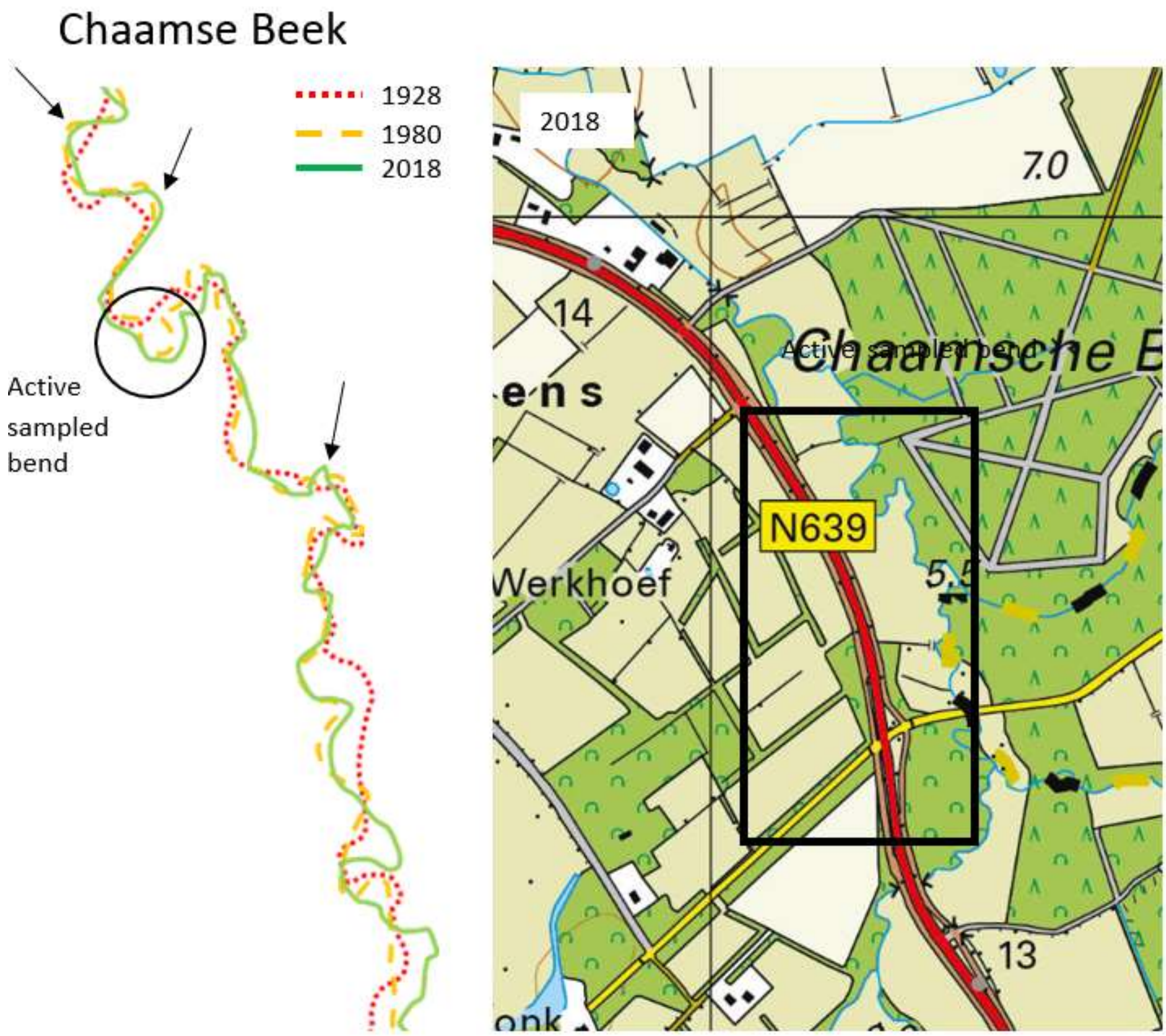

The historical map of the Chaamse beek from 2018 with the stream courses from older maps visualized on the top of the figure. Focus of the stream courses was put in the area mark by the black box in the 2018 map of the Chaamse Beek. Overall the stream course is rather unstable. The sampled bend is indicated by the circle. Some bends where potential lateral migration might have taken place are indicated by arrows.

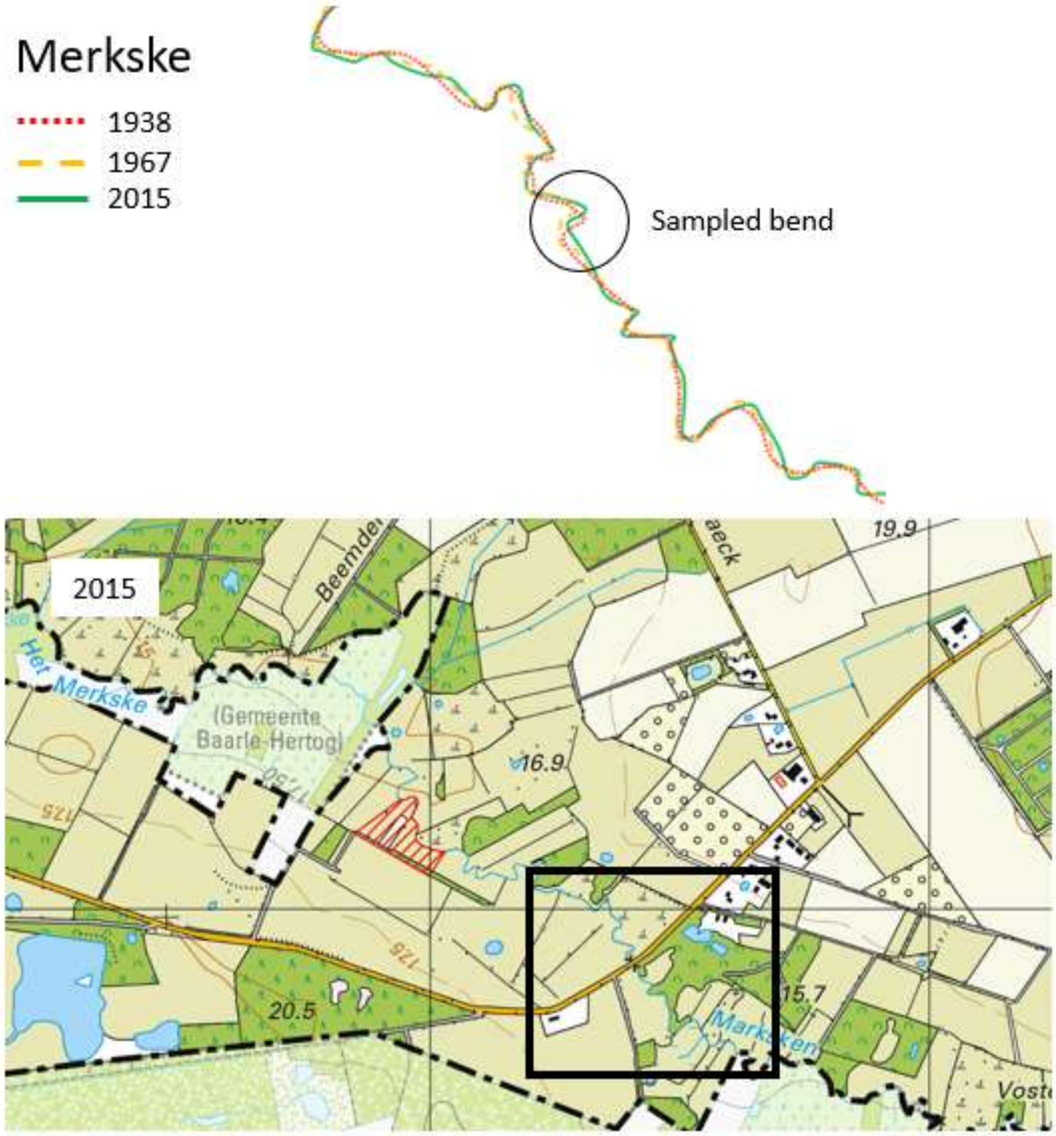

The historical map of the Merkske from 2015 with the stream courses from older maps visualized on the top of the figure. Focus of the stream courses was put in the area mark by the black box in the 2018 map of the Chaamse Beek. Overall the stream course is rather stable. The sampled bend is indicated by the circle. No general trends can be seen, if the stream courses do not match completely this might be caused by map inaccuracies.

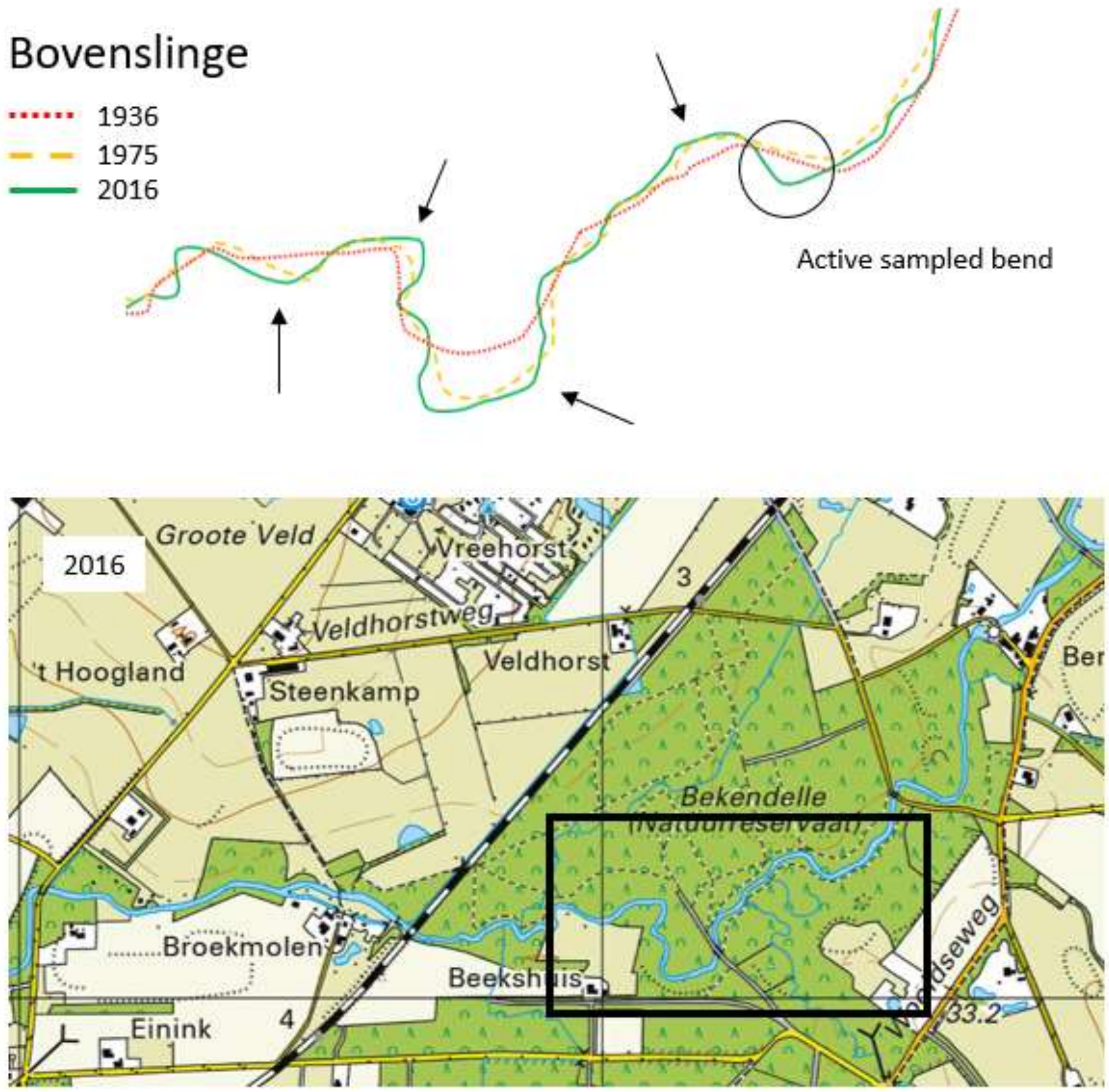

The historical map of the Bovenslinge from 2016 with the stream courses from older maps visualized on the top of the figure. Focus of the stream courses was put in the area mark by the black box in the 2015 map of the Bovenslinge. Overall the stream course is rather unstable. The sampled bend is indicated by the circle. Some bends where potential lateral migration might have taken place are indicated by arrows.